doi.org/10.26434/chemrxiv.13726513.v1

A Versatile New Reagent for Nitrosation under Mild Conditions

Jordan D. Galloway, Cristian Sarabia, James C. Fettinger, Hrant Hratchian, Ryan Baxter

Submitted date: 07/02/2021 • Posted date: 08/02/2021

Citation information: Galloway, Jordan D.; Sarabia, Cristian; Fettinger, James C.; Hratchian, Hrant; Baxter, Ryan (2021): A Versatile New Reagent for Nitrosation under Mild Conditions. ChemRxiv. Preprint. https://doi.org/10.26434/chemrxiv.13726513.v1

We report a new chemical reagent for transnitrosation under mild experimental conditions. This new reagent is stable to air and moisture across a broad range of temperatures, and is effective for transnitrosation in multiple solvents. Compared to traditional nitrosation methods, our reagent shows high functional group tolerance for substrates that are susceptible to oxidation or reversible transnitrosation. Several challenging nitroso-compounds are accessed here for the first time, including 15N isotopologues. X-ray data confirms two rotational isomers of the reagent are configurationally stable at room temperature, although only one isomer is effective for transnitrosation. Computational analysis describes the energetics of rotamer interconversion, including interesting geometry-dependent hybridization ef-fects.

File list (4)

5 February, 2021

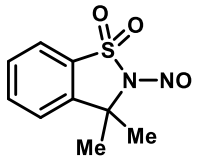

NO-1

3,3-dimethyl-2-nitroso-2,3-dihydrobenzo[d]isothiazole 1,1-dioxide (NO-1)

A yellow block with approximate orthogonal dimensions 0.060 x 0.154 x 0.338mm^3 was placed and optically centered on the Bruker Duo[1] APEXII CCD system at –183°C(90K). Indexing of the unit cell used a random set of reflections collected from three series of 0.5° wide ω-scans, 10 seconds per frame, and 30 frames per series that were well distributed in reciprocal space. Five ω-scan data frame series were collected [MoK$_\alpha$] with 0.3° wide scans, 15 seconds per frame and 606 frames collected per series at varying φ angles (φ=0°, 72°, 144°, 216°, 288°). The crystal to detector distance was 5.15cm, thus providing a complete sphere of data to $2\theta_{max}$=61.01°.

Structural determination and Refinement:

All crystallographic calculations were performed on an Intel Xeon E5-1620v2 at 3.70GHz an eight core processor and 16GB of extended memory. Data collected were corrected for Lorentz and polarization effects with Saint[1] and absorption using Blessing's method and merged as incorporated with the program Sadabs[2,3]. The SHELXTL[4] program package was implemented to determine the probable space group and set up the initial files. System symmetry, systematic absences and intensity statistics indicated the centrosymmetric monoclinic space group $P2_1/n$ (no. 14). The structure was determined by direct methods with the non-hydrogen atoms being located directly for the molecule using the program XT[5]. The structure was refined with XL[6]. The 20407 data collected were merged, based upon identical indices to 11861 data, then for least squares refinement to 3091 unique data [R(int)=0.0224]. All non-hydrogen atoms were refined anisotropically. A disorder was modeled for the terminal N-O, group with the final ratio 0.87:0.13. Hydrogen atoms were idealized initially and then allowed to refine freely throughout the final refinement stage. The final structure was refined to convergence with R(F)=3.63%, wR(F^2)=8.27%, GOF=1.065 for all 3091 unique reflections [R(F)=3.08, wR(F^2)=7.87% for those 2706 data with Fo > 4σ(Fo)]. The final difference-Fourier map was featureless indicating that the structure is both correct and complete.

Table 1. Crystal data and structure refinement for [$C_9H_{10}N_2O_3S$].

Identification code	JF2913FMI (JDGR2)
Empirical formula	C9 H10 N2 O3 S
Formula weight	226.25
Temperature	90(2) K
Wavelength	0.71073 Å

Crystal system	Monoclinic	
Space group	$P2_1/n$	
Unit cell dimensions	a = 7.7236(7) Å	α= 90°.
	b = 9.8965(9) Å	β= 94.6681(13)°.
	c = 13.3301(12) Å	γ = 90°.
Volume	1015.53(16) $Å^3$	
Z	4	
Density (calculated)	1.480 Mg/m^3	
Absorption coefficient	0.307 mm^{-1}	
F(000)	472	
Crystal size	0.338 x 0.154 x 0.060 mm^3	
Crystal color and habit	Yellow Block	
Diffractometer	Bruker APEX-II CCD	
Theta range for data collection	2.566 to 30.509°.	
Index ranges	-11<=h<=11, -14<=k<=14, -19<=l<=19	
Reflections collected	11861	
Independent reflections	3091 [R(int) = 0.0224]	
Observed reflections (I > 2sigma(I))	2706	
Completeness to theta = 25.242°	100.0 %	
Absorption correction	Semi-empirical from equivalents	
Max. and min. transmission	0.9575 and 0.8766	
Solution method	SHELXT (Sheldrick, 2014)	
Refinement method	SHELXL-2018/3 (Sheldrick, 2018) Full-matrix least-squares on F^2	
Data / restraints / parameters	3091 / 14 / 194	
Goodness-of-fit on F^2	1.065	
Final R indices [I>2sigma(I)]	R1 = 0.0308, wR2 = 0.0787	
R indices (all data)	R1 = 0.0363, wR2 = 0.0827	
Largest diff. peak and hole	0.470 and -0.392 $e.Å^{-3}$	

Table 2. Atomic coordinates (x 10^4) and equivalent isotropic displacement parameters ($Å^2$x 10^3) for JF2913FMI. U(eq) is defined as one third of the trace of the orthogonalized U^{ij} tensor.

	x	y	z	U(eq)
S(1)	4763(1)	2078(1)	2767(1)	15(1)
O(1)	3101(1)	1688(1)	3080(1)	27(1)
O(2)	4988(1)	2114(1)	1712(1)	26(1)
N(1)	6354(1)	1119(1)	3387(1)	14(1)
N(2)	6463(5)	-229(2)	3272(2)	20(1)
O(3)	5421(1)	-686(1)	2611(1)	25(1)
N(2B)	6240(30)	-193(10)	3105(16)	19(2)
O(3B)	7244(9)	-925(7)	3622(6)	26(1)
C(1)	7391(1)	1780(1)	4250(1)	12(1)
C(2)	6875(1)	3255(1)	4121(1)	13(1)
C(3)	5548(1)	3530(1)	3384(1)	14(1)
C(4)	6827(2)	1211(1)	5241(1)	16(1)
C(5)	9330(1)	1573(1)	4149(1)	18(1)
C(6)	4931(2)	4826(1)	3157(1)	20(1)
C(7)	5712(2)	5886(1)	3705(1)	24(1)
C(8)	7030(2)	5636(1)	4460(1)	23(1)
C(9)	7620(2)	4329(1)	4680(1)	18(1)

Table 3. Bond lengths [Å] and angles [°] for JF2913FMI.

S(1)-O(2)	1.4308(9)	N(1)-S(1)-C(3)	91.20(5)
S(1)-O(1)	1.4346(9)	N(2)-N(1)-C(1)	119.06(11)
S(1)-N(1)	1.7109(9)	N(2B)-N(1)-C(1)	130.6(6)
S(1)-C(3)	1.7400(11)	N(2)-N(1)-S(1)	122.93(11)
N(1)-N(2)	1.3461(18)	N(2B)-N(1)-S(1)	111.8(6)
N(1)-N(2B)	1.352(9)	C(1)-N(1)-S(1)	116.55(7)
N(1)-C(1)	1.4976(13)	O(3)-N(2)-N(1)	113.74(15)
N(2)-O(3)	1.230(2)	O(3B)-N(2B)-N(1)	112.8(11)
N(2B)-O(3B)	1.229(10)	N(1)-C(1)-C(2)	102.34(8)
C(1)-C(2)	1.5196(14)	N(1)-C(1)-C(5)	109.90(9)
C(1)-C(5)	1.5283(15)	C(2)-C(1)-C(5)	111.63(9)
C(1)-C(4)	1.5324(15)	N(1)-C(1)-C(4)	109.30(8)
C(2)-C(3)	1.3877(15)	C(2)-C(1)-C(4)	111.10(9)
C(2)-C(9)	1.3955(15)	C(5)-C(1)-C(4)	112.11(9)
C(3)-C(6)	1.3931(15)	C(3)-C(2)-C(9)	118.54(10)
C(4)-H(4A)	0.976(15)	C(3)-C(2)-C(1)	116.11(9)
C(4)-H(4B)	0.969(16)	C(9)-C(2)-C(1)	125.35(10)
C(4)-H(4C)	0.964(17)	C(2)-C(3)-C(6)	123.65(10)
C(5)-H(5A)	0.986(17)	C(2)-C(3)-S(1)	112.43(8)
C(5)-H(5B)	0.938(18)	C(6)-C(3)-S(1)	123.91(9)
C(5)-H(5C)	0.968(17)	C(1)-C(4)-H(4A)	110.8(9)
C(6)-C(7)	1.3877(18)	C(1)-C(4)-H(4B)	109.1(9)
C(6)-H(6)	0.956(16)	H(4A)-C(4)-H(4B)	109.6(13)
C(7)-C(8)	1.394(2)	C(1)-C(4)-H(4C)	109.7(9)
C(7)-H(7)	0.924(19)	H(4A)-C(4)-H(4C)	108.2(13)
C(8)-C(9)	1.3939(17)	H(4B)-C(4)-H(4C)	109.4(13)
C(8)-H(8)	0.926(18)	C(1)-C(5)-H(5A)	108.7(10)
C(9)-H(9)	0.959(15)	C(1)-C(5)-H(5B)	109.6(11)
		H(5A)-C(5)-H(5B)	109.8(14)
O(2)-S(1)-O(1)	118.40(6)	C(1)-C(5)-H(5C)	112.1(10)
O(2)-S(1)-N(1)	110.40(5)	H(5A)-C(5)-H(5C)	108.9(14)
O(1)-S(1)-N(1)	109.57(5)	H(5B)-C(5)-H(5C)	107.7(14)
O(2)-S(1)-C(3)	112.20(6)	C(7)-C(6)-C(3)	117.06(11)
O(1)-S(1)-C(3)	111.73(5)	C(7)-C(6)-H(6)	122.9(10)

C(3)-C(6)-H(6)	120.0(10)	C(9)-C(8)-H(8)	119.6(11)
C(6)-C(7)-C(8)	120.44(11)	C(7)-C(8)-H(8)	118.8(11)
C(6)-C(7)-H(7)	119.5(11)	C(8)-C(9)-C(2)	118.70(11)
C(8)-C(7)-H(7)	120.1(11)	C(8)-C(9)-H(9)	121.4(9)
C(9)-C(8)-C(7)	121.59(11)	C(2)-C(9)-H(9)	119.9(9)

Symmetry transformations used to generate equivalent atoms:

Table 4. Anisotropic displacement parameters ($Å^2 x\ 10^3$) for JF2913FMI. The anisotropic displacement factor exponent takes the form: $-2\pi^2[\ h^2\ a^{*2}U^{11} + ...\ + 2\ h\ k\ a^*\ b^*\ U^{12}\ ]$

	U^{11}	U^{22}	U^{33}	U^{23}	U^{13}	U^{12}
S(1)	13(1)	19(1)	14(1)	-2(1)	-2(1)	2(1)
O(1)	14(1)	29(1)	38(1)	-8(1)	1(1)	-4(1)
O(2)	33(1)	32(1)	12(1)	-2(1)	-4(1)	9(1)
N(1)	16(1)	12(1)	14(1)	-1(1)	-1(1)	1(1)
N(2)	27(1)	14(1)	19(1)	-2(1)	5(1)	-1(1)
O(3)	32(1)	21(1)	23(1)	-9(1)	4(1)	-8(1)
N(2B)	25(3)	14(3)	20(3)	2(2)	9(3)	2(2)
O(3B)	27(3)	20(3)	31(3)	-1(3)	4(3)	3(3)
C(1)	12(1)	13(1)	12(1)	0(1)	-1(1)	0(1)
C(2)	14(1)	13(1)	13(1)	0(1)	4(1)	-1(1)
C(3)	14(1)	14(1)	14(1)	0(1)	3(1)	1(1)
C(4)	19(1)	17(1)	14(1)	2(1)	1(1)	-3(1)
C(5)	13(1)	21(1)	21(1)	2(1)	1(1)	2(1)
C(6)	23(1)	19(1)	18(1)	5(1)	6(1)	7(1)
C(7)	33(1)	13(1)	27(1)	3(1)	15(1)	4(1)
C(8)	29(1)	14(1)	26(1)	-4(1)	12(1)	-7(1)
C(9)	19(1)	17(1)	18(1)	-2(1)	4(1)	-5(1)

Table 5. Hydrogen coordinates (x 10^4) and isotropic displacement parameters ($Å^2$x 10^3) for JF2913FMI.

	x	y	z	U(eq)
H(4A)	5570(20)	1298(16)	5272(11)	20(4)
H(4B)	7420(20)	1698(16)	5798(12)	22(4)
H(4C)	7120(20)	266(17)	5294(12)	25(4)
H(5A)	9560(20)	596(17)	4100(12)	27(4)
H(5B)	9970(20)	1934(17)	4714(13)	31(4)
H(5C)	9710(20)	2018(17)	3558(13)	27(4)
H(6)	4010(20)	4955(16)	2645(12)	23(4)
H(7)	5330(20)	6759(19)	3577(13)	33(5)
H(8)	7520(20)	6358(18)	4823(13)	31(4)
H(9)	8530(20)	4161(15)	5198(12)	19(4)

Table 6. Torsion angles [°] for JF2913FMI.

O(2)-S(1)-N(1)-N(2)	-68.4(2)	N(1)-S(1)-C(3)-C(2)	-6.36(8)
O(1)-S(1)-N(1)-N(2)	63.8(2)	O(2)-S(1)-C(3)-C(6)	60.31(11)
C(3)-S(1)-N(1)-N(2)	177.4(2)	O(1)-S(1)-C(3)-C(6)	-75.39(11)
O(2)-S(1)-N(1)-N(2B)	-65.0(14)	N(1)-S(1)-C(3)-C(6)	172.96(10)
O(1)-S(1)-N(1)-N(2B)	67.1(14)	C(2)-C(3)-C(6)-C(7)	0.36(16)
C(3)-S(1)-N(1)-N(2B)	-179.3(14)	S(1)-C(3)-C(6)-C(7)	-178.89(9)
O(2)-S(1)-N(1)-C(1)	125.60(8)	C(3)-C(6)-C(7)-C(8)	-1.28(17)
O(1)-S(1)-N(1)-C(1)	-102.28(8)	C(6)-C(7)-C(8)-C(9)	0.83(18)
C(3)-S(1)-N(1)-C(1)	11.33(8)	C(7)-C(8)-C(9)-C(2)	0.61(17)
C(1)-N(1)-N(2)-O(3)	172.4(2)	C(3)-C(2)-C(9)-C(8)	-1.50(15)
S(1)-N(1)-N(2)-O(3)	6.7(4)	C(1)-C(2)-C(9)-C(8)	178.68(10)
C(1)-N(1)-N(2B)-O(3B)	-5(3)		
S(1)-N(1)-N(2B)-O(3B)	-172.2(17)		
N(2)-N(1)-C(1)-C(2)	-178.7(2)		
N(2B)-N(1)-C(1)-C(2)	-179.1(17)		
S(1)-N(1)-C(1)-C(2)	-12.12(10)		
N(2)-N(1)-C(1)-C(5)	62.6(2)		
N(2B)-N(1)-C(1)-C(5)	62.2(17)		
S(1)-N(1)-C(1)-C(5)	-130.84(8)		
N(2)-N(1)-C(1)-C(4)	-60.9(2)		
N(2B)-N(1)-C(1)-C(4)	-61.2(17)		
S(1)-N(1)-C(1)-C(4)	105.72(9)		
N(1)-C(1)-C(2)-C(3)	7.11(12)		
C(5)-C(1)-C(2)-C(3)	124.60(10)		
C(4)-C(1)-C(2)-C(3)	-109.45(10)		
N(1)-C(1)-C(2)-C(9)	-173.06(10)		
C(5)-C(1)-C(2)-C(9)	-55.57(14)		
C(4)-C(1)-C(2)-C(9)	70.38(13)		
C(9)-C(2)-C(3)-C(6)	1.05(16)		
C(1)-C(2)-C(3)-C(6)	-179.11(10)		
C(9)-C(2)-C(3)-S(1)	-179.63(8)		
C(1)-C(2)-C(3)-S(1)	0.21(12)		
O(2)-S(1)-C(3)-C(2)	-119.01(8)		
O(1)-S(1)-C(3)-C(2)	105.30(9)		

Symmetry transformations used to generate equivalent atoms:

Table 7. Hydrogen bonds for JF2913FMI [Å and °].

D-H...A	d(D-H)	d(H...A)	d(D...A)	<(DHA)
C(4)-H(4B)...O(2)#1	0.969(16)	2.530(16)	3.4309(14)	154.8(13)
C(4)-H(4C)...O(3B^b)	0.964(17)	2.531(18)	3.058(7)	114.4(12)
C(5)-H(5A)...O(3B^b)	0.986(17)	2.385(18)	3.003(7)	120.0(12)
C(6)-H(6)...O(1)#2	0.956(16)	2.503(16)	3.3121(15)	142.4(13)

Symmetry transformations used to generate equivalent atoms:

#1 x+1/2,-y+1/2,z+1/2 #2 -x+1/2,y+1/2,-z+1/2

References:

1. Bruker (2014) APEX2 (Version 2014.9) and (2016) SAINT (Version 8.37a). Bruker AXS Inc., Madison, Wisconsin, USA.
2. An Empirical Correction for Absorption Anisotropy, Blessing, R. H. (1995). Acta Cryst., A51, 33-38.
3. Sheldrick, G.M., SADABS (2016) Version 2016/2, 'Siemens Area Detector Absorption Correction' Universität Göttingen: Göttingen, Germany.
4. Sheldrick, G.M., (2002). SHELXTL. Version 6.1. Bruker AXS Inc., Madison, Wisconsin, USA.
5. Sheldrick, G. M., (2014) SHELXT, Universität Göttingen: Göttingen, Germany. Structure determination program. Private communication.
6. Sheldrick, G. M., (2017). SHELXL2017/1. Universität Göttingen: Göttingen, Germany.

Acknowledgment: We thank the National Science Foundation (Grant CHE-0840444) for the Dual Source X-ray diffractometer.

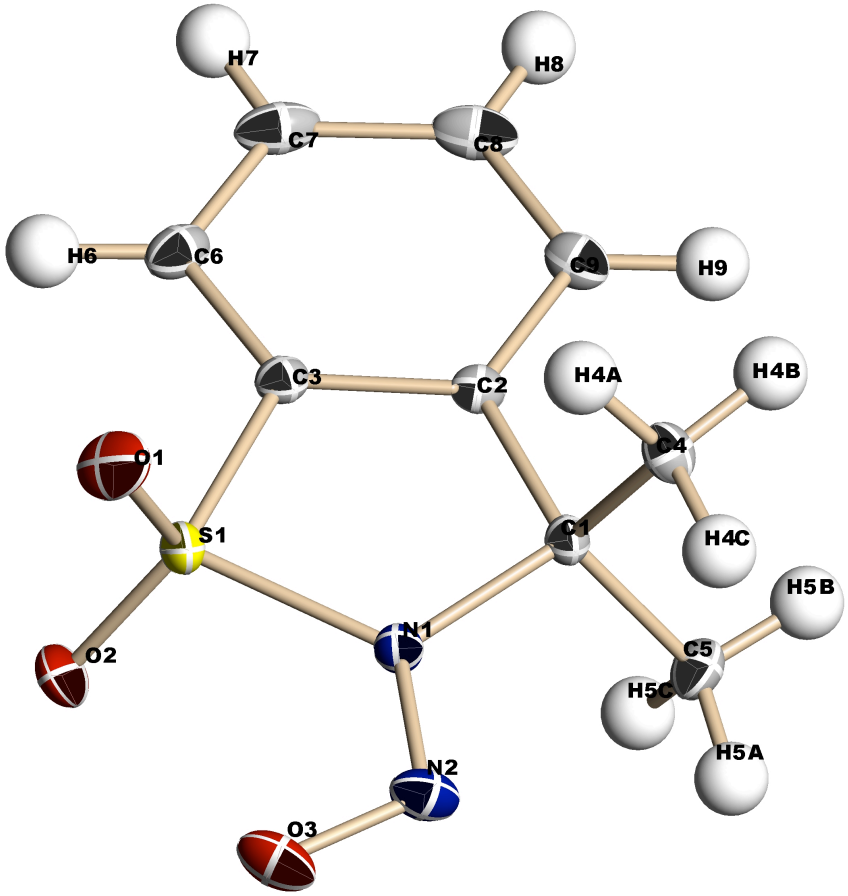
H7
H8
C7
C8
H6
C6
C9
H9
C3
C2
H4A
H4B
C4
O1
S1
C1
H4C
H5B
N1
O2
C5
H5C
H5A
N2
O3

Supporting Information

A Versatile New Reagent for Nitrosation under Mild Conditions

*Jordan D. Galloway[1], Cristian Sarabia[1], James C. Fettinger[2], Hrant P. Hratchian[1], and Ryan D. Baxter[1]**

[1]Department of Chemistry and Chemical Biology, University of California, Merced
5200 North Lake Road, Merced, California, 95343

[2]Department of Chemistry, University of California, Davis
1 Shields Avenue, Davis, California 95616

[*]Corresponding Authors: rbaxter@ucmerced.edu

Table of Contents

1. Calculation Set Up

Geometries for the NO-1a, NO-1a (sp^3), and NO-1b reagent were all calculated using the B3LYP/6-311+G(2p, d) model chemistry with the PCM(acetonitrile) solvent model.[1,3,4] Additionally, vibrational frequency analysis was performed to confirm that all geometries were true minima.[2] Once the ground state geometries were confirmed the Nitrogen-Nitrogen bond dihedral angle was scanned/rotated using a scan job in gaussian, changing the dihedral angle by ten degrees all the way until three-hundred sixty degrees is reached, calculating a ground state energy. The NO-1a was scanned constrained to sp^2 hybridization and constrained to sp^3 hybridization represented as the green and blue curve respectively in the bottom of Figure 4. While NO-1a unconstrained to any hybridization was scanned to produce the top of Figure 4. Scheme SC1 shows the scanned coordinate and potential energy surface path.

2. Optimized Geometries

Scheme SC1. Coordinate Scan

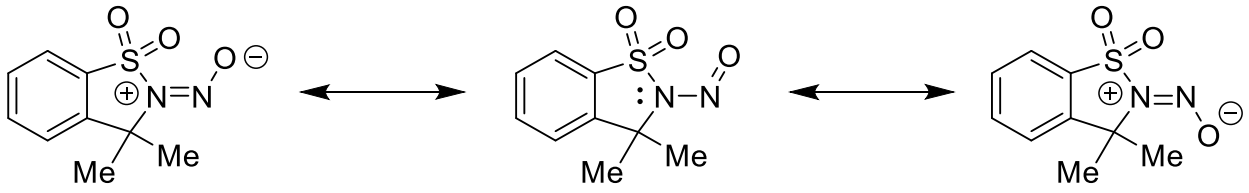

NO-1a NO-1a (sp^3) NO-1b

Table SC1. Optimized Geometries of NO-1a(sp^2), NO-1(sp^3) and NO-1b (sp^2)

NO-1a

C	-0.933083	-0.727194	0.000033
C	-1.058869	0.653554	0.000094
C	-2.341557	1.195960	0.000182
C	-3.444025	0.349781	0.000209
C	-3.288206	-1.037978	0.000155
C	-2.018543	-1.595824	0.000066
C	0.224207	1.469915	0.000070
H	-2.485907	2.268836	0.000227
H	-4.439564	0.775365	0.000274
H	-4.158114	-1.681716	0.000184
H	-1.879742	-2.669187	0.000027
N	1.291554	0.420849	-0.000050
S	0.746074	-1.263299	-0.000093
O	1.114532	-1.900630	-1.246495
O	1.114659	-1.900792	1.246188
N	2.563560	0.761552	-0.000123
O	3.366339	-0.163605	-0.000315
C	0.348161	2.323369	-1.270527
H	-0.454626	3.060496	-1.297233
H	1.300982	2.852965	-1.273130
H	0.282299	1.703862	-2.165369
C	0.348298	2.323220	1.270754
H	1.301114	2.852826	1.273311
H	-0.454493	3.060335	1.297638

H	0.282545	1.703606	2.165530

NO-1b

C	1.098032	-0.584041	-0.000222
C	0.870591	0.783703	-0.000023
C	1.975677	1.631523	-0.000086
C	3.255541	1.090132	-0.000350
C	3.454395	-0.292235	-0.000552
C	2.366598	-1.152251	-0.000488
H	1.845128	2.706135	0.000073
H	4.111992	1.752509	-0.000395
H	4.458364	-0.696048	-0.000760
H	2.502295	-2.225848	-0.000637
S	-0.396144	-1.509953	-0.000084
C	-0.896596	2.048510	1.275927
H	-0.269379	2.940245	1.303635
H	-1.938946	2.359939	1.284301
H	-0.691134	1.454232	2.166546
C	-0.896953	2.048723	-1.275248
H	-1.939397	2.359848	-1.283439
H	-0.270011	2.940657	-1.302796
H	-0.691401	1.454725	-2.166034
O	-0.617402	-2.222191	1.240512
O	-0.617796	-2.221973	-1.240734
N	-2.648274	-0.261763	0.000339
N	-1.337862	-0.042993	0.000204
C	-0.578381	1.252433	0.000228
O	-3.361010	0.730061	0.000464

NO-1a (sp^3)

C	-0.932566	-0.728299	-0.017228
C	-1.061717	0.649635	-0.036856
C	-2.345722	1.187769	-0.029639
C	-3.444073	0.334963	-0.004711
C	-3.282566	-1.051729	0.010066
C	-2.009868	-1.604747	0.003267
C	0.228589	1.452488	-0.021230
H	-2.496339	2.259138	-0.046809
H	-4.441649	0.755855	-0.003000
H	-4.149929	-1.698827	0.021439
H	-1.862866	-2.676802	0.007739
N	1.275399	0.464334	-0.497864
S	0.754051	-1.228800	-0.002601
O	1.047633	-2.179219	-1.052525
O	1.210930	-1.496794	1.346034
N	2.547824	0.733903	-0.141135
O	3.294036	-0.223268	-0.115508
C	0.206877	2.610218	-1.026372
H	-0.540009	3.349016	-0.734922
H	1.179003	3.104041	-1.042754
H	-0.024545	2.251415	-2.029454
C	0.526530	1.958233	1.401119
H	1.452083	2.533309	1.413215
H	-0.287931	2.606217	1.726287
H	0.611119	1.132854	2.108360

Table SC1. Total energy values for the singlet in Scheme 1 calculated with B3LYP/6-311+G(2p,d) model chemistry.

Structure	SCF Energy (Hartree)	Thermal Correction (Hartree)	ZPE Correction (Hartree)
NO-1a with PCM (MeCN)	-1082.466148	-1082.266828	-1082.280440
NO-1b with PCM (MeCN)	-1082.464226	-1082.264849	-1082.278433
NO-1a (sp^3) with	-1082.456008	-1082.257089	-1082.270638

PCM (MeCN)			

3. Full Gaussian Citation

As stated previously in this SI document and in the communication text, a local development version of the GAUSSIAN suite of electronic structure programs was used for all calculations. The full citation for the program is:

M. J. Frisch, G. W. Trucks, H. B. Schlegel, G. E. Scuseria, M. A. Robb, J. R. Cheeseman, G. Scalmani, V. Barone, G. A. Petersson, H. Nakatsuji, X. Li, M. Caricato, A. V. Marenich, J. Bloino, B. G. Janesko, R. Gomperts, B. Mennucci, H. P. Hratchian, J. V. Ortiz, A. F. Izmaylov, J. L. Sonnenberg, D. Williams-Young, F. Ding, F. Lipparini, F. Egidi, J. Goings, B. Peng, A. Petrone, T. Henderson, D. Ranasinghe, V. G. Zakrzewski, J. Gao, N. Rega, G. Zheng, W. Liang, M. Hada, M. Ehara, K. Toyota, R. Fukuda, J. Hasegawa, M. Ishida, T. Nakajima, Y. Honda, O. Kitao, H. Nakai, T. Vreven, K. Throssell, J. A. Montgomery, Jr., J. E. Peralta, F. Ogliaro, M. J. Bearpark, J. J. Heyd, E. N. Brothers, K. N. Kudin, V. N. Staroverov, T. A. Keith, R. Kobayashi, J. Normand, K. Raghavachari, A. P. Rendell, J. C. Burant, S. S. Iyengar, J. Tomasi, M. Cossi, J. M. Millam, M. Klene, C. Adamo, R. Cammi, J. W. Ochterski, R. L. Martin, K. Morokuma, O. Farkas, J. B. Foresman, and D. J. Fox, GAUSSIAN, Development Version, Revision I.10+, Gaussian, Inc., Wallingford CT, 2016.

4. References

1. Hratchian, H. P.; Schlegel, H. B. Finding Minima, Transition States, and Following Reaction Pathways on Ab Initio Potential Energy Surfaces. In *Theory and Applications of Computational Chemistry*; Elsevier, 2005; pp 195–249.

2. Marenich, A. V.; Cramer, C. J.; Truhlar, D. G. Universal Solvation Model Based on Solute Electron Density and on a Continuum Model of the Solvent Defined by the Bulk Dielectric Constant and Atomic Surface Tensions. *J. Phys. Chem. B* **2009**, *113* (18), 6378–6396.

3. Becke, A. D. Density□functional Thermochemistry. III. The Role of Exact Exchange. *J. Chem. Phys.* **1993**, *98* (7), 5648–5652.

4. Wang, Y.; Perdew, J. P. Spin Scaling of the Electron-Gas Correlation Energy in the High-Density Limit. *Phys. Rev. B Condens. Matter* **1991**, *43* (11), 8911–8916.

A Versatile New Reagent for Nitrosation under Mild Conditions

Jordan D. Galloway[1], Cristian Sarabia[1], Hrant P. Hratchian[1], James C. Fettinger[2], and Ryan D. Baxter[1]*

[1]Department of Chemistry and Chemical Biology, University of California, Merced. Merced, California 95343, United States. [2]Department of Chemistry, University of California, Davis. Davis, California 95616.

Supporting Information

Experimental procedures, characterization data for reported compounds, and copies of NMR spectra

Table of Contents

General Considerations. Reagents and solvents were purchased and used without purification. Yields refer to homogenous material that is purified by silica-gel chromatography and spectroscopically pure (>95%) by ^{1}H NMR and 13C NMR. Yields in the Supporting Information describe the result of a single experiment, whereas the yields reported in Schemes 1–3 are an average of two or more experiments. Reactions were monitored by thin-layer chromatography using 0.25 mm E. Merck silica gel plates (60F-254). NMR spectra were recorded on a Varian-INOVA 400 Mhz or 500 Mhz spectrometer, calibrated using residual undeuterated solvent as an internal reference ($CDCl_3$ – ^{1}H NMR 7.26 ppm, ^{13}C NMR -77.16 ppm). The following abbreviations were used to explain multiplicities (s–singlet, d–doublet, t–triplet, q–quartet, m–multiplet).

Procedure for synthesis of NO-1.

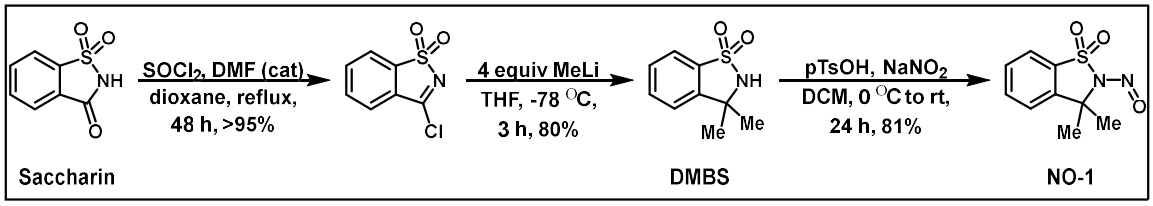

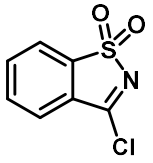

3-chlorobenzo[*d*]isothiazole 1,1-dioxide

3-chlorobenzo[d]isothiazole 1,1-dioxide. To a 500 mL round bottom with a stir bar atop a heating mantle 10.1 g (55 mmol) of saccharin, 10.0 mL (138 mmol) of $SOCl_2$, and a catalytic amount of DMF (1 ml) was added in 250 mL of 1,4-dioxane. The reaction was heated for 48 hours at reflux. The clear brown solution was concentrated in vacuo in a rotary evaporator in a heating bath. The residue was used in the next step without further purification. The data matches those previously reported.[1]

^{1}H NMR (500 MHz, $CDCl_3$): 7.93 (d, *J* = 7.3 Hz, 1H), 7.91 – 7.80 (m, 3H).
^{13}C NMR (125 MHz, $CDCl_3$): 166.3, 140.6, 135.1, 134.6, 129.9, 125.3, 122.6.

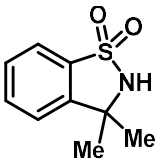

DMBS

3,3-dimethyl-2,3-dihydrobenzo[d]isothiazole 1,1-dioxide (DMBS). To a 250 mL round bottom 100 mL of dry diethyl ether was added to 11 g of **3-chlorobenzo[d]isothiazole 1,1-dioxide** (55 mmol). The reaction was cooled to -10 °C. Slowly added to the chilled solution was 4 equivalents of 1.6 M MeLi. The reaction was stirred for 30 min at -10 °C. The reaction was warmed to RT and allowed to stir for 2.5 h. Once reaction is complete pour into 150 mL of dilute HCL (5%). The organic layer was separated and washed with water until neutral. The crude reaction was absorbed onto silica and purified with EtOAc/Hexanes (50/50). R_f = 0.4. The product isolated as a pale yellow solid in 9.9 g (80% yield). The data matches those previously reported.[2]

^{1}H NMR (500 MHz, $CDCl_3$): 7.63 (d, *J* = 7.8 Hz, 1H), 7.57 – 7.52 (m, 1H), 7.44 – 7.38 (m, 1H), 7.34 (d, *J* = 7.8 Hz, 1H), 5.42 (s, 1H), 1.56 (s, 6H).
^{13}C NMR (125 MHz, $CDCl_3$): 146.0, 134.8, 133.3, 128.9, 122.8, 120.8, 60.8, 29.4.
HRMS (ESI-TOF): calcd for $C_9H_{11}NO_2S$ $[M+H]^+$ 198.0583 found 198.05074.

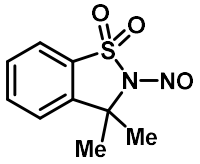

NO-1

3,3-dimethyl-2-nitroso-2,3-dihydrobenzo[d]isothiazole 1,1-dioxide (NO-1). To a large 1L round bottom 10 g (0.50 mol) of **DMBS** was added with 250 mL of DCM and 8.6 g (70 mmol) of *p*TsOH. The mixture was stirred and cooled to 0 °C. Slowly added was 5.0 g (72 mmol) $NaNO_2$. The reaction was left to warm to room temperature and stirred overnight. The was filtered through a Büchner funnel to remove the insoluble material. The filtrate was then absorbed onto silica and purified with column chromatography using DCM (Rf = 0.4) or 10% EtOAc in hexanes as the mobile phase. Isolated was 8.9 g (81% yield) of greenish yellow solid.
^{1}H NMR (500 MHz, $CDCl_3$): 7.88 – 7.75 (m, 2H), 7.64 (t, *J* = 7.7 Hz, 1H), 7.58 (d, *J* = 7.8 Hz, 1H), 1.99 (s, 6H).
^{13}C NMR (125 MHz, $CDCl_3$): 135.5, 130.3, 123.5, 122.0, 65.5, 29.6.
HRMS (ESI-TOF): calcd for $C_9H_{10}N_2O_3S$ $[M+H]^+$ 227.0485 found 227.0482.

Reaction Procedures.

[A] General Procedure for Nitrosation. The threads of a 3 mL borosilicate scintillation vial were thoroughly taped with Teflon tape. To this vial containing a stir bar was added substrate (0.2 mmol, 1 equiv), and **NO-1** (54.0 mg, 0.24 mmol, 1.2 equiv). Dichloromethane (2 mL) was then added and the reaction was stirred at room temperature until completed (thin-layer chromatography). In some reactions, heating is required (80 ºC) and dichloroethane (2 mL) or acetonitrile (2 mL) was used in replacement of dichloromethane.

Upon completion, the solvent was removed under reduced pressure, crude mixture was directly absorbed onto silica and purified by silica gel chromatography to yield the desired product.

[B] General Procedure for Acid Catalyzed Nitrosation. The threads of a 3 mL borosilicate scintillation vial were thoroughly taped with Teflon tape. To this vial containing a stir bar was added substrate (0.2 mmol, 1 equiv), and **NO-1** (54.0 mg, 0.24 mmol, 1.2 equiv). Acetonitrile (2 mL) and trifluoracetic acid (3.1 µL, 20 mol %) was then added and the reaction was stirred at room temperature until completed (thin-layer chromatography).

Upon completion, the solvent was removed under reduced pressure, crude mixture was directly absorbed onto silica and purified by silica gel chromatography to yield the desired product.

Scheme 1 Compounds (1–14)

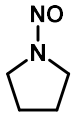

1

1-nitrosopyrrolidine (1). General procedure A was employed using pyrrolidine (17 µL, 0.2 mmol) in dichloromethane. The reaction afforded **1** (18.6 mg, 93% yield) as a pale yellow oil. The data matches those previously reported.[3]

^{1}H NMR (500 MHz, $CDCl_3$): 4.17 (t, *J* = 6.8 Hz, 1H), 3.48 (t, *J* = 7.1 Hz, 1H), 2.04 – 1.88 (m, 2H).
^{13}C NMR (125 MHz, $CDCl_3$): 49.7, 45.1, 23.9, 22.5.
HRMS (ESI-TOF): calcd for $C_4H_8N_2O$ $[M+H]^+$ 101.0709 found 101.0707.

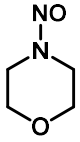

2

4-nitrosomorpholine (2). General procedure A was employed using morpholine (17 mg, 0.2 mmol). The reaction afforded **2** (21.1 mg, 91% yield) as a pale yellow oil. The data matches those previously reported.[3]

^{1}H NMR (500 MHz, $CDCl_3$): 4.33 – 4.25 (m, 1H), 3.92 – 3.83 (m, 2H), 3.65 (t, *J* = 5.2 Hz, 1H).
^{13}C NMR (125 MHz, $CDCl_3$): 67.4, 66.0, 50.1, 40.5.
HRMS (ESI-TOF): calcd for $C_4H_8N_2O_2$ $[M+H]^+$ 117.0659 found 117.0656.

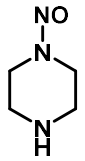

3

1-nitrosopiperazine (3). General procedure A was employed using piperazine (17 µL, 0.2 mmol). The reaction afforded **3** (22.5 mg, 98 % yield) as a pale yellow oil. The data matches those previously reported.[4]

^{1}H NMR (500 MHz, $CDCl_3$): 4.27 – 4.18 (m, 1H), 3.85 – 3.78 (m, 1H), 3.11 – 3.03 (m, 1H), 2.87 – 2.78 (m, 1H), 2.67 (s, 1H).
^{13}C NMR (125 MHz, $CDCl_3$): 51.1, 46.6, 45.1, 40.8.
HRMS (ESI-TOF): calcd for $C_4H_9N_3O$ $[M+H]^+$ 116.0818 found 116.0815.

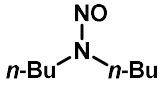

4

N,N-dibutylnitrous amide (4). General procedure A was employed using dibutylamine (36 µL, 0.2 mmol). The reaction afforded **4** (30.7 mg, 97 % yield) as a yellow oil. The data matches those previously reported.[3]

^{1}H NMR (500 MHz, $CDCl_3$): 4.06 (t, *J* = 7.3 Hz, 2H), 3.58 – 3.48 (m, 2H), 1.77 – 1.66 (m, 2H), 1.49 – 1.41 (m, 2H), 1.41 – 1.33 (m, 2H), 1.32 – 1.23 (m, 2H), 0.95 (t, *J* = 7.4 Hz, 3H), 0.90 (t, *J* = 7.3 Hz, 3H).
^{13}C NMR (125 MHz, $CDCl_3$): 52.1, 43.6, 30.4, 28.2, 20.5, 19.9, 13.8, 13.7.
HRMS (ESI-TOF): calcd for $C_{10}H_{11}NO_4$ $[M+H]^+$ 159.1492 found 159.1486.

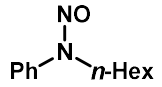

5

N-hexyl-N-phenylnitrous amide (5). General procedure A was employed using N-hexylaniline (40 µL, 0.2 mmol). The reaction afforded **5** (41.0 mg, 93 % yield) as a pale yellow oil.

^{1}H NMR (500 MHz, $CDCl_3$): 7.53 (d, J = 7.6 Hz, 2H), 7.47 (t, J = 7.4 Hz, 2H), 7.36 (t, J = 6.9 Hz, 1H), 4.08 – 3.95 (m, 2H), 1.54 (s, 2H), 1.27 (s, 6H), 0.86 (s, 3H).
^{13}C NMR (125 MHz, $CDCl_3$): 141.8, 129.6, 127.4, 119.8, 44.1, 31.4, 26.8, 26.6, 22.6, 14.1.

HRMS (ESI-TOF): calcd for $C_{12}H_{18}N_2O$ $[M+H]^+$ **207.1492** found 207.1491.

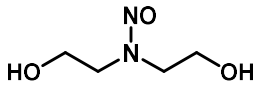

6

N,N-bis(2-hydroxyethyl)nitrous amide (6). General procedure A was employed using diethanolamine (19 µL, 0.2 mmol). The reaction afforded **6** (24.4 mg, 91 % yield) as a pale yellow oil. The data matches those previously reported.[3]

^{1}H NMR (500 MHz, $(CD_3)_2SO$): 4.92 (t, *J* = 5.5 Hz, 1H), 4.85 (t, *J* = 5.5 Hz, 1H), 4.18 (t, *J* = 5.6 Hz, 2H), 3.72 (q, *J* = 5.5 Hz, 2H), 3.66 (t, *J* = 6.0 Hz, 2H), 3.44 (q, *J* = 5.8 Hz, 2H).
^{13}C NMR (125 MHz, $(CD_3)_2SO$): 58.7, 56.8, 55.1, 46.5.
HRMS (ESI-TOF): calcd for $C_4H_{10}N_2O_3$ $[M+H]^+$ **135.0764** found 135.0797.

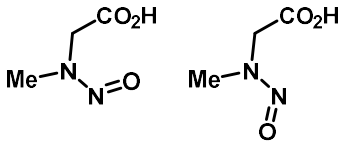

7 (cis) **7 (trans)**

N-methyl-N-nitrosoglycine (7). General procedure A was employed using Sarcosine (18 mg, 0.2 mmol) in dichloroethane. The reaction afforded **7(trans)** and **7(cis)** as a mixture of rotamers in a 1:1 ratio (21.2 mg, 90% yield) as a pale yellow oil.

(7 trans) and (7 cis)
^{1}H NMR (500 MHz, $CDCl_3$): 10.25 (s, 1H), 5.02 (s, 2H), 4.31 (s, 2H), 3.91 (s, 3H), 3.14 (s, 3H).
^{13}C NMR (125 MHz, $CDCl_3$): 172.6, 170.7, 54.4, 46.7, 40.1, 32.9.
HRMS (ESI-TOF): calcd for $C_3H_6N_2O_3$ $[M+H]^+$ 119.0451 found 119.0448.

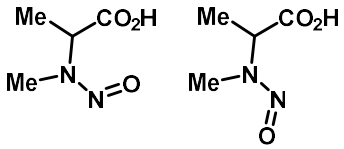

8 (cis) **8 (trans)**

N-methyl-N-nitrosoalanine. General procedure A was employed using DL-Alanine (21 mg, 0.2 mmol) in dichloroethane. The reaction afforded **8(trans)** and **8(cis)** as a mixture of rotamers in a 1:3 ratio (25.6 mg, 97% yield) as a pale yellow oil.

(8 trans) and (8 cis)
^{1}H NMR (500 MHz, $CDCl_3$): 11.70 (s, 1H), 5.47 (q, *J* = 7.0 Hz, 1H), 5.10 (q, *J* = 7.0 Hz, 1H), 3.81 (s, 3H), 3.05 (s, 3H), 1.71 (d, *J* = 7.1 Hz, 3H), 1.46 (d, *J* = 7.0 Hz, 3H).

^{13}C NMR (125 MHz, $CDCl_3$): 174.4, 173.5, 61.0, 52.0, 36.7, 30.3, 15.5, 12.9.
HRMS (ESI-TOF): calcd for $C_4H_8N_2O_3$ $[M+H]^+$ **133.0608** found 133.0604.

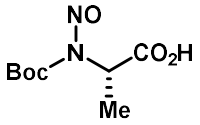

9

N-(tert-butoxycarbonyl)-N-nitroso-L-alanine (9). General procedure B was employed using Boc-Ala-OH (38 mg, 0.2 mmol). The reaction afforded **9** (31.8 mg, 73% yield) as a pale yellow oil.

^{1}H NMR (500 MHz, $CDCl_3$): 5.36 – 5.26 (m, 1H), 1.64 (s, 9H), 1.35 (d, *J* = 7.0 Hz, 3H).
^{13}C NMR (125 MHz, $CDCl_3$): 174.6, 151.1, 86.6, 47.9, 28.1, 13.8.
HRMS (ESI-TOF): calcd for $C_8H_{14}N_2O_5$ $[M+H]^+$ 219.0975 found 219.1006.

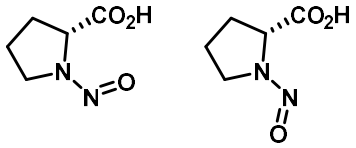

10 (cis) **10 (trans)**

nitroso-D-proline (10). General procedure A was employed using D-Proline (23 mg, 0.2 mmol) in dichlorethane. The reaction afforded **10 (trans)** and **10 (cis)** as a mixture of rotamers (28.2 mg, 98% yield) as a pale yellow oil.

^{1}H NMR (500 MHz, $CDCl_3$): 5.26 (dd, *J* = 8.6, 3.2 Hz, 1H), 4.49 – 4.38 (m, 3H), 4.31 (dt, *J* = 11.7, 6.6 Hz, 2H), 3.64 – 3.55 (m, 2H), 2.47 – 2.32 (m, 3H), 2.32 – 2.25 (m, 1H), 2.21 – 2.13 (m, 1H), 2.12 – 1.99 (m, 3H).
^{13}C NMR (125 MHz, $CDCl_3$): 243.0, 240.7, 132.9, 129.0, 120.9, 116.5, 99.5, 98.5, 93.8, 91.8.
HRMS (ESI-TOF): calcd for $C_5H_8N_2O_3$ $[M+H]^+$ 145.0608 found 145.0601.

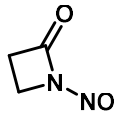

11

1-nitrosoazetidin-2-one (11). General procedure A was employed using 2-Azetidinone (16 mg, 0.2 mmol) in dicheloethane. The reaction afforded **11** (18.2 mg, 91% yield) as a yellow oil.

^{1}H NMR (400 MHz, $CDCl_3$): 3.65 (t, *J* = 5.9 Hz, 2H), 3.18 (t, *J* = 5.9 Hz, 2H).
^{13}C NMR (100 MHz, $CDCl_3$): 160.8, 40.7, 33.9.
HRMS (ESI-TOF): calcd for $C_3H_4N_2O_2$ $[M+H]^+$ 101.0346 found 101.0585.

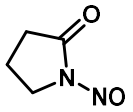

12

1-nitrosopyrrolidin-2-one (12). General procedure A was employed using 2-Pyrrolidinone (16 µL, 0.2 mmol) in dichloroethane. The reaction afforded **12** (21.4 mg, 94 % yield) as a pale yellow oil. The data matches those previously reported.[5]

^{1}H NMR (500 MHz, $CDCl_3$): 3.73 – 3.63 (m, 2H), 2.79 (t, *J* = 8.1 Hz, 2H), 2.25 – 2.09 (m, 2H).
^{13}C NMR (125 MHz, $CDCl_3$): 173.1, 42.7, 31.0, 15.9.
HRMS (ESI-TOF): calcd for $C_4H_6N_2O_2$ $[M+H]^+$ **115.0502** found 115.0499.

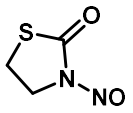

13

3-nitrosothiazolidin-2-one (13). General procedure B was employed using 1,3-thiazolidin-2-one (21 mg, 0.2 mmol). The reaction afforded **13** (20.6 mg, 78 % yield) as a pale yellow oil.

^{1}H NMR (500 MHz, $CDCl_3$): 4.00 (t, *J* = 7.3 Hz, 1H), 3.39 (t, *J* = 7.3 Hz, 1H).
^{13}C NMR (125 MHz, $CDCl_3$): 171.1, 43.0, 23.8.
HRMS (ESI-TOF): calcd for $C_{10}H_{11}NO_4$ $[M+H]^+$ 133.0066 found 133.0075.

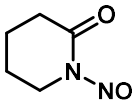

14

1-nitrosopiperidin-2-one (14). General procedure A was employed using δ-valerolactam (21 mg, 0.2 mmol) in dichloroethane. The reaction afforded **14** (23.8 mg, 93% yield) as a pale yellow oil. The data matches those previously reported.[5]

^{1}H NMR (500 MHz, $CDCl_3$): 3.60 – 3.47 (m, 1H), 2.86 – 2.74 (m, 1H), 1.92 – 1.81 (m, 2H).
^{13}C NMR (125 MHz, $CDCl_3$): 170.2, 43.6, 34.0, 21.4, 20.1.
HRMS (ESI-TOF): calcd for $C_5H_8N_2O_2$ $[M+H]^+$ 129.0659 found 129.0655.

Scheme 2 Compounds (15–36)

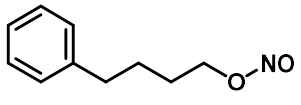

15

4-phenylbutyl nitrite (15). General procedure A was employed using 4-Phenyl-1-butanol (31 µL, 0.2 mmol) in dichloroethane. The reaction afforded **15** (28.6 mg, 80% yield) as a pale yellow oil. When general procedure B was employed (30.8 mg, 86% yield). The data matches those previously reported.[6]

^{1}H NMR (500 MHz, $CDCl_3$): 7.31 (t, *J* = 7.3 Hz, 2H), 7.25 – 7.15 (m, 3H), 4.73 (s, 2H), 2.68 (t, *J* = 7.3 Hz, 2H), 1.84 – 1.69 (m, 4H).
^{13}C NMR (125 MHz, $CDCl_3$): δ 141.9, 128.5, 128.5, 126.0, 68.3, 35.5, 28.7, 27.8.
HRMS (ESI-TOF): calcd for $C_{10}H_{13}NO_2$ $[M+H]^+$ 180.1019 found 180.1034.

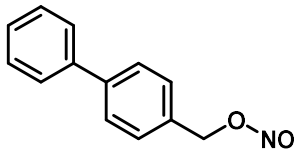

16

[1,1'-biphenyl]-4-ylmethyl nitrite (16). General procedure A was employed using Biphenyl-4-methanol (37 mg, 0.2 mmol) in dichloroethane. The reaction afforded **16** (41.8 mg, 98% yield) as a colorless solid. When general procedure B was employed (30.9 mg, 98% yield).

^{1}H NMR (400 MHz, $CDCl_3$): 7.61 (t, *J* = 7.4 Hz, 4H), 7.41 (qd, *J* = 14.9, 7.3 Hz, 5H), 5.76 (s, 2H).
^{13}C NMR (100 MHz, $CDCl_3$): 141.5, 140.5, 134.5, 128.8, 128.6, 127.6, 127.5, 127.1, 69.7.
HRMS (ESI-TOF): calcd for $C_{13}H_{11}NO_2$ $[M+H]^+$ 214.0863 found 214.0851.

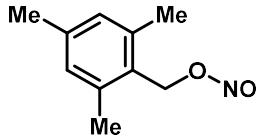

17

2,4,6-trimethylbenzyl nitrite (17). General procedure A was employed using 2,4,6-Trimethylbenzyl alcohol (30 mg, 0.2 mmol) in dichloroethane. The reaction afforded **17** (34.8 mg, 97% yield) as a colorless solid. When general procedure B was employed (34.6 mg, 98% yield). The data matches those previously reported.[7]

^{1}H NMR (400 MHz, $CDCl_3$): 6.91 (s, 2H), 5.72 (s, 2H), 2.34 (s, 6H), 2.30 (s, 3H).
^{13}C NMR (100 MHz, $CDCl_3$): 138.9, 138.2, 129.3, 128.4, 64.8, 21.2, 19.7.
HRMS (ESI-TOF): calcd for $C_{10}H_{13}NO_2$ $[M+H]^+$ 180.1019 found 180.1008.

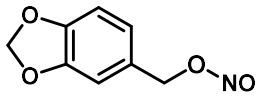

18

benzo[d][1,3]dioxol-5-ylmethyl nitrite (18). General procedure A was employed using Piperonyl alcohol (31 mg, 0.2 mmol) in dichloroethane. The reaction afforded **18** (29.2 mg, 81% yield) as a colorless oil. When general procedure B was employed (34.3 mg, 95% yield).

^{1}H NMR (500 MHz, $CDCl_3$): 6.86 – 6.73 (m, *J* = 7.7 Hz, 3H), 5.97 (s, 2H), 5.61 (s, 2H).
^{13}C NMR (125 MHz, $CDCl_3$): 148.1, 148.0, 129.4, 122.3, 109.0, 108.5, 101.4, 70.2.
HRMS (ESI-TOF): calcd for $C_8H_7NO_4$ $[M+H]^+$ 182.0448 found 182.0415

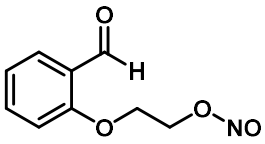

19

2-(2-formylphenoxy)ethyl nitrite (19). General procedure A was employed using 2-(2-Hydroxyethoxy)benzaldehyde (23 µL, 0.2 mmol) in acetonitrile. The reaction afforded **19** (28.7 mg, 74% yield) as a yellow oil. When general procedure B was employed (33.1 mg, 85% yield).

^{1}H NMR (400 MHz, $CDCl_3$): 10.42 (s, 1H), 7.84 (dd, *J* = 7.6, 1.5 Hz, 1H), 7.59 – 7.52 (m, 1H), 7.06 (t, J = 7.5 Hz, 1H), 6.97 (d, *J* = 8.4 Hz, 1H), 5.20 (s, 2H), 4.44 – 4.32 (m, 2H).
^{13}C NMR (100 MHz, $CDCl_3$): 189.6, 160.7, 136.1, 128.7, 125.2, 121.6, 112.5, 66.8, 66.3.
HRMS (ESI-TOF): calcd for $C_9H_9NO_4$ $[M+H]^+$ 196.0604 found 196.0581.

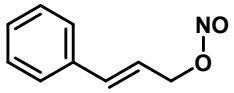

20

cinnamyl nitrite (20). General procedure A was employed using Cinnamyl alcohol (27 µL, 0.2 mmol) in dichloroethane. The reaction afforded **20** (11.7 mg, 36% yield) as a colorless oil. When general procedure B was employed (27.5 mg, 84% yield).

^{1}H NMR (500 MHz, $CDCl_3$): 7.40 (t, *J* = 9.3 Hz, 2H), 7.34 (dd, *J* = 16.5, 8.9 Hz, 2H), 7.31 – 7.26 (m, 1H), 6.69 (d, *J* = 15.9 Hz, 1H), 6.32 (dt, *J* = 15.7, 6.3 Hz, 1H), 5.35 (s, 2H).
^{13}C NMR (125 MHz, $CDCl_3$): 136.1, 134.9, 128.8, 128.4, 126.8, 122.8, 68.7.
HRMS (ESI-TOF): calcd for $C_9H_9NO_2$ $[M+H]^+$ 164.0706 found 164.0698.

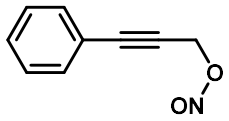

21

3-phenylprop-2-yn-1-yl nitrite (21). General procedure A was employed using 3-Phenyl-2-propyn-1-ol (27 µL, 0.2 mmol) in acetonitrile. The reaction afforded **21** (17.3 mg, 54% yield) as a colorless oil. When general procedure B was employed (19.8 mg, 62% yield).

^{1}H NMR (500 MHz, $CDCl_3$): 7.47 – 7.44 (m, 2H), 7.36 – 7.30 (m, 3H), 5.49 (s, 2H).
^{13}C NMR (125 MHz, $CDCl_3$): 132.0, 131.8, 129.0, 128.5, 122.1, 87.0, 51.9.
HRMS (ESI-TOF): calcd for $C_9H_7NO_2$ $[M+H]^+$ 162.0550 found 162.0548

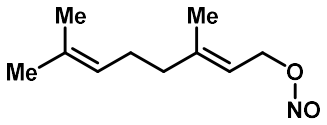

22

(*E*)-3,7-dimethylocta-2,6-dien-1-yl nitrite (22). General procedure A was employed using Geraniol (35 µL, 0.2 mmol) in dichloroethane. The reaction afforded **22** (32.1 mg, 88% yield) as a pale yellow oil. When general procedure B was employed (32.1 mg, 85% yield).

^{1}H NMR (500 MHz, $CDCl_3$): 5.37 (t, *J* = 6.5 Hz, 1H), 5.21 – 5.02 (m, *J* = 22.4, 16.7 Hz, 3), 2.17 – 1.99 (m, 4H), 1.74 (s, 3H), 1.68 (s, 3H), 1.60 (s, 3H).
^{13}C NMR (125 MHz, $CDCl_3$): 143.5, 132.1, 123.7, 117.6, 64.9, 39.7, 26.4, 25.8, 17.8, 16.7.
HRMS (ESI-TOF): calcd for $C_{10}H_{23}NO_3Si$ $[M+H]^+$ **184.1338** found 184.1322.

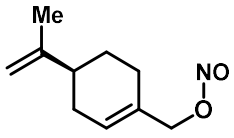

23

(S)-(4-(prop-1-en-2-yl)cyclohex-1-en-1-yl)methyl nitrite (23). General procedure A was employed using (S)-(−)-Perillyl alcohol (38 µL, 0.2 mmol) in dichloroethane. The reaction

afforded **23** (30.2 mg, 84% yield) as a pale yellow oil. When general procedure B was employed (18.7 mg, 52% yield).

^{1}H NMR (400 MHz, $CDCl_3$): 5.80 (s, 1H), 5.08 (s, 2H), 4.72 (d, *J* = 9.1 Hz, 2H), 2.21 – 1.95 (m, 4H), 1.90 – 1.81 (m, 1H), 1.74 (s, 3H), 1.55 – 1.44 (m, 1H).
^{13}C NMR (100 MHz, $CDCl_3$): 149.6, 132.5, 127.1, 109.0, 72.7, 40.9, 30.6, 27.4, 26.6, 20.9.
HRMS (ESI-TOF): calcd for $C_{10}H_{15}NO_2$ $[M+H]^+$ **182.1181** found 182.0698.

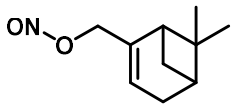

24

(6,6-dimethylbicyclo[3.1.1]hept-2-en-2-yl)methyl nitrite (24). General procedure A was employed using Myrtenol (38 µL, 0.2 mmol) in acetonitrile. The reaction afforded **24** (33.3 mg, 92% yield) as a pale yellow oil. When general procedure B was employed (34.3 mg, 95% yield).

^{1}H NMR (500 MHz, $CDCl_3$): 5.60 (s, 1H), 5.05 (s, 2H), 2.41 (dt, *J* = 8.7, 5.6 Hz, 1H), 2.29 (q, *J* = 18.1 Hz, 2H), 2.11 (d, *J* = 5.2 Hz, 2H), 1.28 (s, 3H), 1.18 (d, *J* = 8.7 Hz, 1H), 0.81 (s, 3H).
^{13}C NMR (125 MHz, $CDCl_3$): 142.9, 122.8, 71.3, 43.7, 40.8, 38.3, 31.6, 31.5, 26.2, 21.2.
HRMS (ESI-TOF): calcd for $C_{10}H_{15}NO_2$ $[M+H]^+$ **182.1171** found 182.1168.

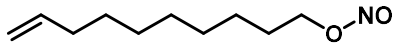

25

dec-9-en-1-yl nitrite (25). General procedure A was employed using 9-Decen-1-ol (36 µL, 0.2 mmol) in acetonitrile. The reaction afforded **25** (33.9 mg, 92% yield) as a pale yellow oil. When general procedure B was employed (35.5 mg, 96% yield).

^{1}H NMR (500 MHz, $CDCl_3$): 5.81 (ddt, *J* = 16.9, 10.1, 6.7 Hz, 1H), 4.99 (d, *J* = 17.1 Hz, 1H), 4.93 (d, *J* = 10.1 Hz, 1H), 4.69 (s, 2H), 2.04 (dd, *J* = 14.0, 6.9 Hz, 2H), 1.79–1.65 (m, 2H), 1.42–1.22 (m, 10H).
^{13}C NMR (125 MHz, $CDCl_3$): 139.3, 114.3, 114.3, 68.6, 33.9, 29.5, 29.3, 29.1, 29.0, 26.0.
HRMS (ESI-TOF): calcd for $C_{10}H_{19}NO_2$ $[M+H]^+$ **186.1494** found 186.1977.

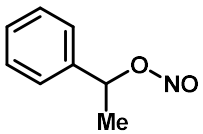

26

1-phenylethyl nitrite (26). General procedure A was employed using 1-Phenylethanol (25 µL, 0.2 mmol) in dichloroethane. The reaction afforded **26** (19.8 mg, 66% yield) as a pale yellow oil. When general procedure B was employed (20.8 mg, 69% yield).

^{1}H NMR (500 MHz, $CDCl_3$): 7.46 – 7.28 (m, 5H), 6.52 – 6.38 (m, 1H), 1.72 (d, *J* = 6.7 Hz, 3H).
^{13}C NMR (125 MHz, $CDCl_3$): 141.3, 128.7, 128.1, 126.2, 77.2, 22.2.
HRMS (ESI-TOF): calcd for $C_8H_9NO_2$ $[M+H]^+$ **152.0712** found 152.0699.

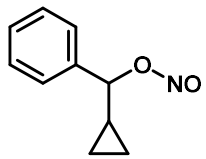

27

cyclopropyl(phenyl)methyl nitrite (27). General procedure A was employed using α-Cyclopropylbenzyl alcohol (29 µL, 0.2 mmol) in dichloroethane. The reaction afforded **27** (16.9 mg, 48% yield) as a pale yellow oil. When general procedure B was employed (13.7 mg, 39% yield).

^{1}H NMR (400 MHz, $CDCl_3$): 7.47 – 7.28 (m, 5H), 5.68 (d, *J* = 8.8 Hz, 1H), 1.54 – 1.41 (m, 1H), 0.75 – 0.68 (m, 2H), 0.52 (dt, *J* = 14.1, 9.2 Hz, 2H).
^{13}C NMR (100 MHz, $CDCl_3$): 140.0, 128.7, 128.3, 126.8, 85.7, 16.7, 4.5, 3.9.
HRMS (ESI-TOF): calcd for $C_{10}H_{11}NO_2$ $[M+H]^+$ 178.0863 found 178.0852.

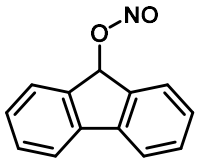

28

9H-fluoren-9-yl nitrite (28). General procedure A was employed using 9-Hydroxyfluorene (36 mg, 0.2 mmol) in dichloroethane. The reaction afforded **28** (28.8 mg, 68% yield) as a colorless solid. When general procedure B was employed (25.5 mg, 60% yield).

^{1}H NMR (500 MHz, $CDCl_3$): 7.71 (d, *J* = 7.5 Hz, 2H), 7.48–7.42 (m, 4H), 7.32 (t, *J* = 7.4 Hz, 2H), 7.27 (s, 1H).
^{13}C NMR (125 MHz, $CDCl_3$): 141.7, 141.0, 129.9, 128.1, 125.7, 120.4, 80.3.
HRMS (ESI-TOF): calcd for $C_{13}H_9NO_2$ $[M+H]^+$ 212.0712 found 212.0731.

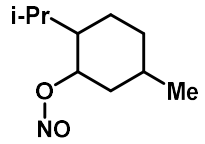

29

2-isopropyl-5-methylcyclohexyl nitrite (29). General procedure A was employed using (±)-menthol (31 mg, 0.2 mmol) in dichloroethane. The reaction afforded **29** (29.6 mg, 80% yield) as a pale yellow oil. When general procedure B was employed (35.5 mg, 96% yield). The data matches those previously reported.[8]

^{1}H NMR (400 MHz, $CDCl_3$): 5.37 – 5.14 (m, 1H), 2.09 – 1.95 (m, 1H), 1.88 – 1.70 (m, 3H), 1.69 – 1.53 (m, 1H), 1.53 – 1.41 (m, 1H), 1.29 – 1.11 (m, 2H), 1.04 – 0.83 (m, 7H), 0.77 (d, J = 6.9 Hz, 3H).
^{13}C NMR (100 MHz, $CDCl_3$): 80.1, 46.7, 42.2, 34.2, 31.9, 25.9, 23.6, 22.2, 20.9, 15.9.
HRMS (ESI-TOF): calcd for $C_{10}H_{19}NO_2$ $[M+H]^+$ 186.1489 found 186.1484.

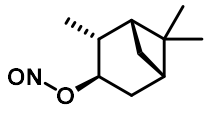

30

(1R,2R,3R,5S)-2,6,6-trimethylbicyclo[3.1.1]heptan-3-yl nitrite (30). General procedure A was employed using (1R,2R,3R,5S)-3-Pinanol (31 mg, 0.2 mmol) in dichloroethane. The reaction afforded **30** (28.4 mg, 78% yield) as a pale yellow oil. When general procedure B was employed (33.2 mg, 91% yield).

^{1}H NMR (500 MHz, $CDCl_3$): 5.69 (s, 1H), 2.71 – 2.57 (m, 1H), 2.46 – 2.36 (m, 1H), 2.22 – 2.12 (m, 1H), 2.04 – 1.95 (m, 1H), 1.93 – 1.88 (m, 1H), 1.88 – 1.81 (m, 1H), 1.27 (s, 3H), 1.14 (d, *J* = 7.4 Hz, 3H), 1.08 – 1.01 (m, 3H).
^{13}C NMR (125 MHz, $CDCl_3$): 79.3, 47.5, 43.8, 41.4, 38.7, 35.9, 33.9, 27.6, 24.0, 20.1.
HRMS (ESI-TOF): calcd for $C_{10}H_{17}NO_2$ $[M+H]^+$ **184.1332** found 184.1326.

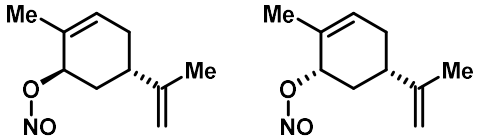

31 (trans) 31 (cis)

(1R,5S)-2-methyl-5-(prop-1-en-2-yl)cyclohex-2-en-1-yl nitrite (31 trans) and (1S,5S)-2-methyl-5-(prop-1-en-2-yl)cyclohex-2-en-1-yl nitrite (31 cis). General procedure A was employed using (-)-carveol (32 µL, 0.2 mmol) in dichloroethane. The reaction afforded **31 (trans)** and **31 (cis)** as

a mixture of rotamers in a 1:1.25 (trans:cis) ratio (27.1 mg, 75% yield) as a pale yellow oil. When general procedure B was employed (33.0 mg, 91% yield).

(31 trans) and (31 cis)
^{1}H NMR (500 MHz, $CDCl_3$): 6.06 – 5.95 (m, 1H), 5.83 – 5.79 (m, 1H), 5.77 (s, 1H), 5.73 – 5.65 (m, 1H), 4.78 – 4.69 (m, 4H), 2.52 – 2.41 (m, 1H), 2.35 – 2.11 (m, 5H), 2.06 – 1.99 (m, 2H), 1.95 – 1.88 (m, 2H), 1.79 – 1.67 (m, 11H), 1.61 (s, 3H).
^{13}C NMR (125 MHz, $CDCl_3$): 148.7, 148.2, 132.4, 123.0, 128.9, 127.0, 109.7, 109.5, 40.8, 35.7, 35.2, 35.0, 30.9, 30.9, 21.0, 20.6, 20.6, 19.3.
HRMS (ESI-TOF): calcd for $C_{10}H_{15}NO_2$ $[M+H]^+$ 182.1176 found 182.1167.

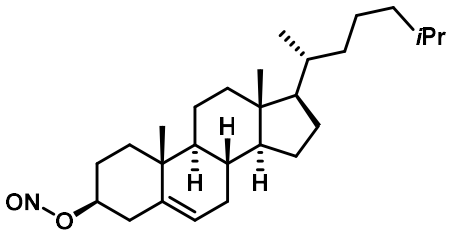

32

(3S,8S,9S,10R,13R,14S,17R)-10,13-dimethyl-17-((R)-6-methylheptan-2-yl)-2,3,4,7,8,9,10,11,12,13,14,15,16,17-tetradecahydro-1H-cyclopenta[a]phenanthren-3-yl nitrite (32). General procedure A was employed using 3β-Hydroxy-5-cholestene (83 mg, 0.2 mmol) in acetonitrile. The reaction afforded **32** (69.0 mg, 83% yield) as a white solid. When general procedure B was employed (70.6 mg, 85% yield).

^{1}H NMR (500 MHz, $CDCl_3$): 5.49 – 5.42 (m, 1H), 5.29 – 5.19 (m, 1H), 2.52 (t, J = 11.6 Hz, 1H), 2.41 (dd, J = 13.1, 3.3 Hz, 1H), 2.09 – 1.92 (m, 4H), 1.90 – 1.68 (m, 3H), 1.65 – 1.45 (m, 6H), 1.43 – 1.24 (m, 6H), 1.23 – 0.98 (m, 12H), 0.93 (d, J = 6.5 Hz, 3H), 0.88 (dd, J = 6.5, 1.9 Hz, 6H), 0.70 (s, 3H).
^{13}C NMR (125 MHz, $CDCl_3$): 139.6, 123.2, 79.6, 56.9, 56.3, 50.3, 42.5, 39.9, 39.7, 38.9, 37.3, 36.8, 36.4, 36.0, 32.1, 32.0, 28.5, 28.4, 28.2, 24.5, 24.0, 23.0, 22.7, 21.2, 19.5, 18.9, 12.0.
HRMS (ESI-TOF): calcd for $C_{27}H_{47}NO_2$ $[M+H]^+$ 416.3523 found 416.3260.

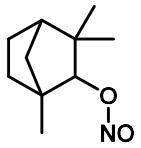

33

1,3,3-trimethylbicyclo[2.2.1]heptan-2-yl nitrite (33). General procedure B was employed using Fenchyl alcohol (32 mg, 0.2 mmol). The reaction afforded **33** (19.4 mg, 53% yield) as a pale yellow oil.

^{1}H NMR (500 MHz, $CDCl_3$): 4.93 (s, 1H), 1.81 (d, J = 3.0 Hz, 1H), 1.70 (d, J = 10.8 Hz, 2H), 1.65 – 1.57 (m, 1H), 1.53 – 1.44 (m, 1H), 1.29 (d, J = 10.6 Hz, 1H), 1.13 (s, 3H), 1.06 (s, 3H), 0.73 (s, 3H).
^{13}C NMR (125 MHz, $CDCl_3$): 91.3, 48.7, 48.3, 41.8, 40.3, 30.3, 26.7, 26.0, 21.2, 19.2.
HRMS (ESI-TOF): calcd for $C_{10}H_{17}NO_2$ $[M+H]^+$ **184.1332** found 184.1326.

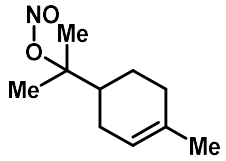

34

(R)-2-(4-methylcyclohex-3-en-1-yl)propan-2-yl nitrite (34). General procedure B was employed using α-Terpineol (33 μL, 0.2 mmol). The reaction afforded **34** (23.0 mg, 63% yield) as a teal oil. ***34** consistently appeared to decompose into an unknown compound during characterization. Tabulated data reflects desired product.

^{1}H NMR (500 MHz, $CDCl_3$): 5.39 (s,1), 2.10 – 1.75 (m, 5H), 1.66 (s, 3H), 1.57 (d, J = 5.9 Hz, 6H).
^{13}C NMR (125 MHz, $CDCl_3$): 134.3, 120.2, 87.2, 44.0, 30.9, 26.7, 25.4, 24.4, 24.0, 23.4.
HRMS (ESI-TOF): calcd for $C_{10}H_{17}NO_2$ $[M+H]^+$ **184.2585** found 183.1291.

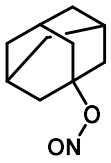

35

adamantan-1-yl nitrite (35). General procedure A was employed using 1-Adamantanol (31 mg, 0.2 mmol) in acetonitrile. The reaction afforded **35** (19.2 mg, 53 % yield) as a colorless solid. When general procedure B was employed (22.8 mg, 63% yield).

^{1}H NMR (500 MHz, $CDCl_3$): 2.29 (s, 3H), 2.13 (s, 6H), 1.76 (s, 6H).
^{13}C NMR (125 MHz, $CDCl_3$): 82.3, 42.9, 36.2, 30.9.
HRMS (ESI-TOF): calcd for $C_{10}H_{15}NO_2$ $[M+H]^+$ **182.1176** found 182.1168.

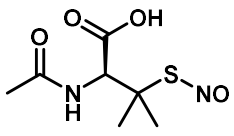

36

S-nitroso-N-acetylpenicillamine (36). General procedure B was employed using N-Acetyl-D-penicillamine (38 mg, 0.2 mmol). The reaction afforded **36** (31.7 mg, 72 % yield) as a blue solid. The data matches those previously reported.[9]

^{1}H NMR (500 MHz, $(CD_3)_2SO$): 13.17 (bs, 1H), 8.51 (d, J = 9.5 Hz, 1H), 5.17 (d, J = 9.5 Hz, 1H), 3.39 (bs, 1H), 1.97 (s, 3H), 1.94 (s, 3H), 1.87 (s, 3H).
^{13}C NMR (125 MHz, $(CD_3)_2SO$): 170.9, 169.6, 59.2, 58.4, 26.3, 25.3, 22.2.
HRMS (ESI-TOF): calcd for $C_7H_{12}N_2O_4S$ $[M+H]^+$ 221.0591 found 221.0585.

Procedure for synthesis of ^{15}N-labeled NO-1.

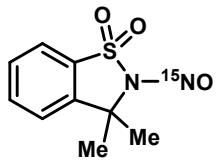

(NO-1)-^{15}N Labeled

3,3-dimethyl-2-[nitroso-^{15}N]-2,3-dihydrobenzo[d]isothiazole 1,1-dioxide (NO-1). To a large 1L round bottom 986.3 mg (5 mmol) of **DMBS** was added with 10 mL of DCM and 1.3 g (7.0 mmol) of *p*TsOH. The mixture was stirred and cooled to 0 °C. Slowly added was 500.0 mg (7.14 mmol) $NaNO_2$. The reaction was left to warm to room temperature and stirred overnight. The was filtered through a Büchner funnel to remove the insoluble material. The filtrate was then absorbed onto silica and purified with column chromatography using DCM (Rf = 0.4) or 10% EtOAc in hexanes as the mobile phase. Isolated was 886.2 mg (78% yield) of greenish yellow solid.
^{1}H NMR (500 MHz, $CDCl_3$): 7.89 – 7.77 (m, 2H), 7.64 (t, *J* = 7.6 Hz, 1H), 7.53 (d, *J* = 7.9 Hz, 1H), 2.00 (s, 6H).
^{13}C NMR (125 MHz, $CDCl_3$): 139.6, 135.4, 131.6, 130.3, 123.4, 122.3, 65.5, 29.8.
HRMS (ESI-TOF): calcd for $C_9H_{10}N^{15}NO_3S$ $[M+H]^+$ 228.0455 found 228.0446.

Scheme 3 Compounds (37–39)

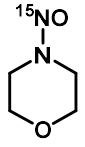

37

4-nitrosomorpholine (37). General procedure A was employed using morpholine (17 mg, 0.2 mmol) in dichloromethane. The reaction afforded **37** (22.9 mg, 98% yield) as a pale yellow oil.

^{1}H NMR (500 MHz, $CDCl_3$): 4.32 – 4.24 (m, 1H), 3.90 – 3.86 (m, 1H), 3.86 – 3.82 (m, 1H), 3.68 – 3.61 (m, 1H).
^{13}C NMR (125 MHz, $CDCl_3$): 67.4 (s), 66.0 (s), 50.0 (d, *J* = 6.0 Hz), 40.4 (d, *J* = 1.8 Hz).

HRMS (ESI-TOF): calcd for $C_4H_8N^{15}NO_2$ $[M+H]^+$ 118.0629 found 118.0631.

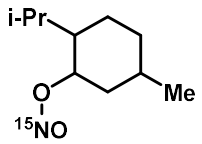

38

^{15}N-labeled 2-isopropyl-5-methylcyclohexyl nitrite (38). General procedure A was employed using (±)-menthol (31 mg, 0.2 mmol) in dichloroethane. The reaction afforded **38** (29.8 mg, 81% yield) as a pale yellow oil.

^{1}H NMR (500 MHz, $CDCl_3$): 5.36 – 5.16 (m, 1H), 2.02 (d, J = 11.6 Hz, 1H), 1.90 – 1.69 (m, 3H), 1.69 – 1.54 (m, 1H), 1.48 (t, J = 11.6 Hz, 1H), 1.28 – 1.14 (m, 2H), 1.02 – 0.84 (m, 7H), 0.77 (d, J = 6.8 Hz, 3H).
^{13}C NMR (125 MHz, $CDCl_3$): 80.1, 46.7, 42.2, 34.2, 31.9, 25.9, 23.6, 22.2, 20.9, 15.9.
HRMS (ESI-TOF): calcd for $C_{10}H_{19}{}^{15}NO_2$ $[M+H]^+$ 187.1459 found 187.1451.

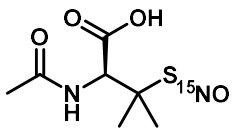

39

S-[nitroso-^{15}N]-N-acetylpenicillamine (39). General procedure B was employed using N-Acetyl-D-penicillamine (38 mg, 0.2 mmol). The reaction afforded **39** (31.7 mg, 72% yield) as a blue solid.

^{1}H NMR (500 MHz, DMSO): 13.10 (s, 1H), 8.50 (d, *J* = 9.5 Hz, 1H), 5.16 (d, *J* = 9.5 Hz, 1H), 1.97 (s, 3H), 1.94 (s, 3H), 1.87 (s, 3H).
^{13}C NMR (125 MHz, DMSO): 170.8, 170.0, 59.1, 58.3, 26.2, 25.2, 22.2.
HRMS (ESI-TOF): calcd for $C_7H_{12}N^{15}NO_4S$ $[M+H]^+$ 222.0561 found 222.0563.

References

[1] Helberg, J.; Ampßler, T.; Zipse, H. Pyridinyl Amide Ion Pairs As Lewis Base Organocatalysts. *J. Org. Chem.* **2020**, *85*, 5390–5402.

[2] Porter, N. A.; Carter, R. L.; Mero, C. L.; Roepel, M. G.; Curran, D. P. Penultimate Group Effects in Free Radical Telomerizations of Acrylamides. *Tetrahedron* **1996**, *52*, 4181–4198.

[3] Zhang, J.; Jiang, J.; Li, Y.; Wan, X. Iodide-Catalyzed Synthesis of N-Nitrosamines via C–N Cleavage of Nitromethane. *J. Org. Chem* **2013**, *78*, 11366–11372.

[4] Cochrane, S. A.; Li, X.; He, S.; Yu, M.; Wu, M.; Vederas, J. C. Synthesis of Tridecaptin–Antibiotic Conjugates with in Vivo Activity against Gram-Negative Bacteria. *Journal of Medicinal Chemistry* **2015**, *58* (24), 9779–9785.

[5] Torra, N.; Urpí, F.; Vilarrasa, J. N-Nitrosation and N-Nitration of Lactams. From Macrolactams to Macrolactones. *Tetrahedron* **1989**, *45*, 863–868.

[6] Doyle, M. P.; Zuidema, L. J.; Bade, T. R. Cyclic Ether Formation in Oxidations of Primary Alcohols by Cerium(IV). Reactions of 5-Phenyl-1-Pentanol, 4-Phenyl-1-Butanol, and 3-Phenyl-1-Propanol with Ceric Ammonium Nitrate. *J. Org. Chem.* **1975**, *40*, 1454–1456.

[7] Suzuki, H.; Nakano, K.; Mishina, T.; Hanafusa, T. *Nip. Kag. Kai.* **1978**, *7*, 1049–1052.

[8] Holan, M.; Jahn, U. Anaerobic Nitroxide-Catalyzed Oxidation of Alcohols Using the NO+/NO· Redox Pair. *Org. Lett.* **2013**, *16*, 58–61.

[9] Roy, B.; D'hardemare, A. D. M.; Fontecave, M. New Thionitrites: Synthesis, Stability, and Nitric Oxide Generation. *J. Org. Chem* **1994**, *59*, 7019–7026.

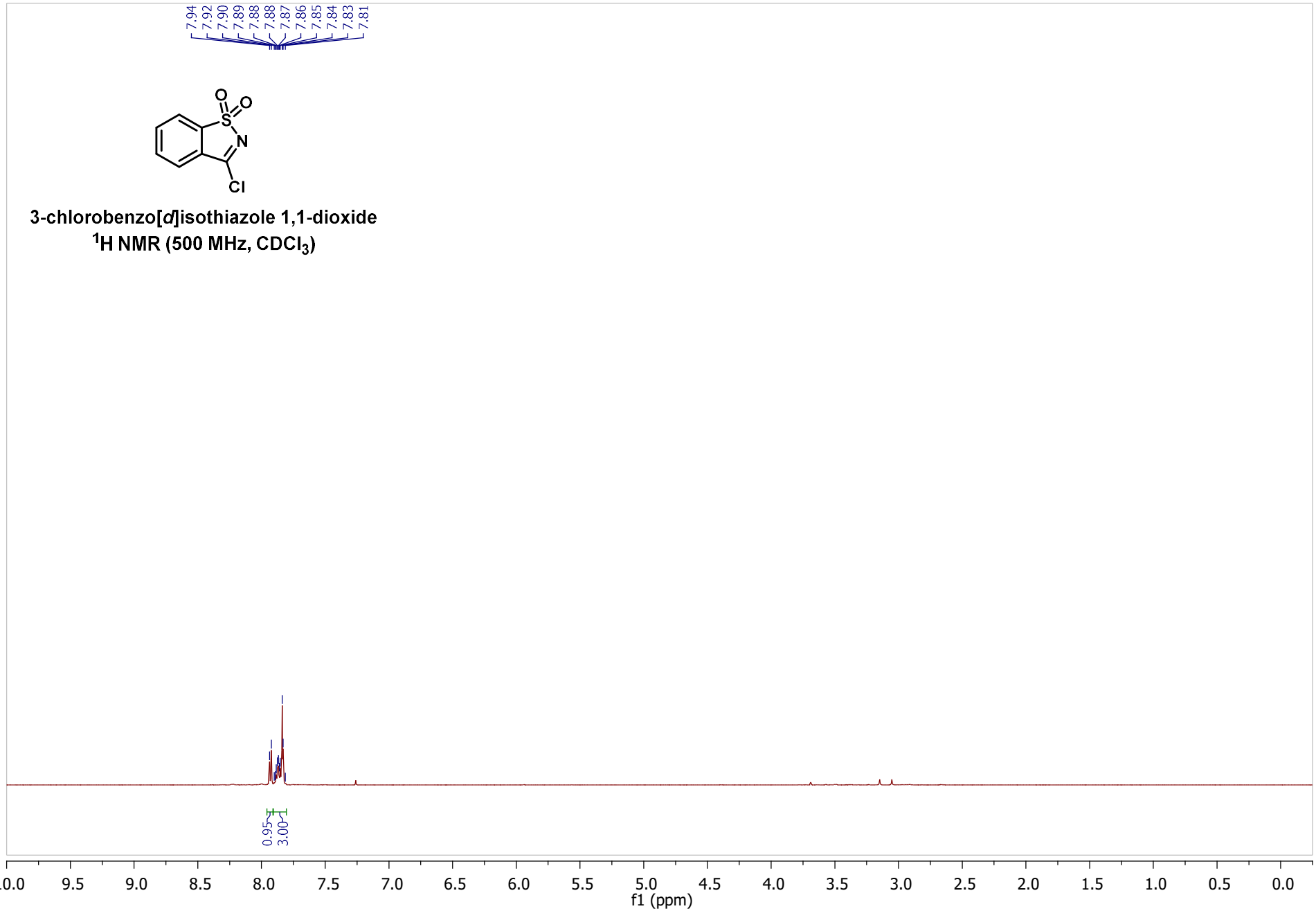

3-chlorobenzo[*d*]isothiazole 1,1-dioxide
^{1}H NMR (500 MHz, $CDCl_3$)

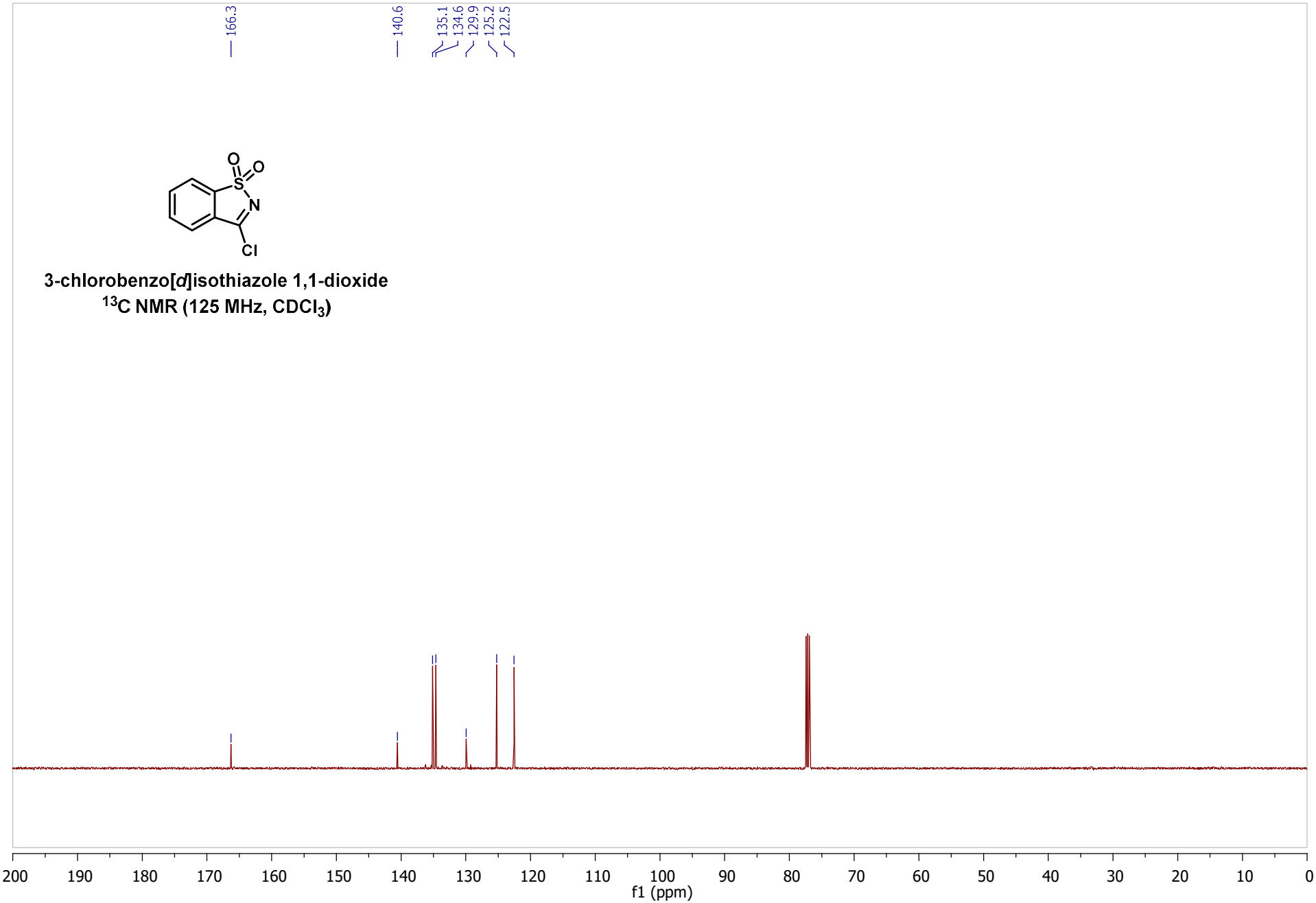

3-chlorobenzo[*d*]isothiazole 1,1-dioxide

^{13}C NMR (125 MHz, $CDCl_3$)

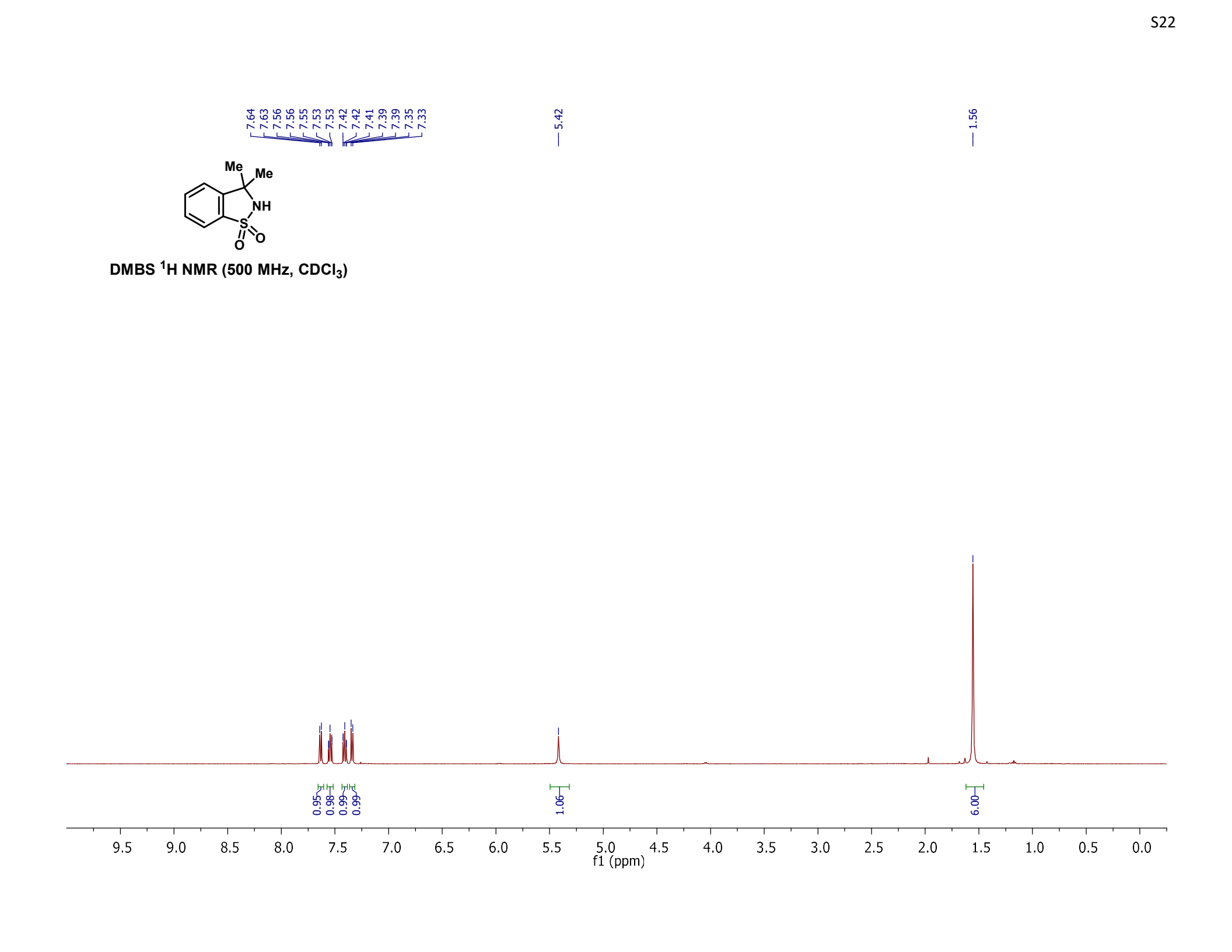

DMBS ^{1}H NMR (500 MHz, $CDCl_3$)

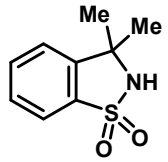

DMBS ^{13}C NMR (125 MHz, $CDCl_3$)

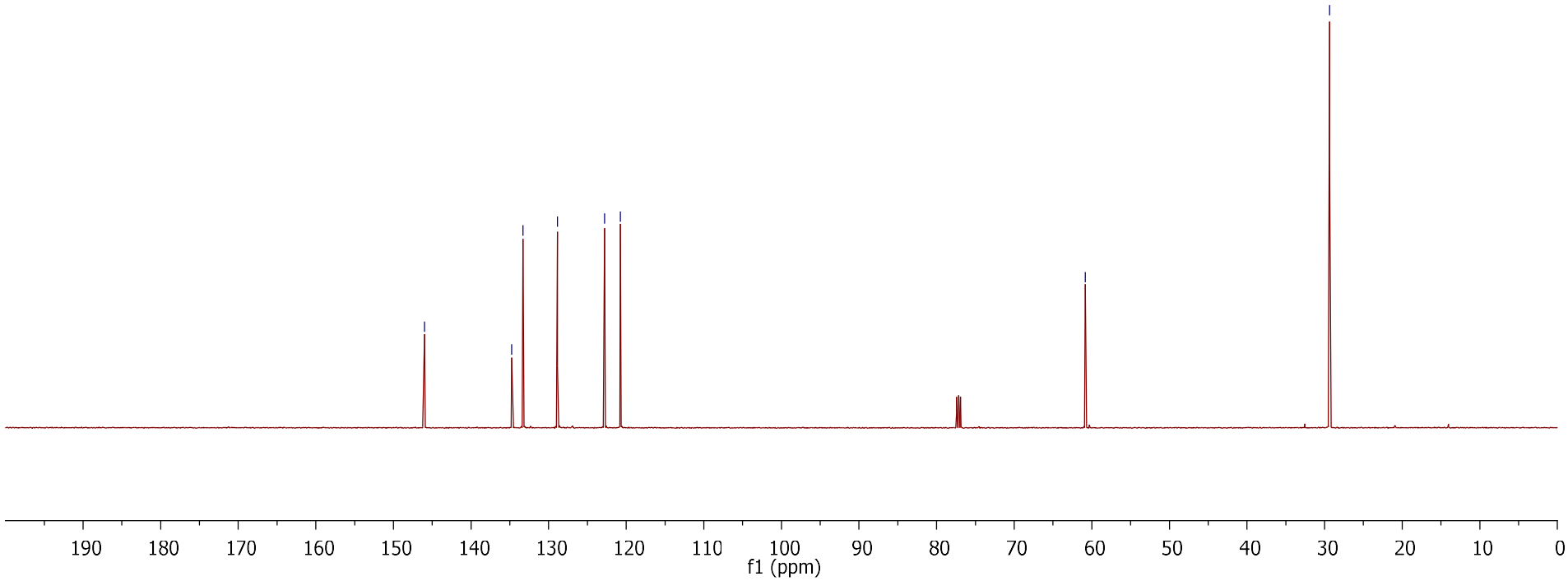

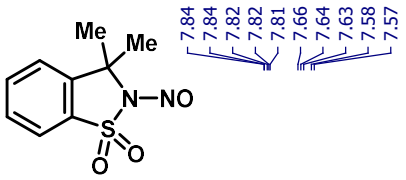

NO-1 ^{1}H NMR (500 MHz, $CDCl_3$)

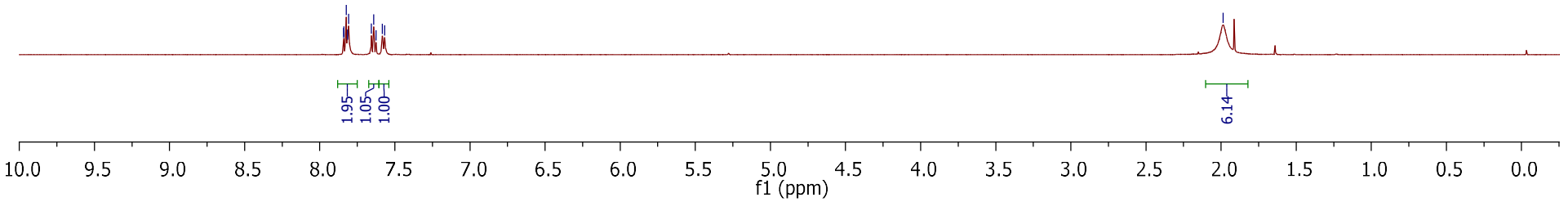

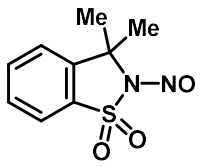

NO-1 ^{13}C NMR (125 MHz, $CDCl_3$)

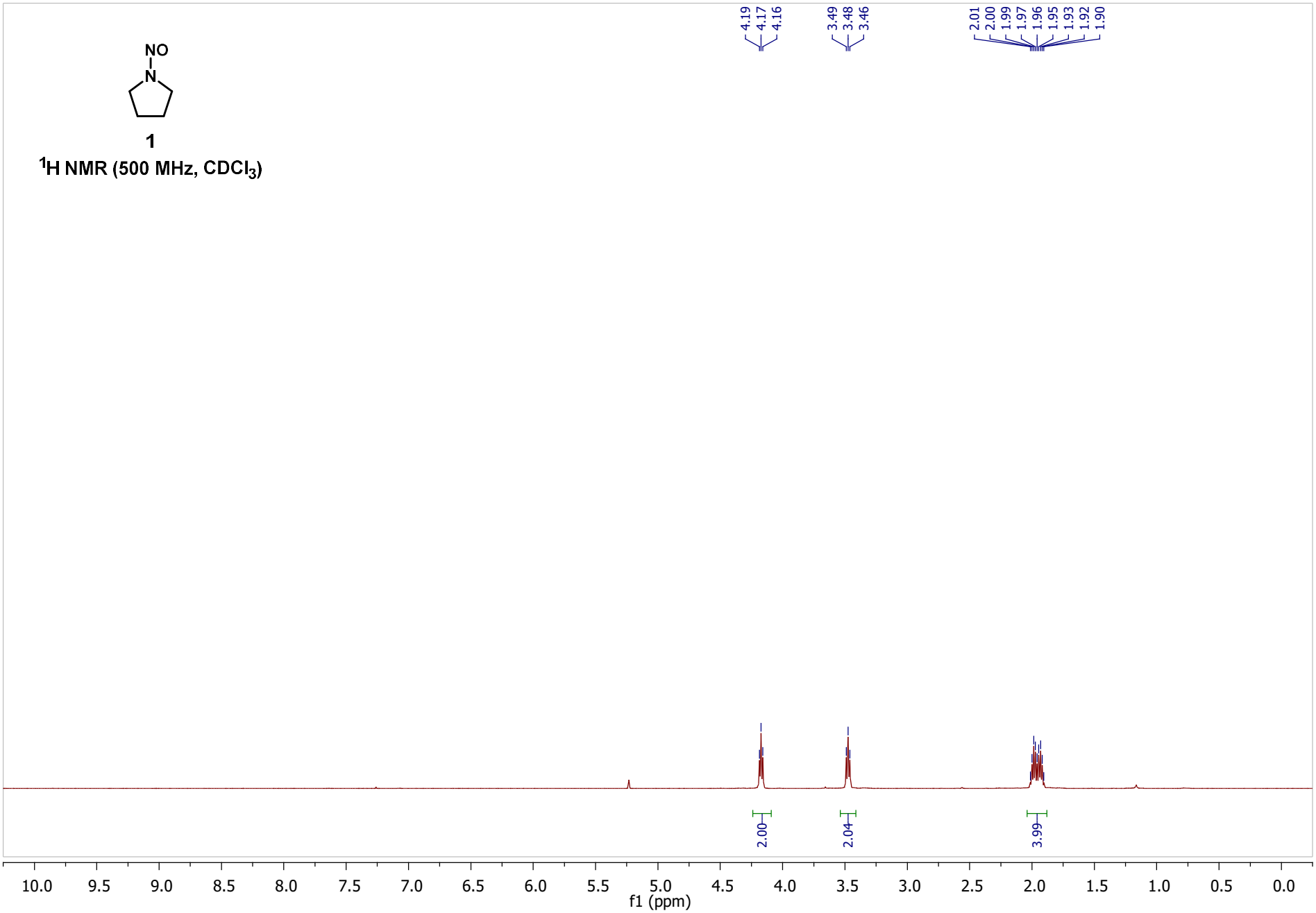
NO
N
1
1H NMR (500 MHz, CDCl3)
4.19
4.17
4.16
3.49
3.48
3.46
2.01
2.00
1.99
1.97
1.96
1.95
1.93
1.92
1.90
2.00
2.04
3.99
10.0
9.5
9.0
8.5
8.0
7.5
7.0
6.5
6.0
5.5
5.0
4.5
4.0
3.5
3.0
2.5
2.0
1.5
1.0
0.5
0.0
f1 (ppm)

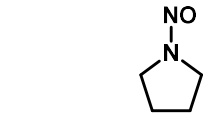

1

^{13}C NMR (125 MHz, $CDCl_3$)

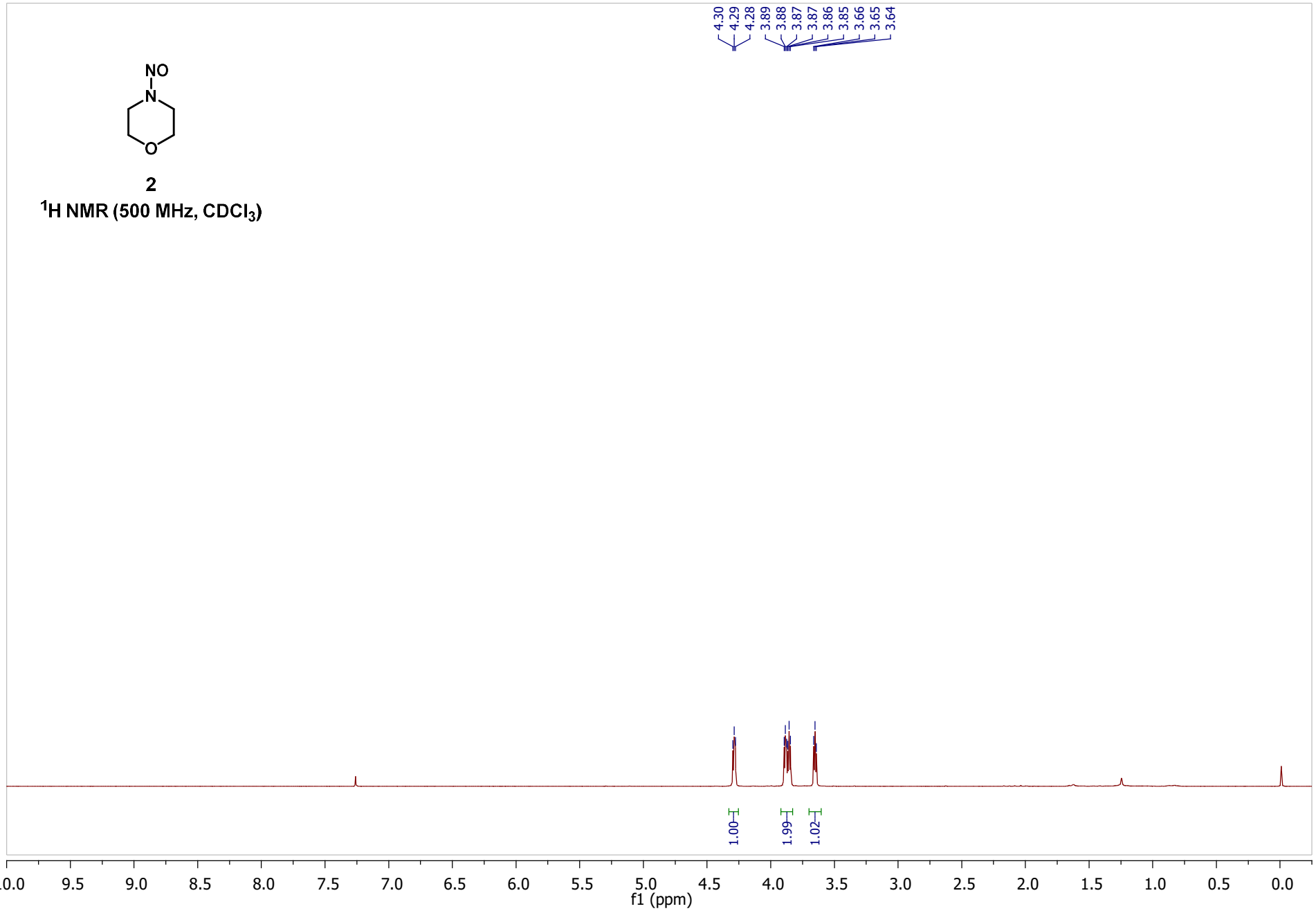
NO
N
O
2
1H NMR (500 MHz, CDCl3)
4.30
4.29
4.28
3.89
3.88
3.87
3.87
3.86
3.85
3.66
3.65
3.64
1.00
1.99
1.02
10.0
9.5
9.0
8.5
8.0
7.5
7.0
6.5
6.0
5.5
5.0
4.5
4.0
3.5
3.0
2.5
2.0
1.5
1.0
0.5
0.0
f1 (ppm)

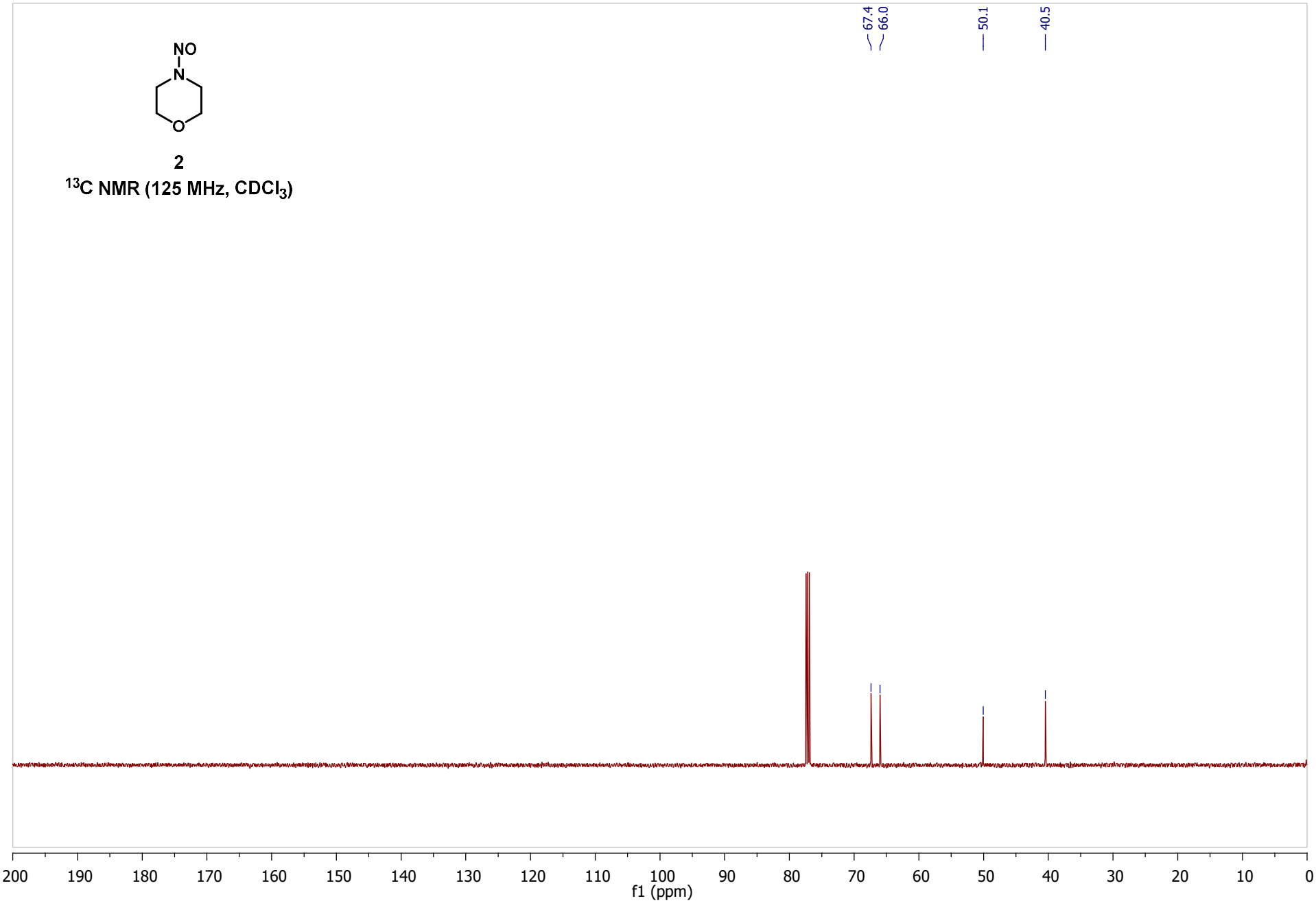
NO
N
O
2
13C NMR (125 MHz, CDCl3)
67.4
66.0
50.1
40.5
200
190
180
170
160
150
140
130
120
110
100
90
80
70
60
50
40
30
20
10
0
f1 (ppm)

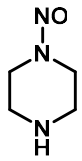

3

^{1}H NMR (500 MHz, $CDCl_3$)

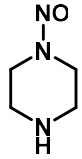

3

^{13}C NMR (125 MHz, $CDCl_3$)

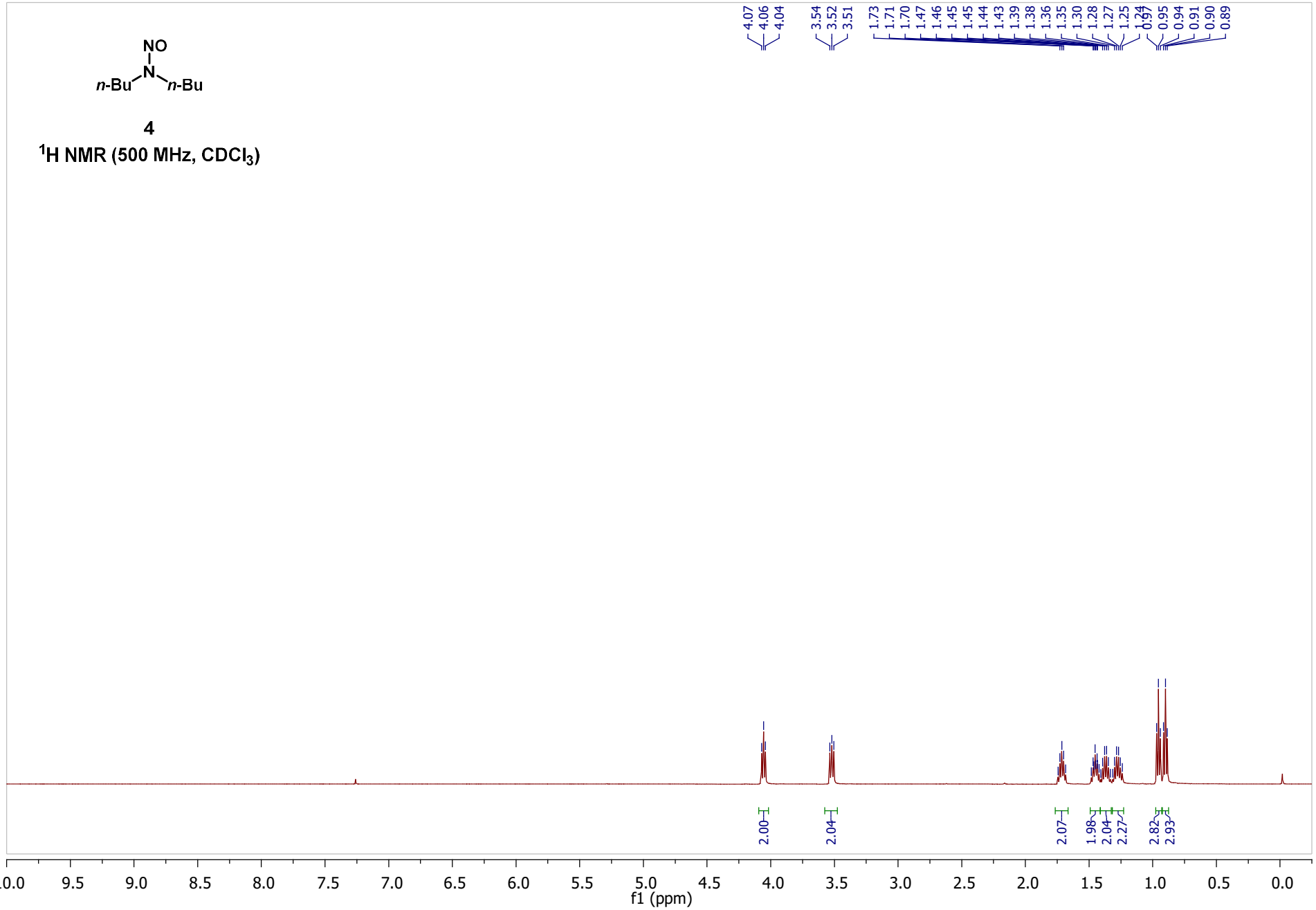
NO
N
n-Bu
n-Bu
4
1H NMR (500 MHz, CDCl3)
4.07
4.06
4.04
3.54
3.52
3.51
1.73
1.71
1.70
1.47
1.46
1.45
1.45
1.44
1.43
1.39
1.38
1.36
1.35
1.30
1.28
1.27
1.25
0.97
0.95
0.94
0.91
0.90
0.89
2.00
2.04
2.07
1.98
2.04
2.27
2.82
2.93
10.0
9.5
9.0
8.5
8.0
7.5
7.0
6.5
6.0
5.5
5.0
4.5
4.0
3.5
3.0
2.5
2.0
1.5
1.0
0.5
0.0
f1 (ppm)

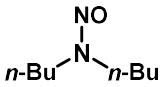

4

^{13}C NMR (125 MHz, $CDCl_3$)

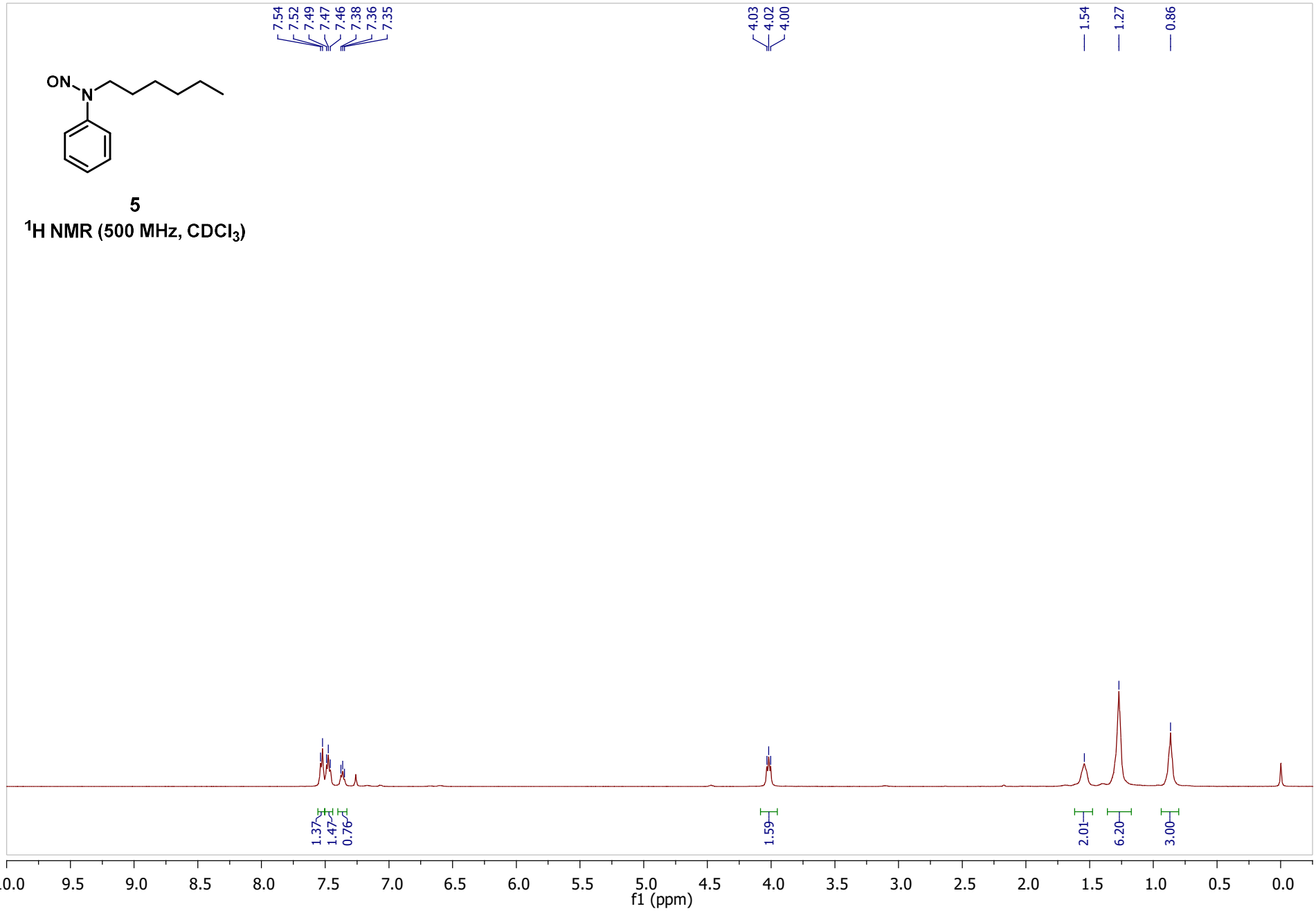

5

^{1}H NMR (500 MHz, $CDCl_3$)

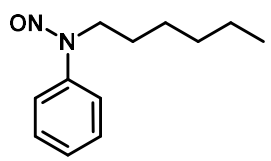

5

^{13}C NMR (125 MHz, $CDCl_3$)

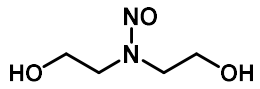

6

^{1}H NMR (500 MHz, $(CD_3)_2SO$)

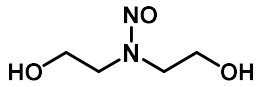

6

^{13}C NMR (125 MHz, $(CD_3)_2SO$)

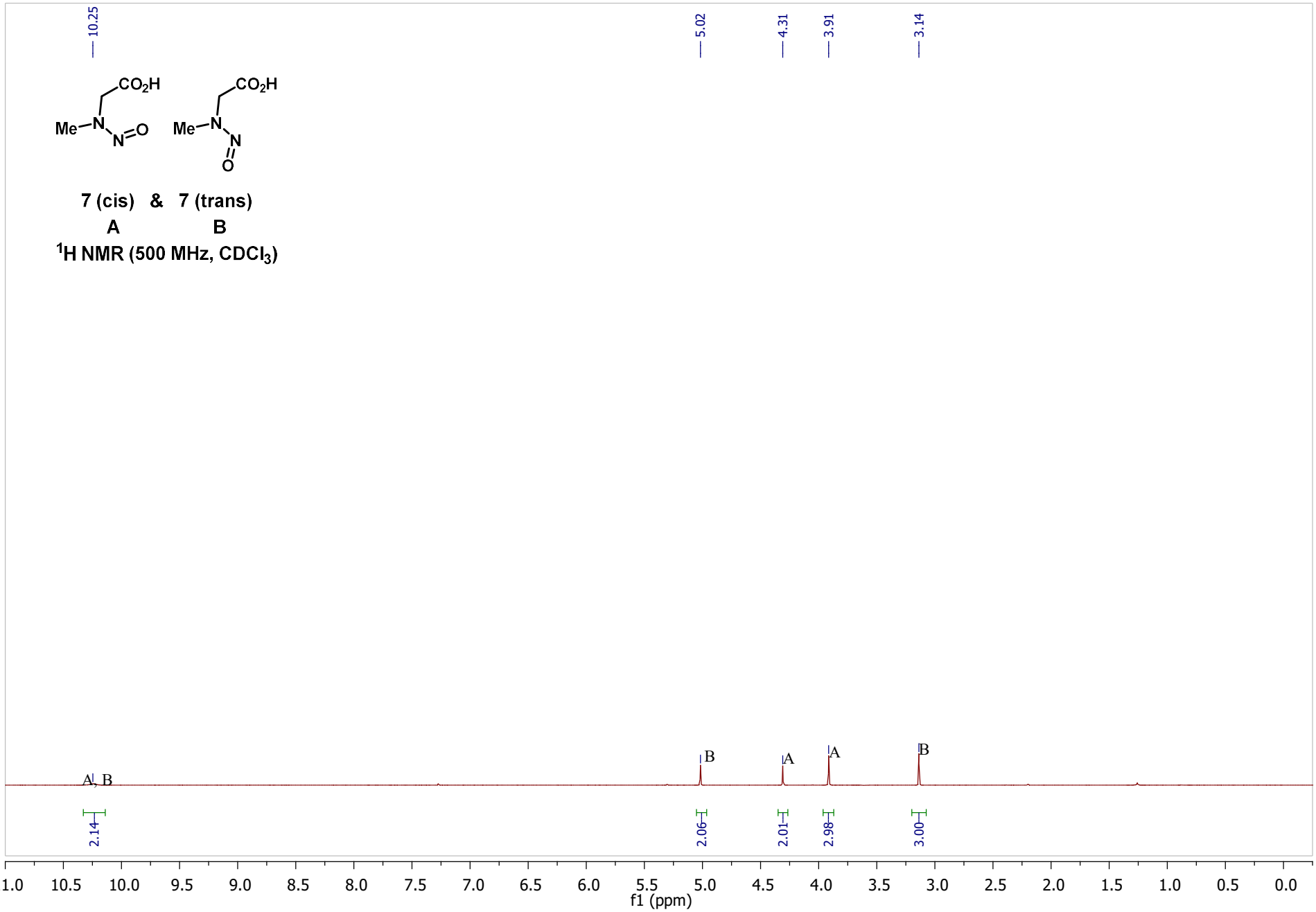
10.25
5.02
4.31
3.91
3.14
CO2H
Me
N
N
O
CO2H
Me
N
N
O
7 (cis) & 7 (trans)
A B
1H NMR (500 MHz, CDCl3)
A, B
B
A
A
B
2.14
2.06
2.01
2.98
3.00
11.0 10.5 10.0 9.5 9.0 8.5 8.0 7.5 7.0 6.5 6.0 5.5 5.0 4.5 4.0 3.5 3.0 2.5 2.0 1.5 1.0 0.5 0.0
f1 (ppm)

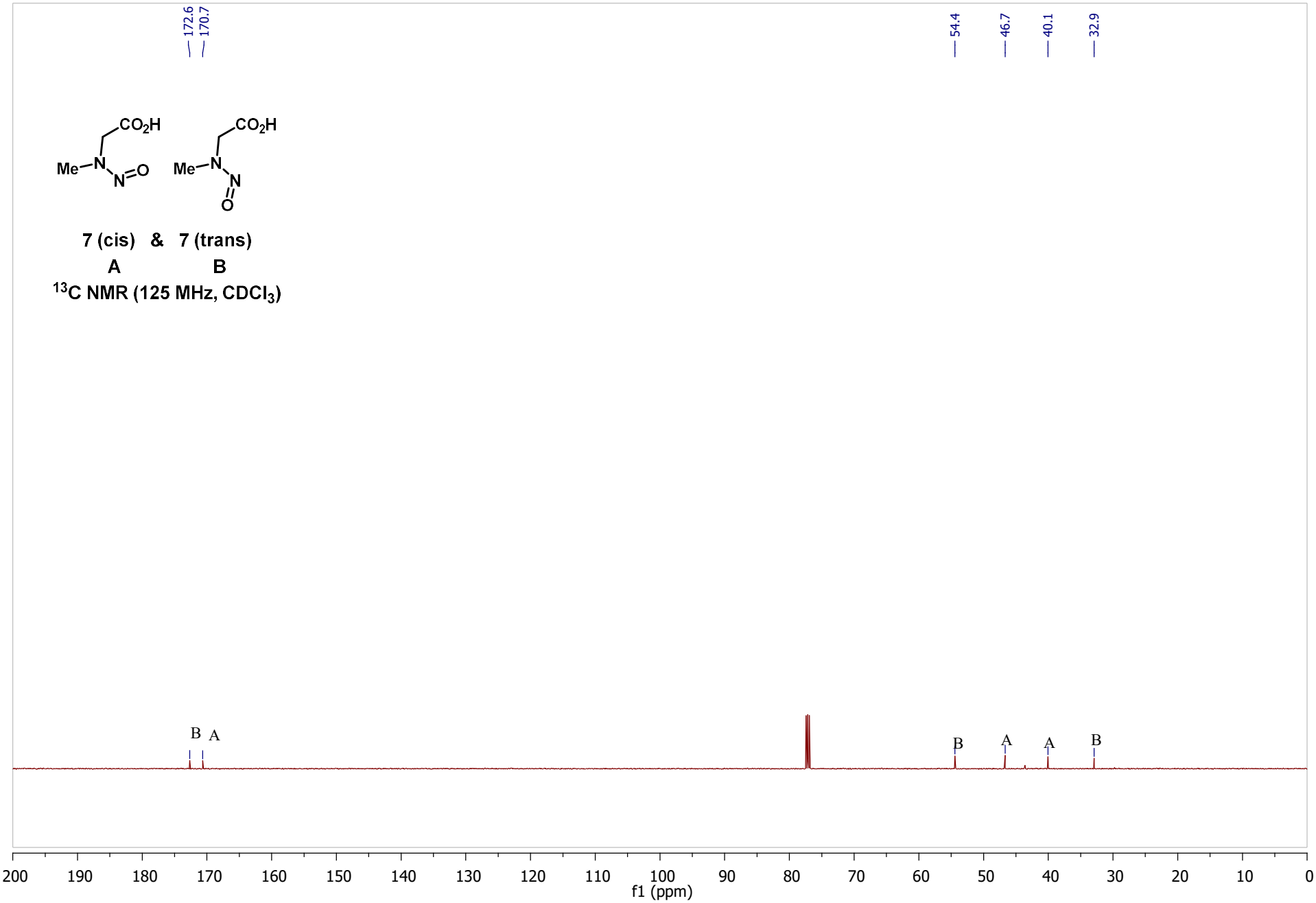
172.6
170.7
54.4
46.7
40.1
32.9
CO2H
Me
N
N
O
CO2H
Me
N
N
O
7 (cis) & 7 (trans)
A B
13C NMR (125 MHz, CDCl3)
B A
B A A B
200 190 180 170 160 150 140 130 120 110 100 90 80 70 60 50 40 30 20 10 0
f1 (ppm)

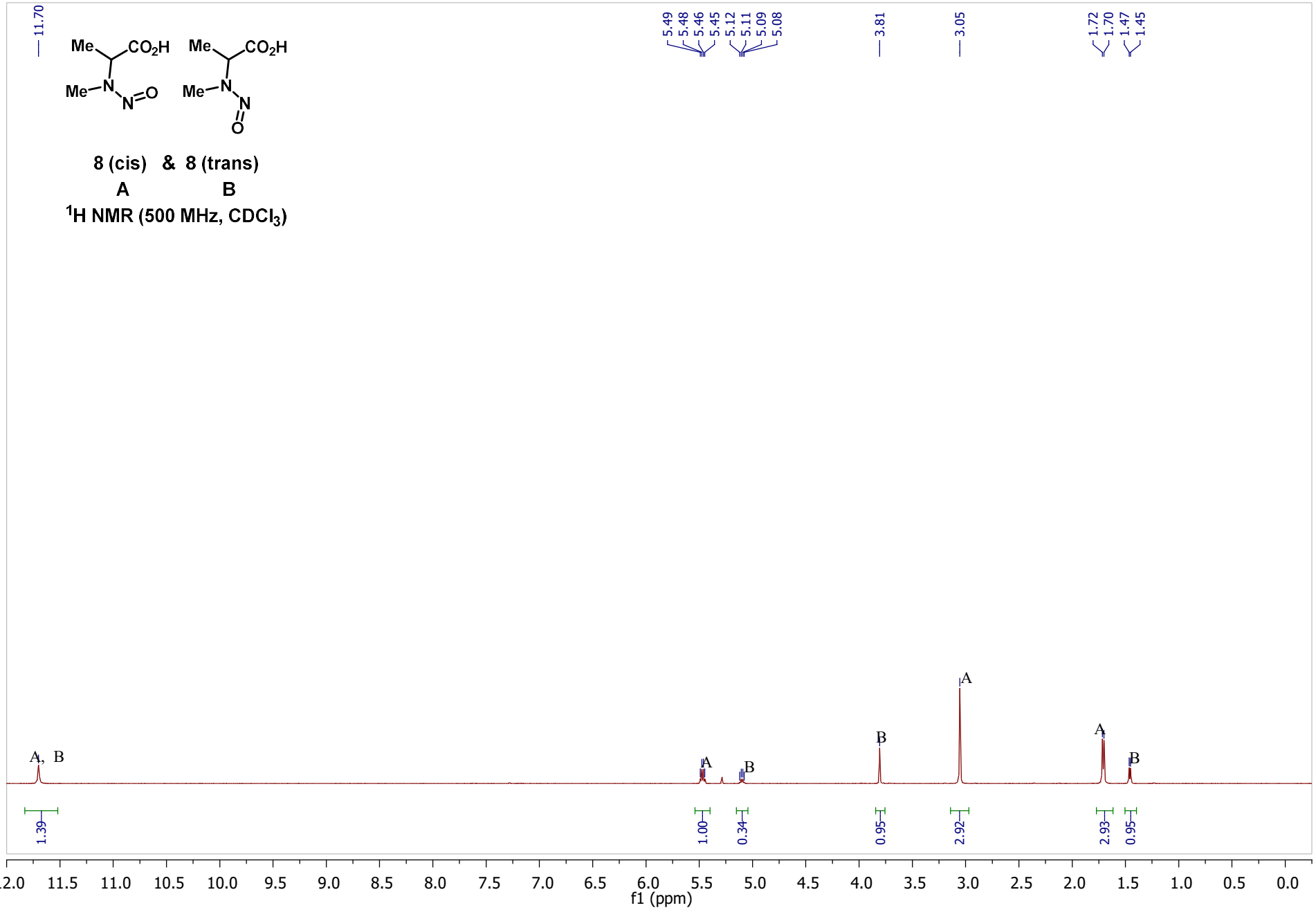
11.70
5.49
5.48
5.46
5.45
5.12
5.11
5.09
5.08
3.81
3.05
1.72
1.70
1.47
1.45
Me
CO2H
Me
N
N
O
Me
CO2H
Me
N
N
O
8 (cis) & 8 (trans)
A B
1H NMR (500 MHz, CDCl3)
A, B
A
B
B
A
A
B
1.39
1.00
0.34
0.95
2.92
2.93
0.95
12.0 11.5 11.0 10.5 10.0 9.5 9.0 8.5 8.0 7.5 7.0 6.5 6.0 5.5 5.0 4.5 4.0 3.5 3.0 2.5 2.0 1.5 1.0 0.5 0.0
f1 (ppm)

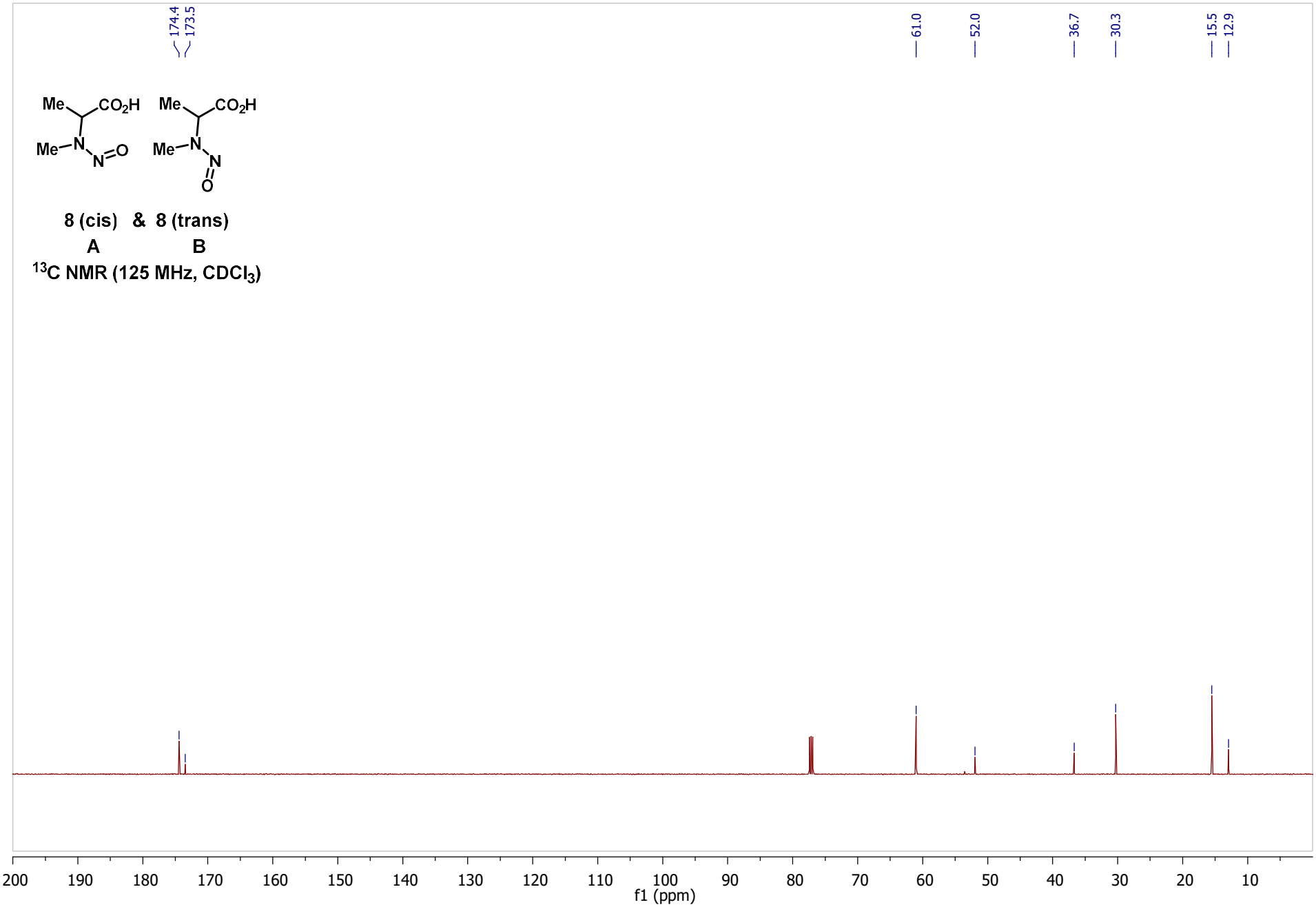
174.4
173.5
61.0
52.0
36.7
30.3
15.5
12.9
Me
CO2H
Me
N
N
O
Me
CO2H
Me
N
N
O
8 (cis) & 8 (trans)
A
B
13C NMR (125 MHz, CDCl3)
200
190
180
170
160
150
140
130
120
110
100
90
80
70
60
50
40
30
20
10
f1 (ppm)

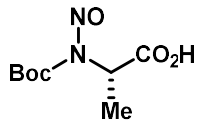

9

^{1}H NMR (500 MHz, $CDCl_3$)

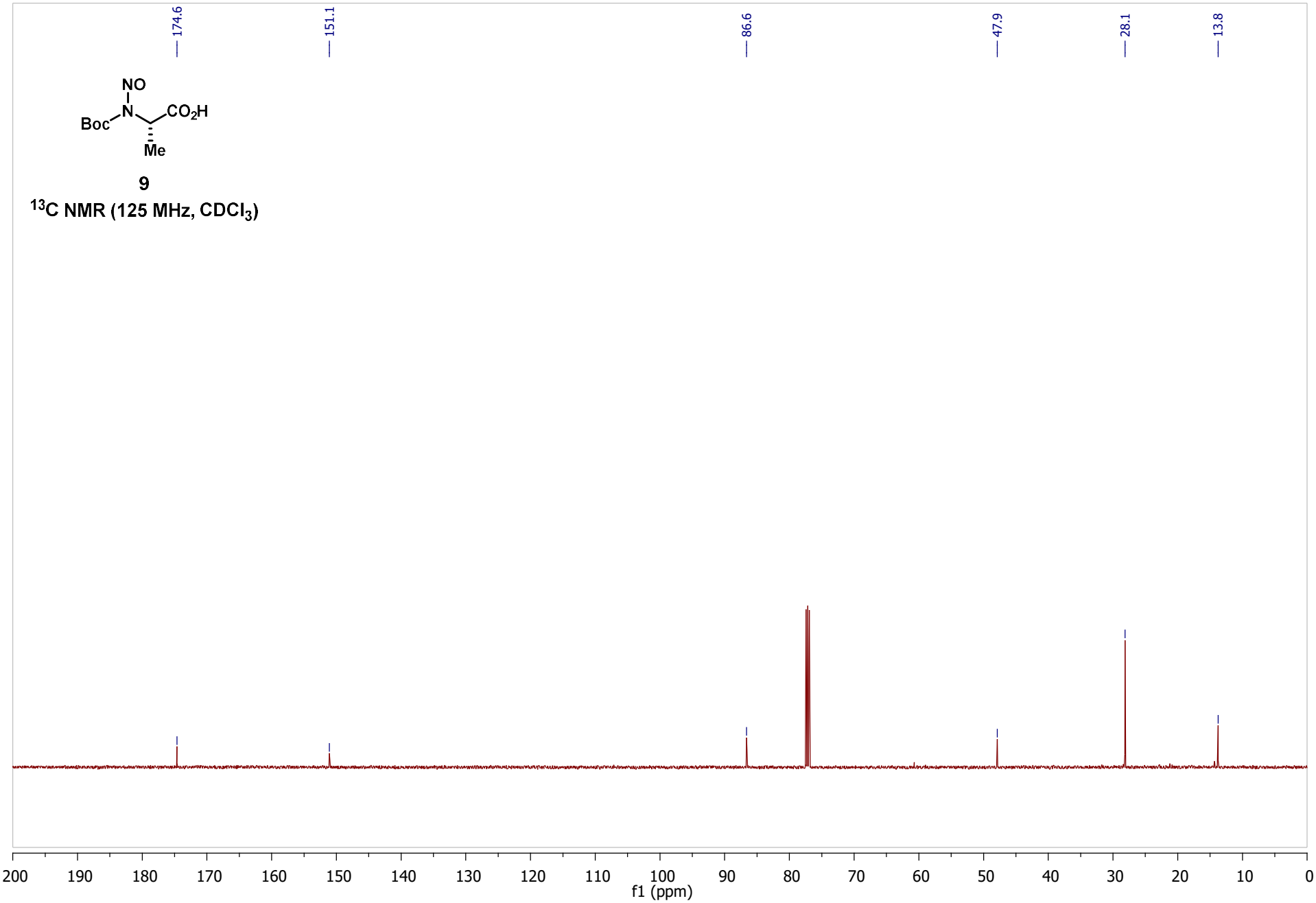

9

^{13}C NMR (125 MHz, $CDCl_3$)

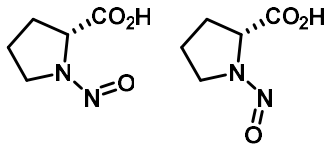

10 (cis) & 10 (trans)

^{1}H NMR (500 MHz, $CDCl_3$)

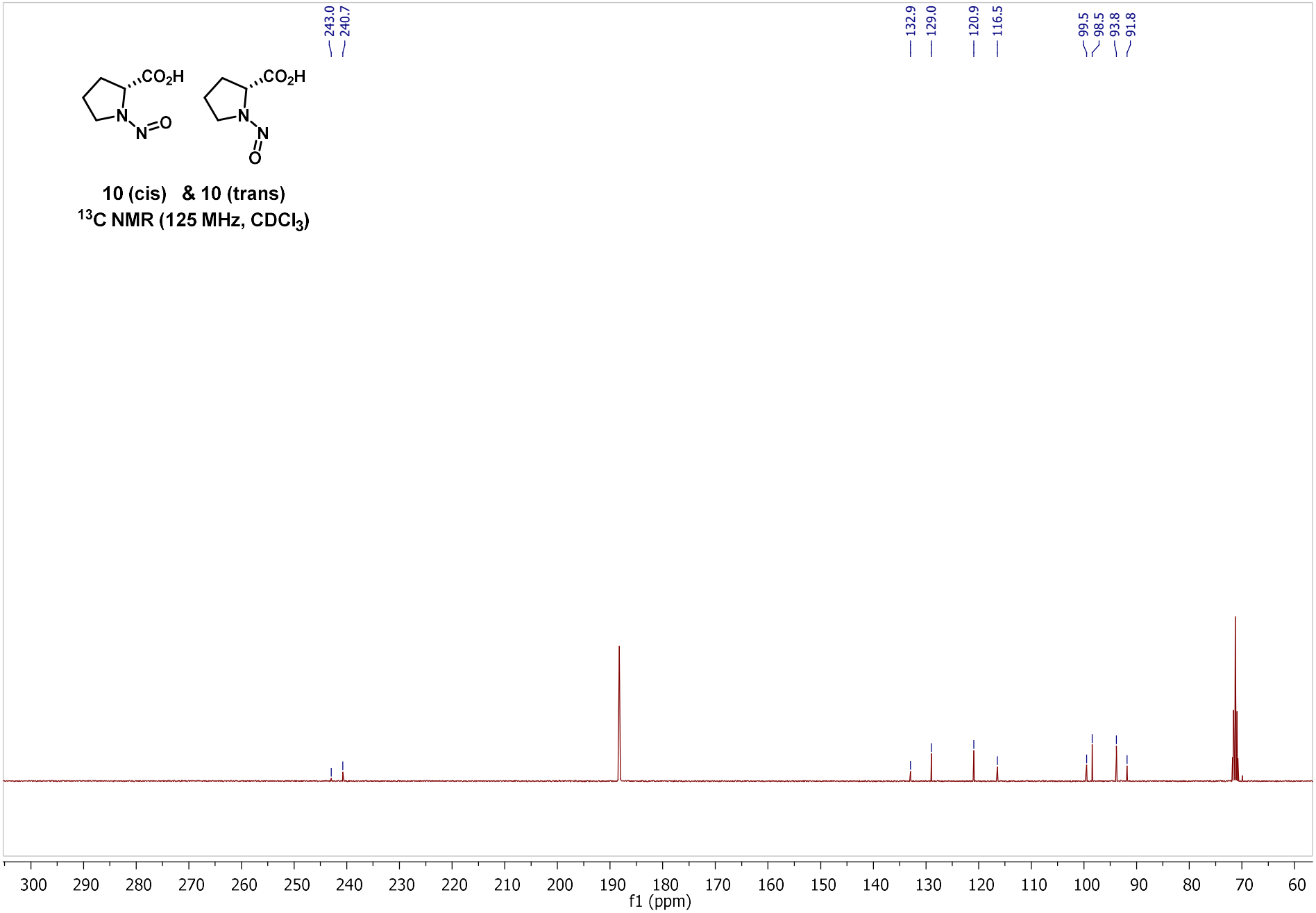
243.0
240.7
132.9
129.0
120.9
116.5
99.5
98.5
93.8
91.8
CO2H
N
N=O
CO2H
N
N
O
10 (cis) & 10 (trans)
13C NMR (125 MHz, CDCl3)
300 290 280 270 260 250 240 230 220 210 200 190 180 170 160 150 140 130 120 110 100 90 80 70 60
f1 (ppm)

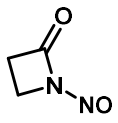

11

^{1}H NMR (400 MHz, $CDCl_3$)

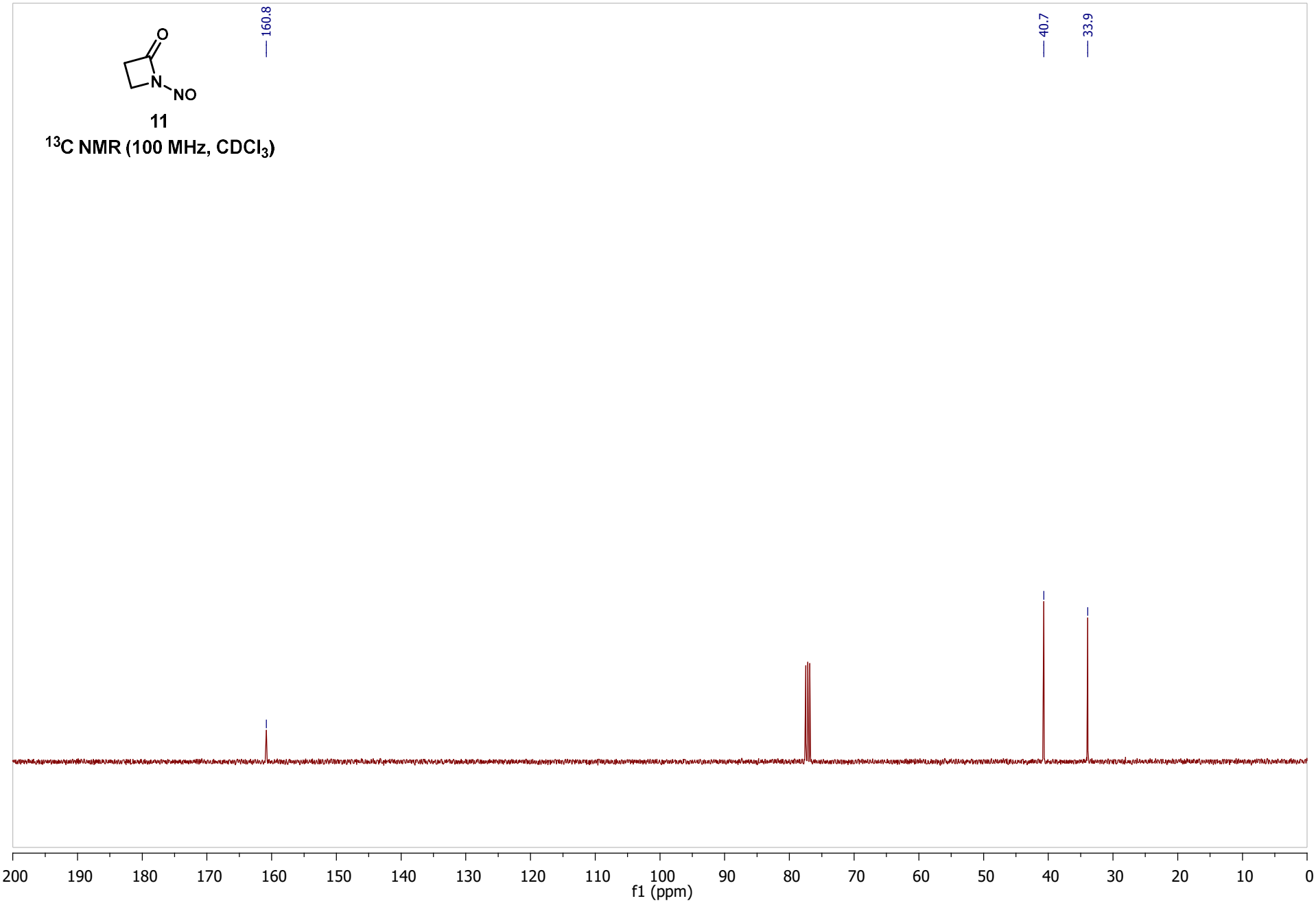

11

^{13}C NMR (100 MHz, $CDCl_3$)

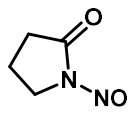

12

^{1}H NMR (500 MHz, $CDCl_3$)

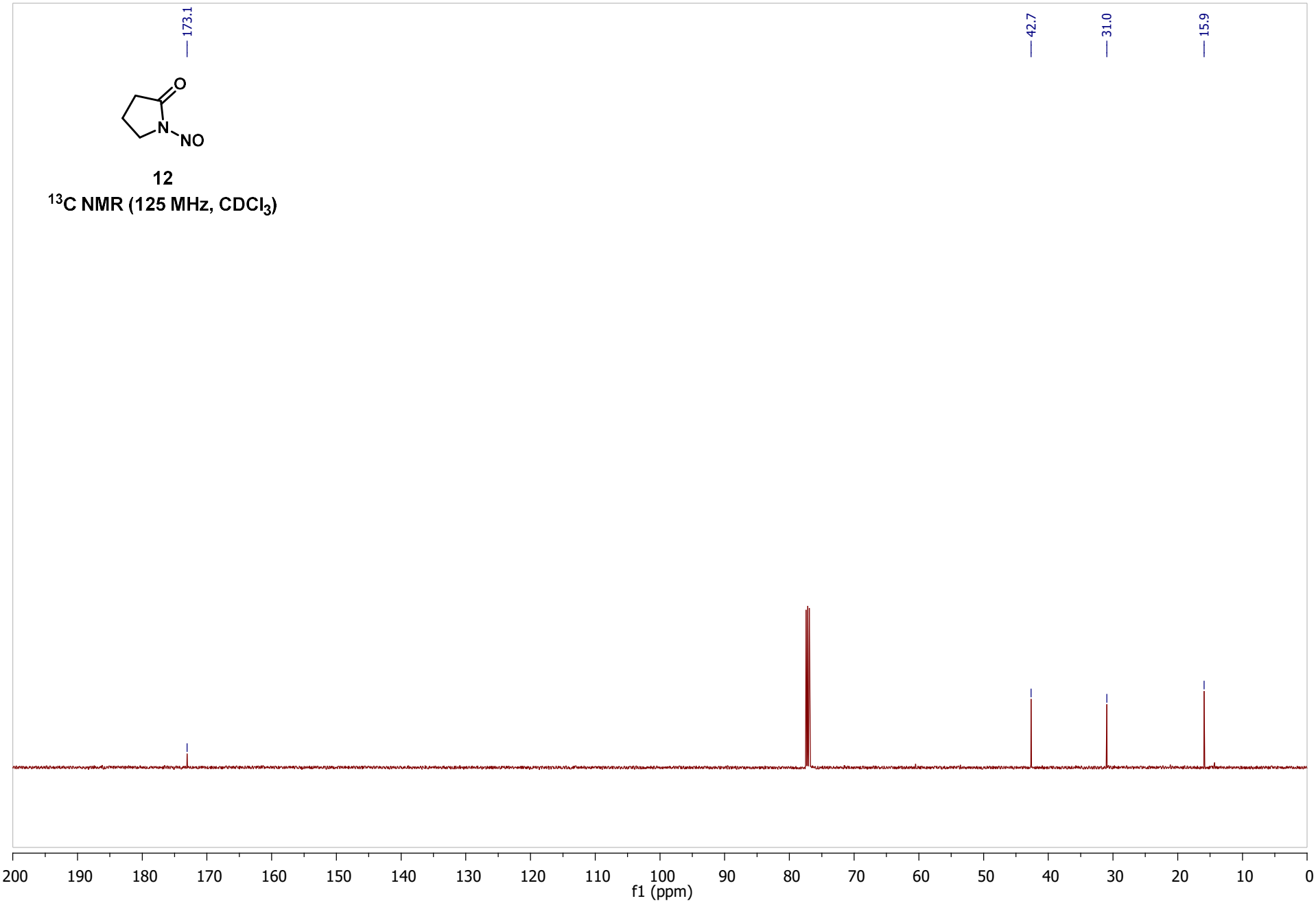

12

^{13}C NMR (125 MHz, $CDCl_3$)

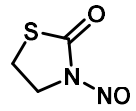

13

^{1}H NMR (500 MHz, $CDCl_3$)

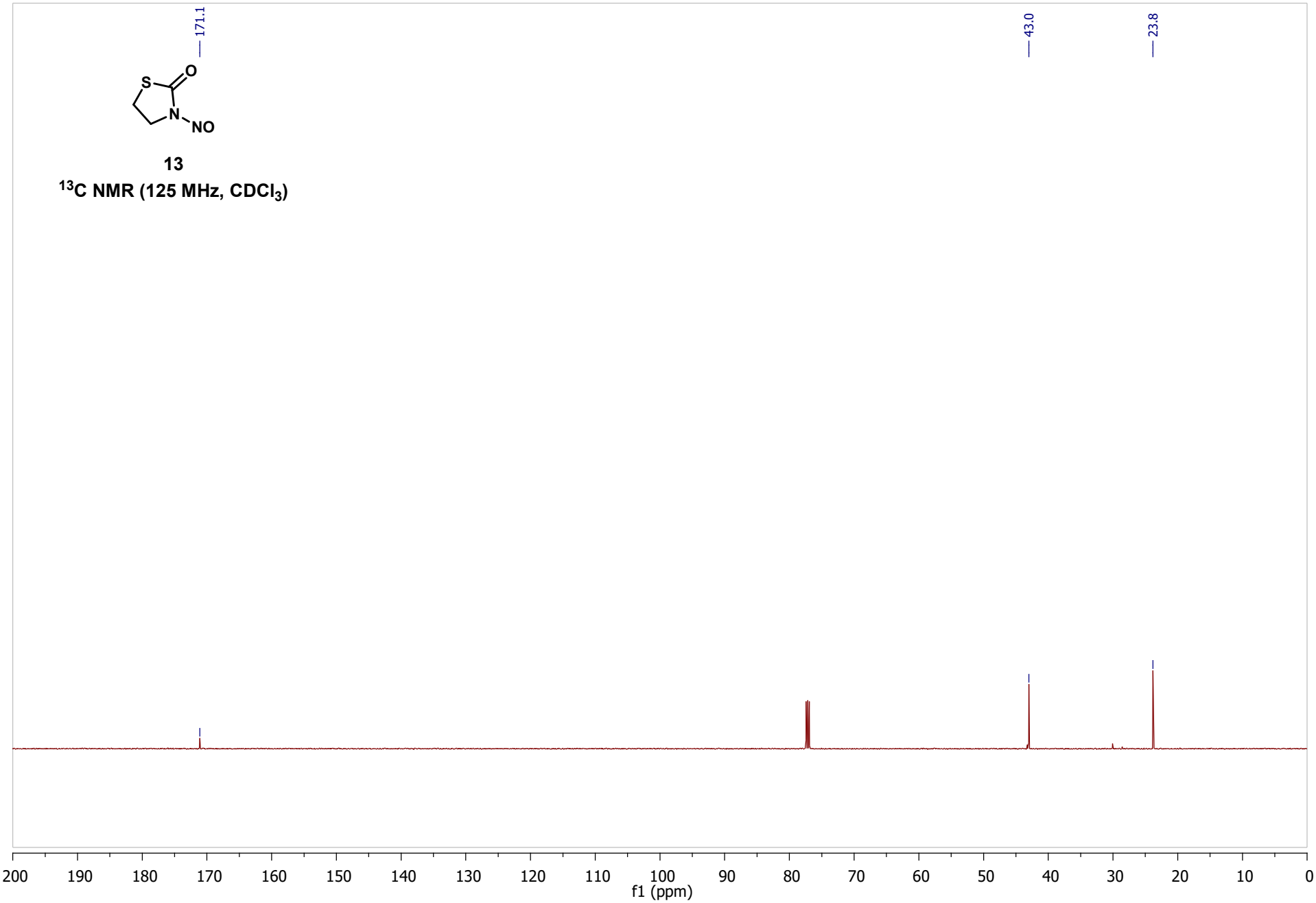

13

^{13}C NMR (125 MHz, $CDCl_3$)

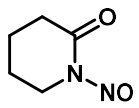

14

^{1}H NMR (500 MHz, $CDCl_3$)

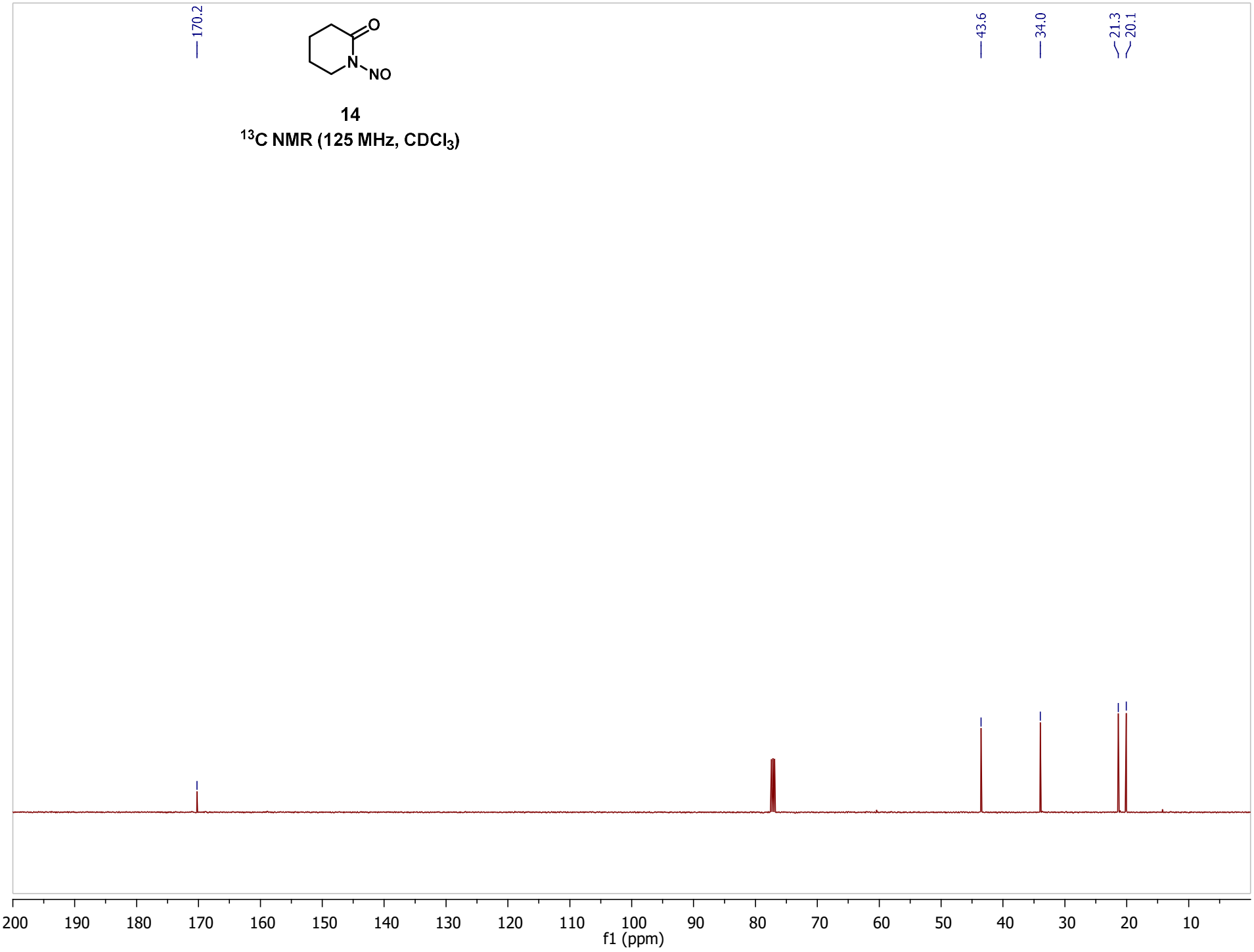

14

^{13}C NMR (125 MHz, $CDCl_3$)

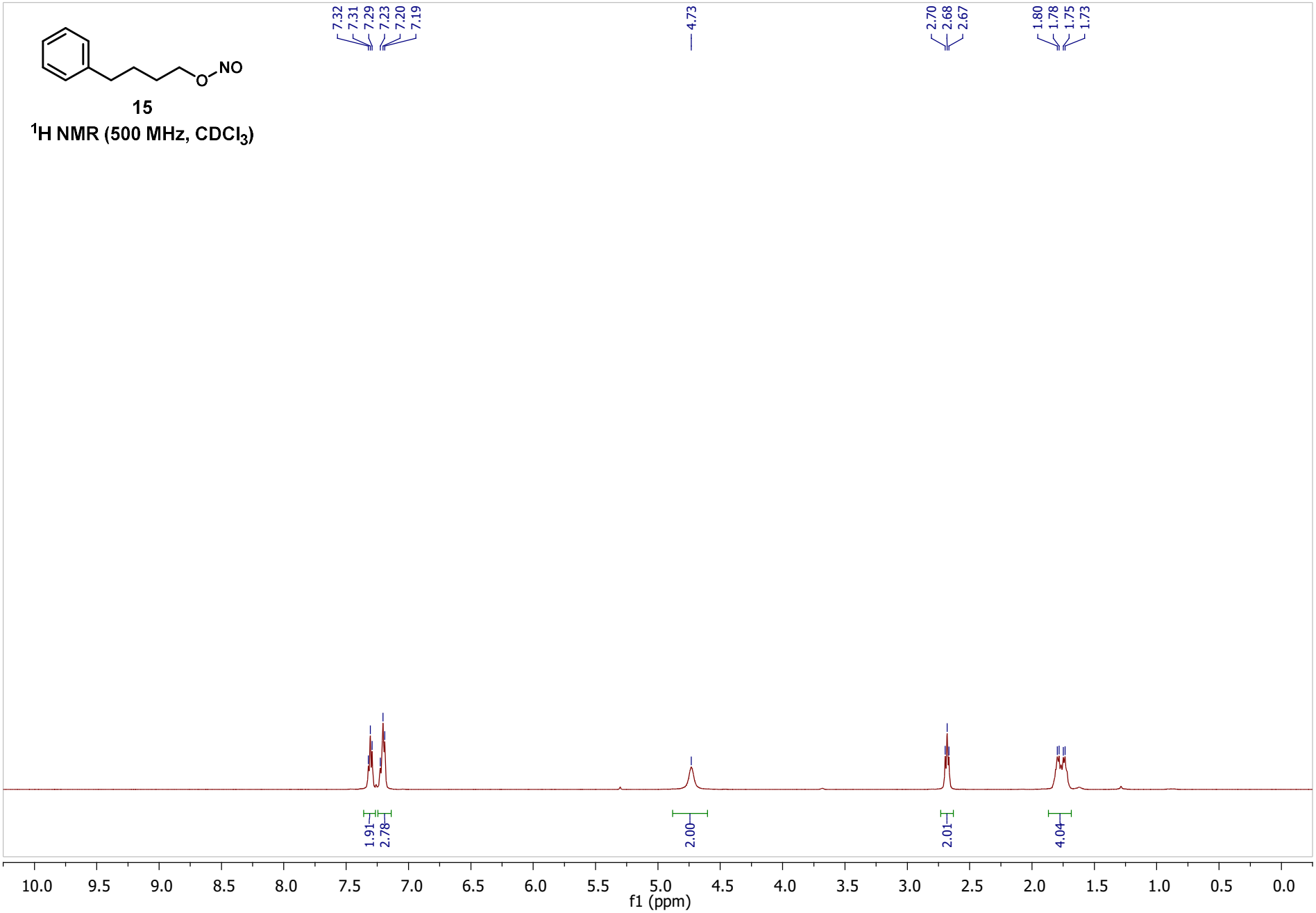
NO
O
15
1H NMR (500 MHz, CDCl3)
7.32
7.31
7.29
7.23
7.20
7.19
4.73
2.70
2.68
2.67
1.80
1.78
1.75
1.73
1.91
2.78
2.00
2.01
4.04
10.0
9.5
9.0
8.5
8.0
7.5
7.0
6.5
6.0
5.5
5.0
4.5
4.0
3.5
3.0
2.5
2.0
1.5
1.0
0.5
0.0
f1 (ppm)

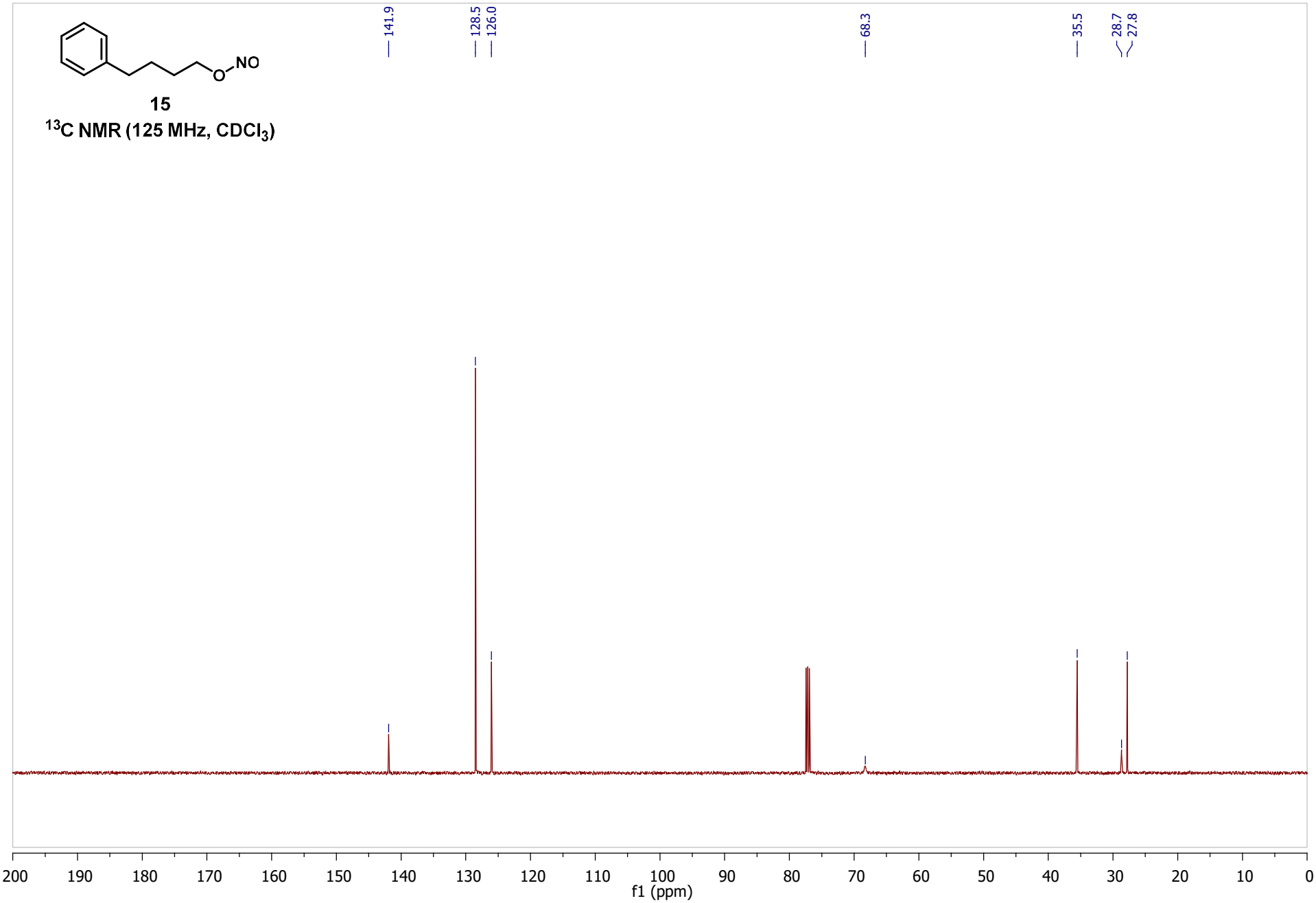
141.9
128.5
126.0
68.3
35.5
28.7
27.8
NO
O
15
13C NMR (125 MHz, CDCl3)
200
190
180
170
160
150
140
130
120
110
100
90
80
70
60
50
40
30
20
10
0
f1 (ppm)

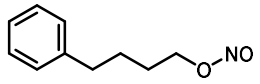

15

^{1}H—^{13}C HSQC NMR (500 MHz, $CDCl_3$)

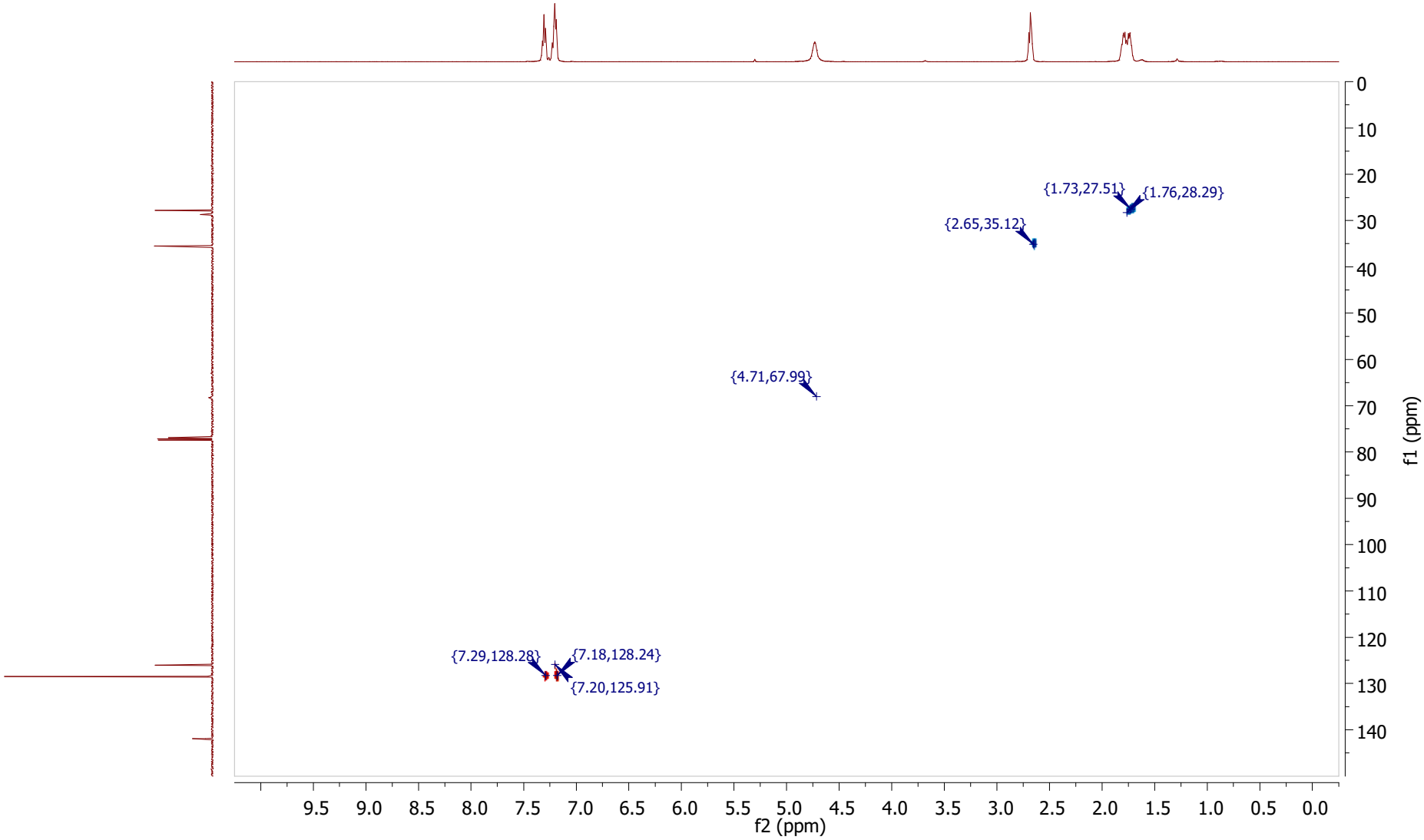

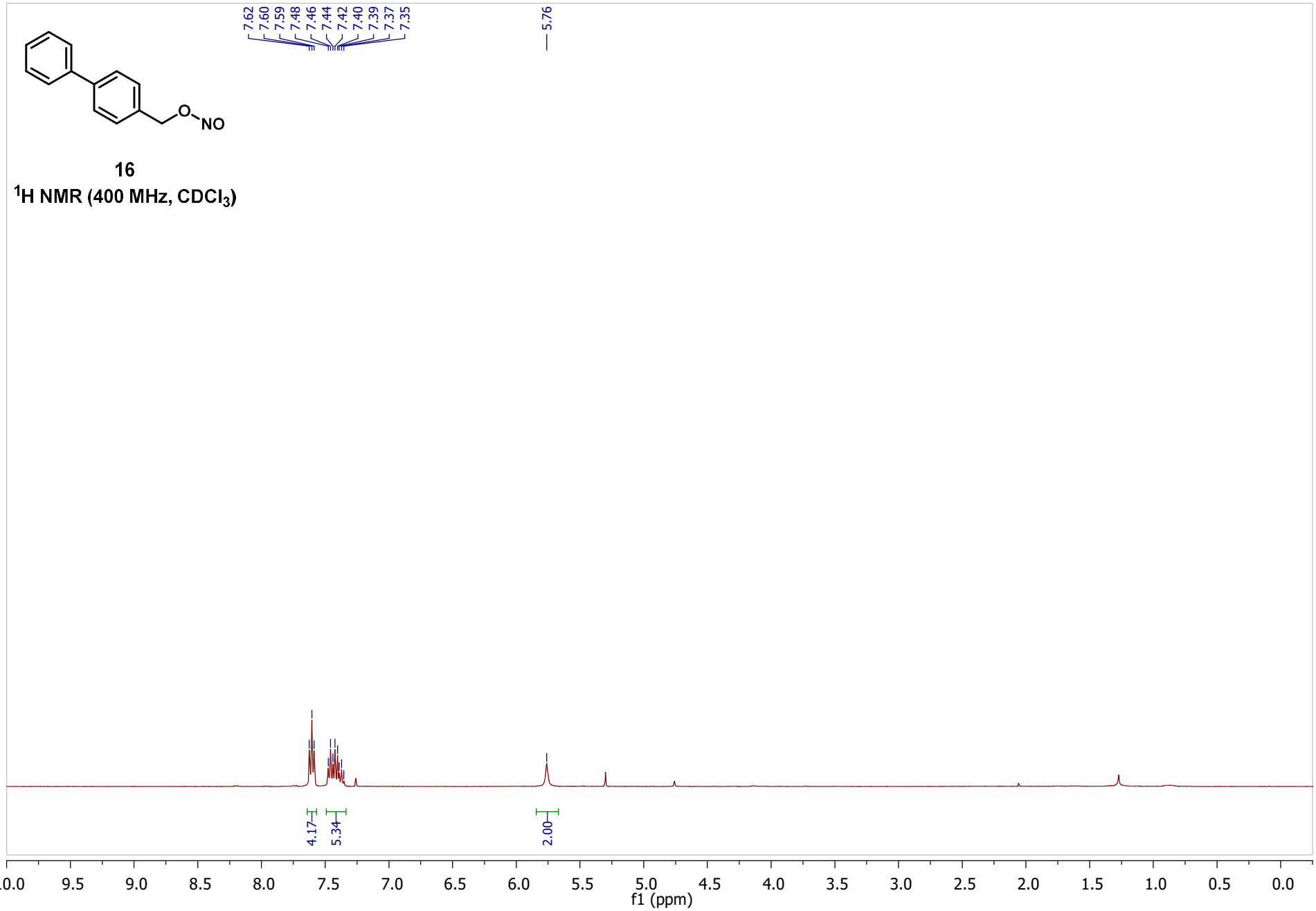

16

^{1}H NMR (400 MHz, $CDCl_3$)

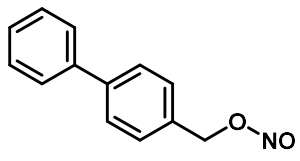

16

^{13}C NMR (100 MHz, $CDCl_3$)

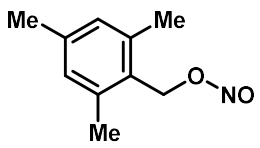

17

^{1}H NMR (400 MHz, $CDCl_3$)

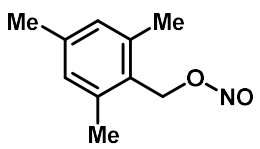

17

^{13}C NMR (100 MHz, $CDCl_3$)

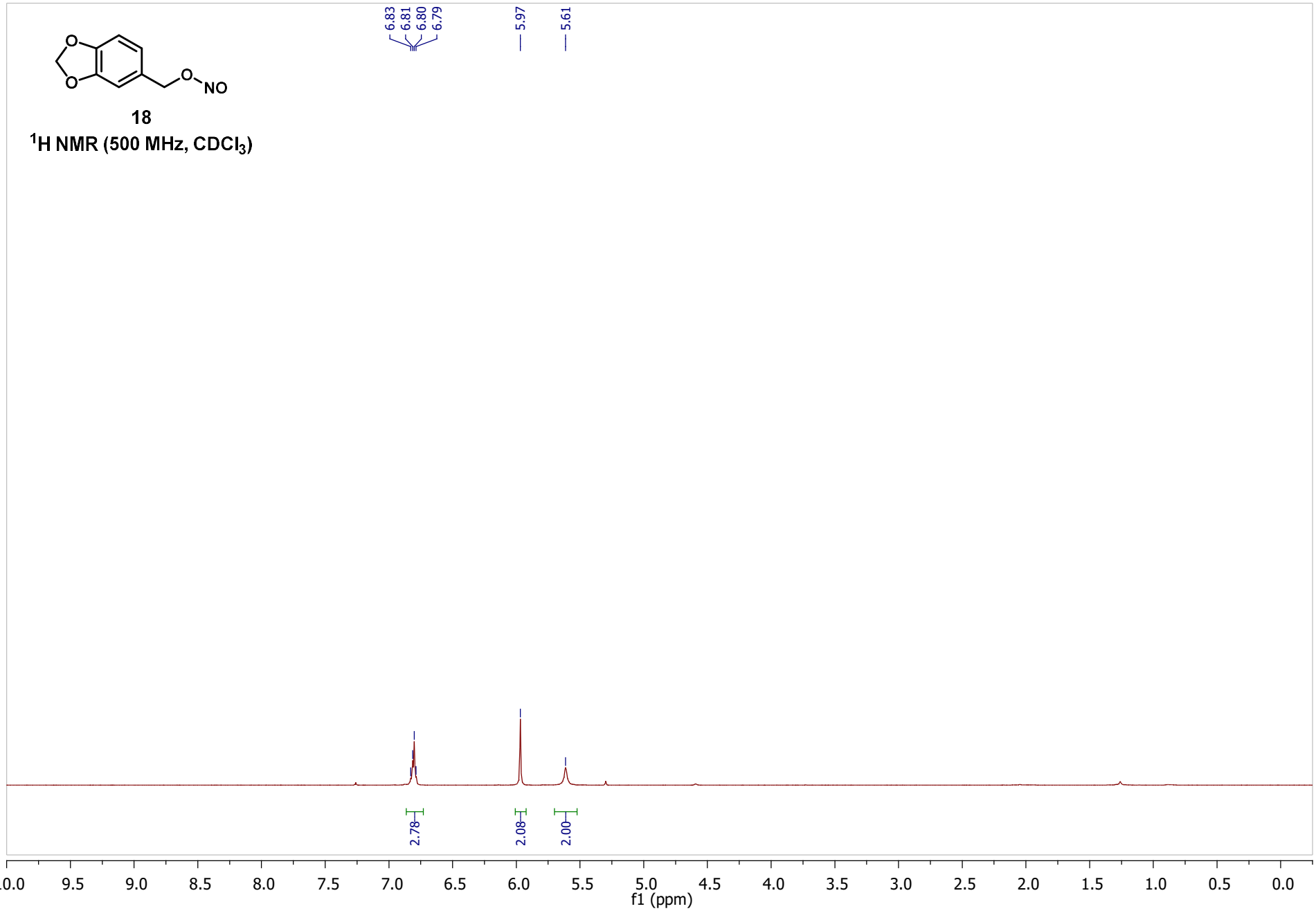
6.83
6.81
6.80
6.79
5.97
5.61
O
O
O
NO
18
1H NMR (500 MHz, CDCl3)
2.78
2.08
2.00
10.0
9.5
9.0
8.5
8.0
7.5
7.0
6.5
6.0
5.5
5.0
4.5
4.0
3.5
3.0
2.5
2.0
1.5
1.0
0.5
0.0
f1 (ppm)

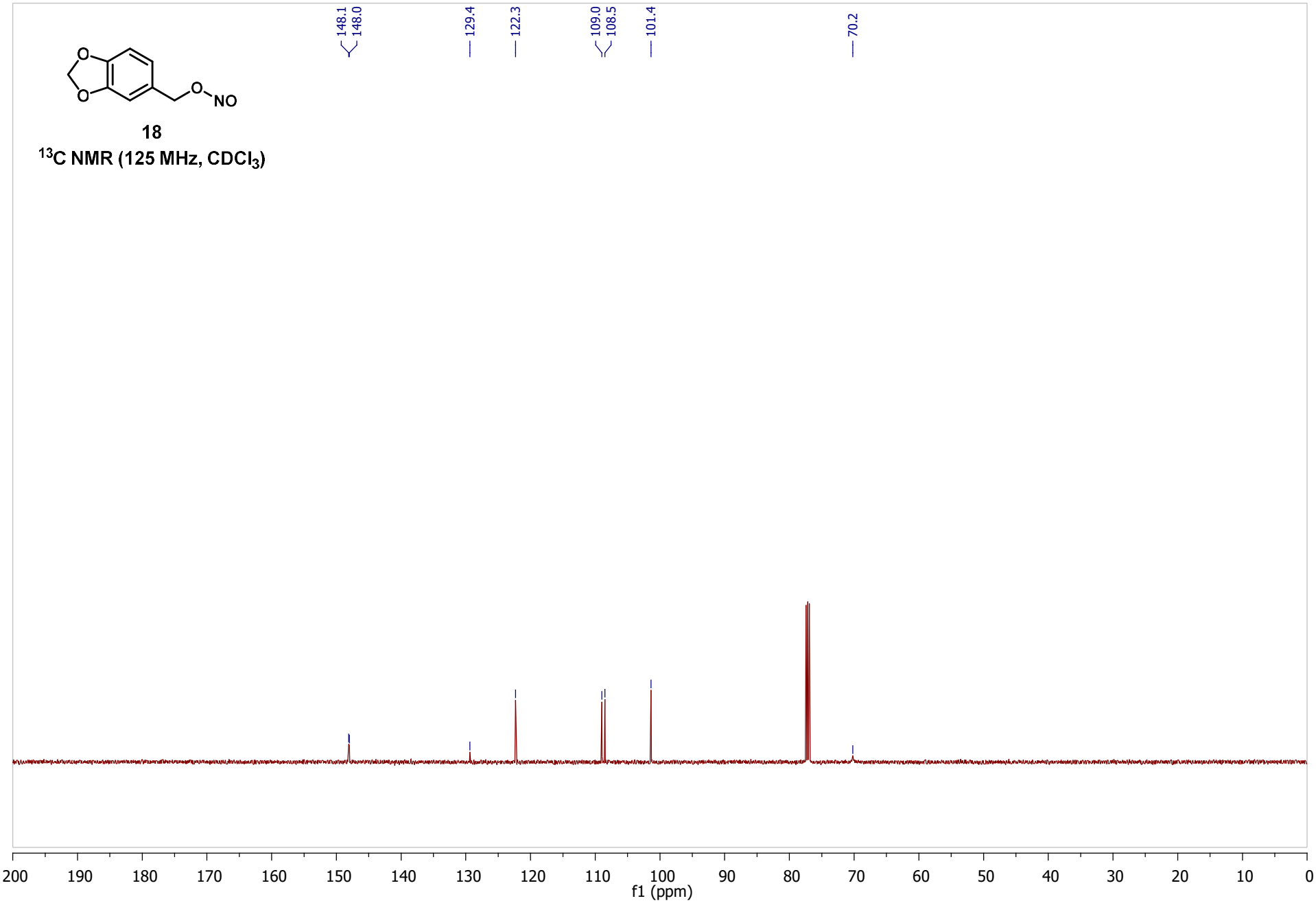
148.1
148.0
129.4
122.3
109.0
108.5
101.4
70.2
O
O
O
NO
18
13C NMR (125 MHz, CDCl3)
200
190
180
170
160
150
140
130
120
110
100
90
80
70
60
50
40
30
20
10
0
f1 (ppm)

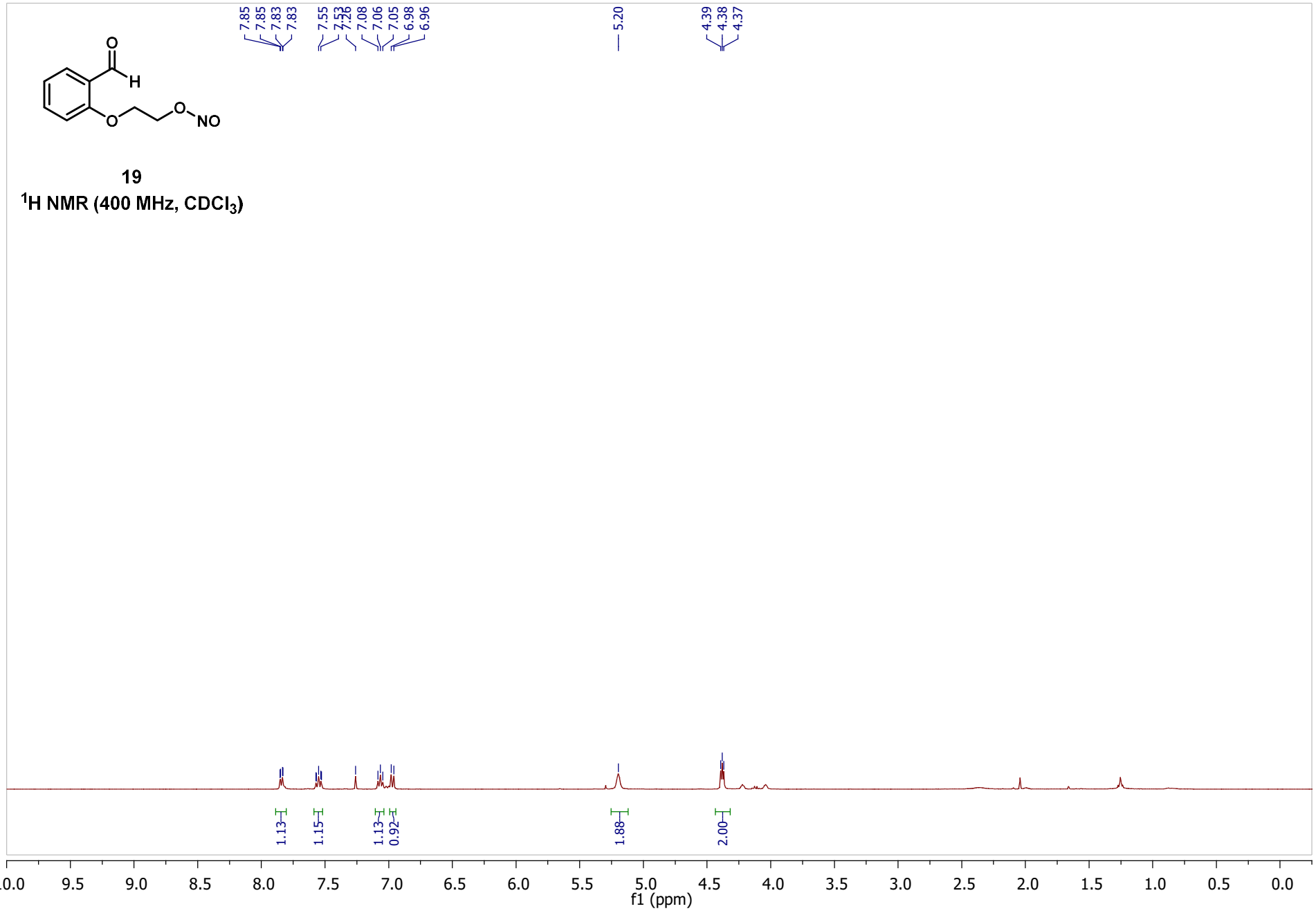

19

^{1}H NMR (400 MHz, $CDCl_3$)

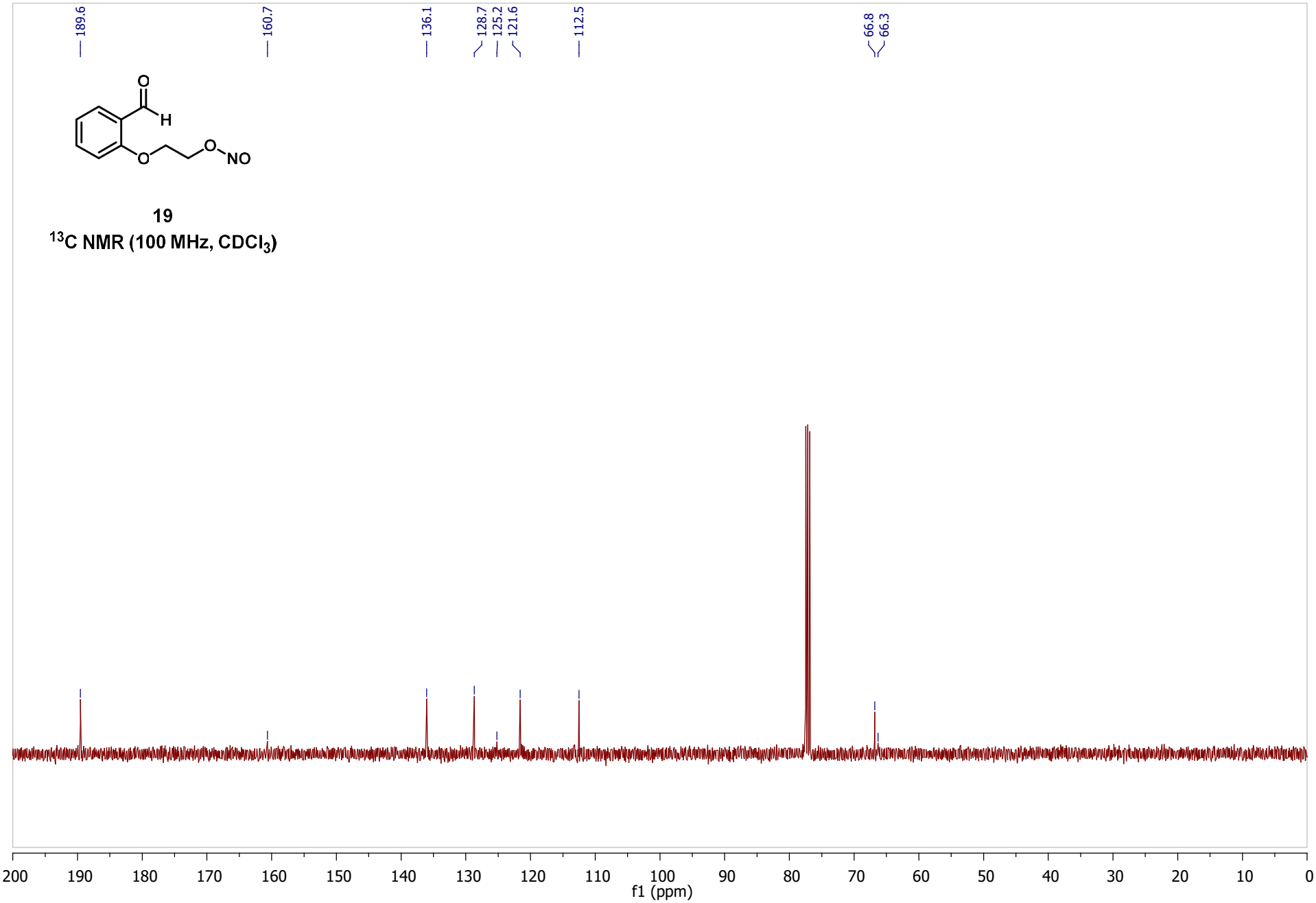

19

^{13}C NMR (100 MHz, $CDCl_3$)

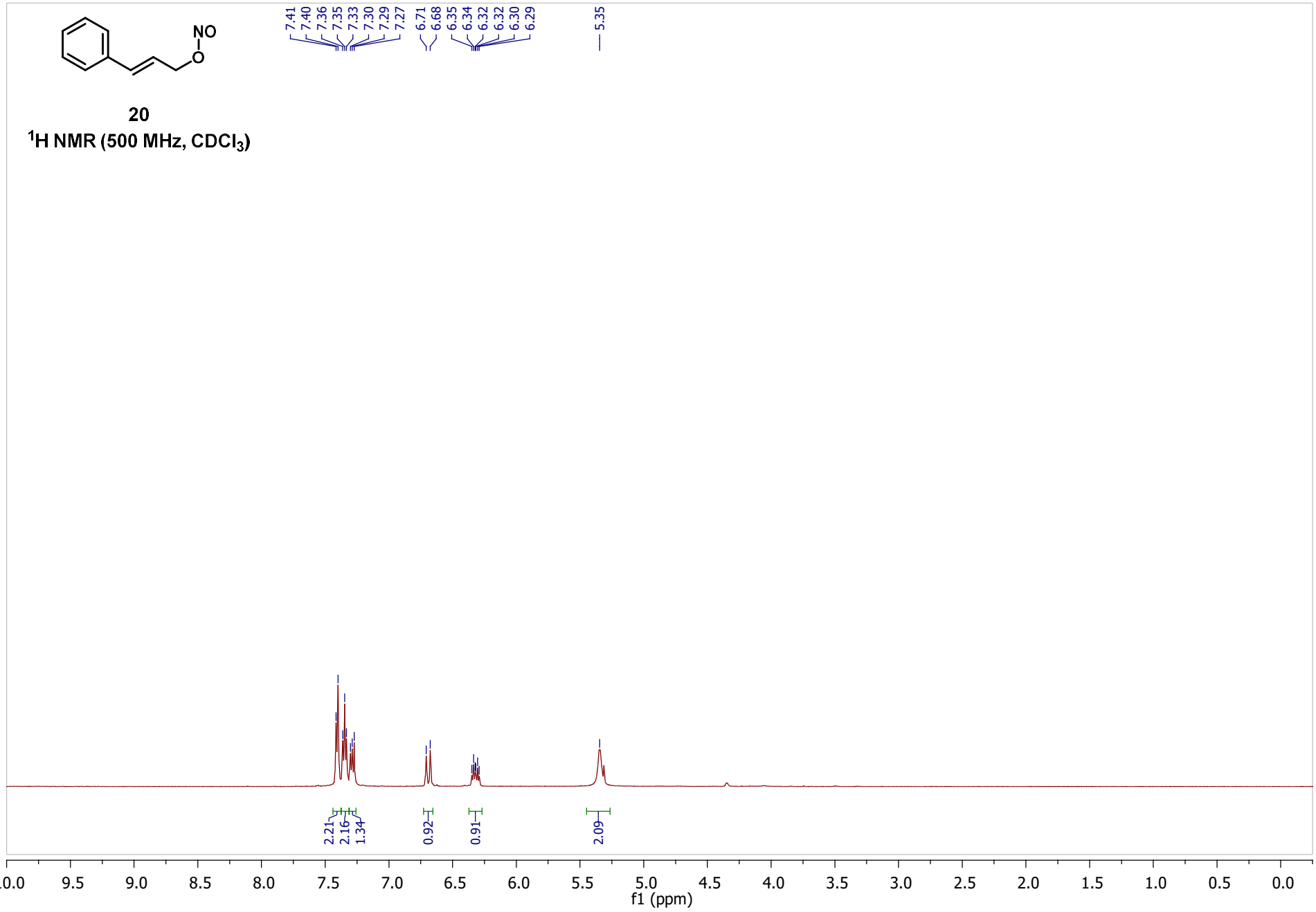
NO
O
20
1H NMR (500 MHz, CDCl3)
7.41
7.40
7.36
7.35
7.33
7.30
7.29
7.27
6.71
6.68
6.35
6.34
6.32
6.32
6.30
6.29
5.35
2.21
2.16
1.34
0.92
0.91
2.09
10.0
9.5
9.0
8.5
8.0
7.5
7.0
6.5
6.0
5.5
5.0
4.5
4.0
3.5
3.0
2.5
2.0
1.5
1.0
0.5
0.0
f1 (ppm)

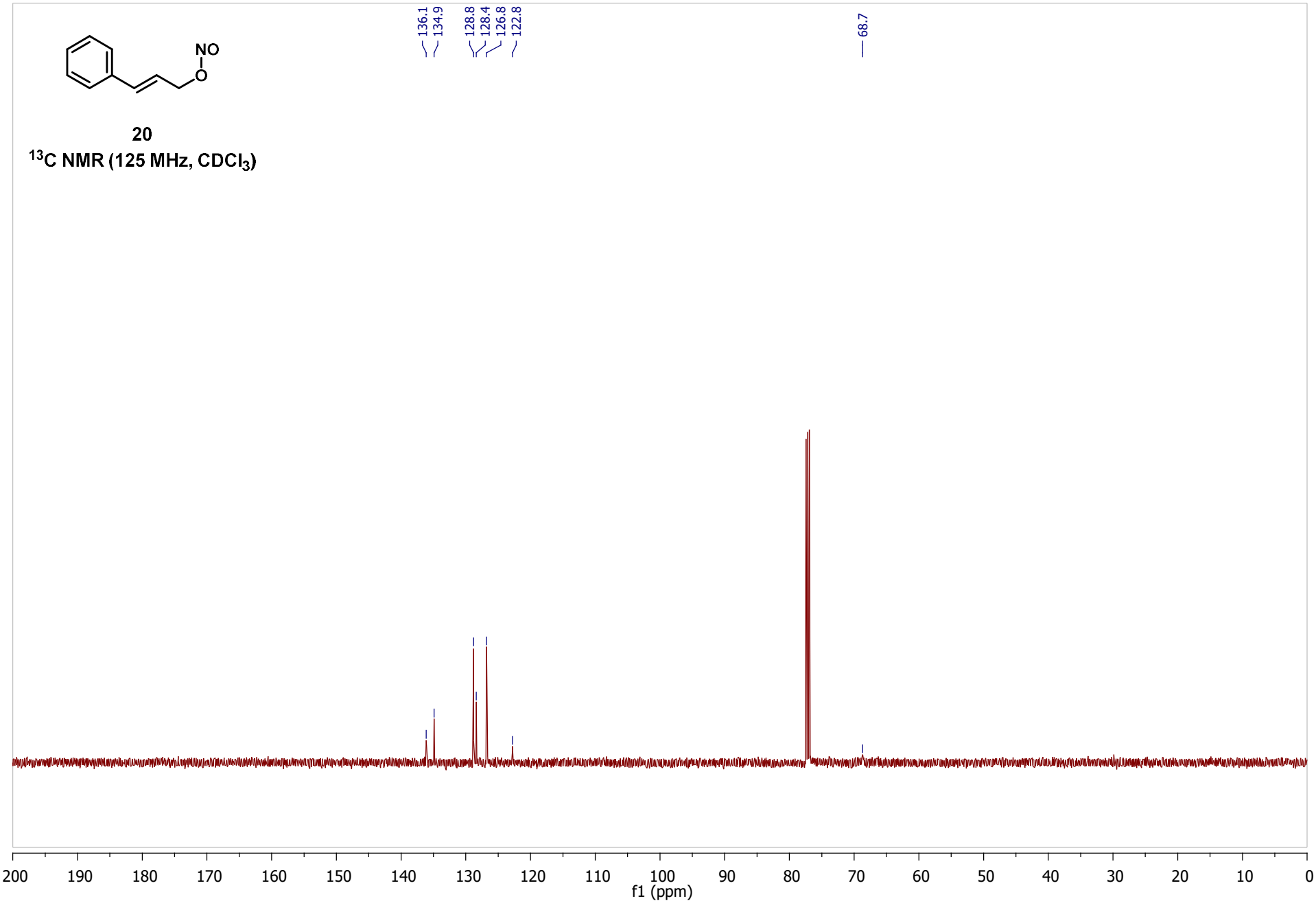

20

^{13}C NMR (125 MHz, $CDCl_3$)

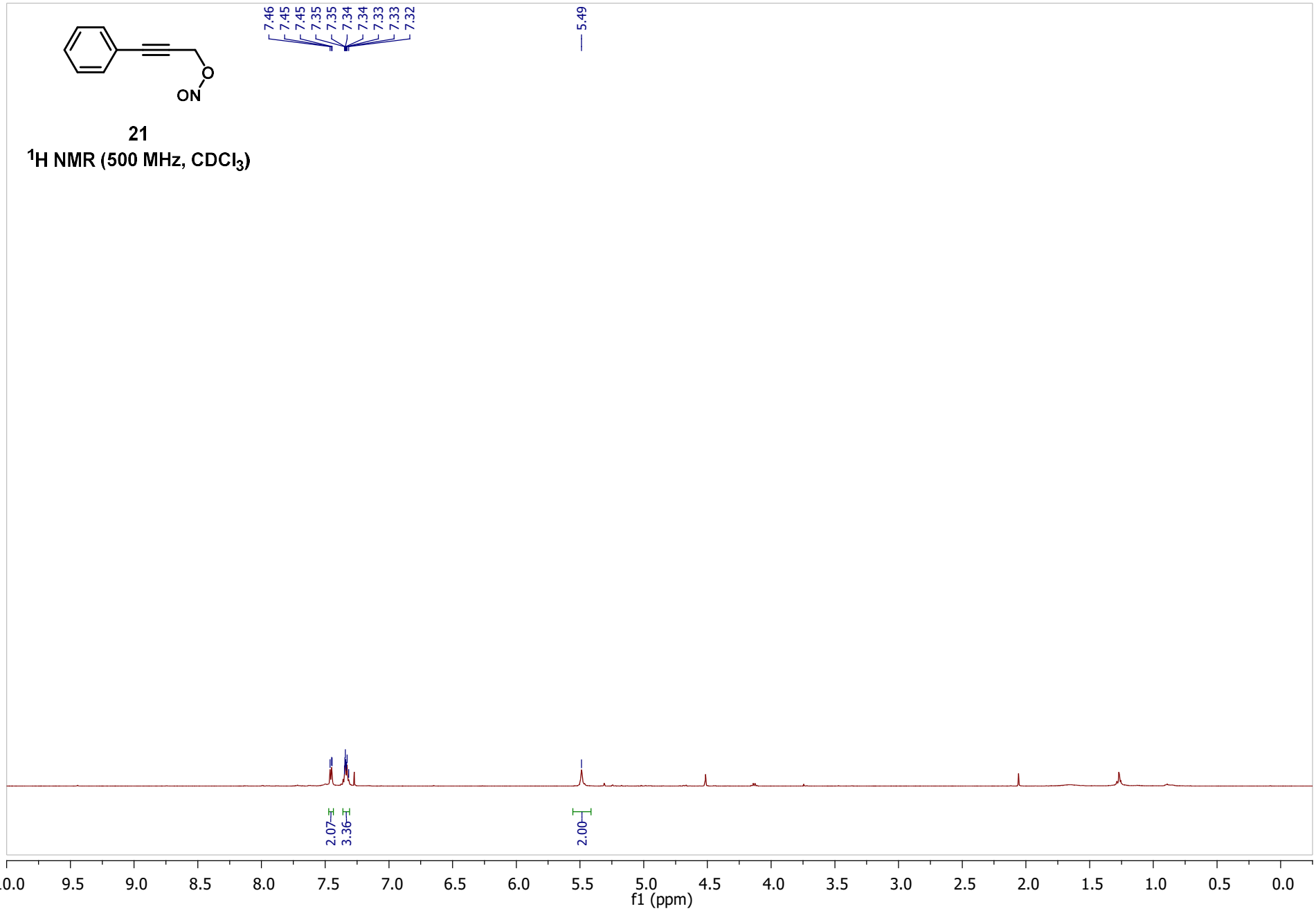

21

^{1}H NMR (500 MHz, $CDCl_3$)

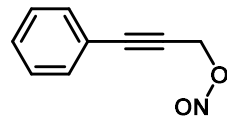

21

^{13}C NMR (125 MHz, $CDCl_3$)

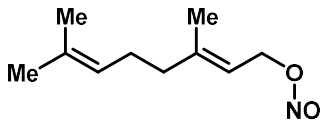

22

^{1}H NMR (500 MHz, $CDCl_3$)

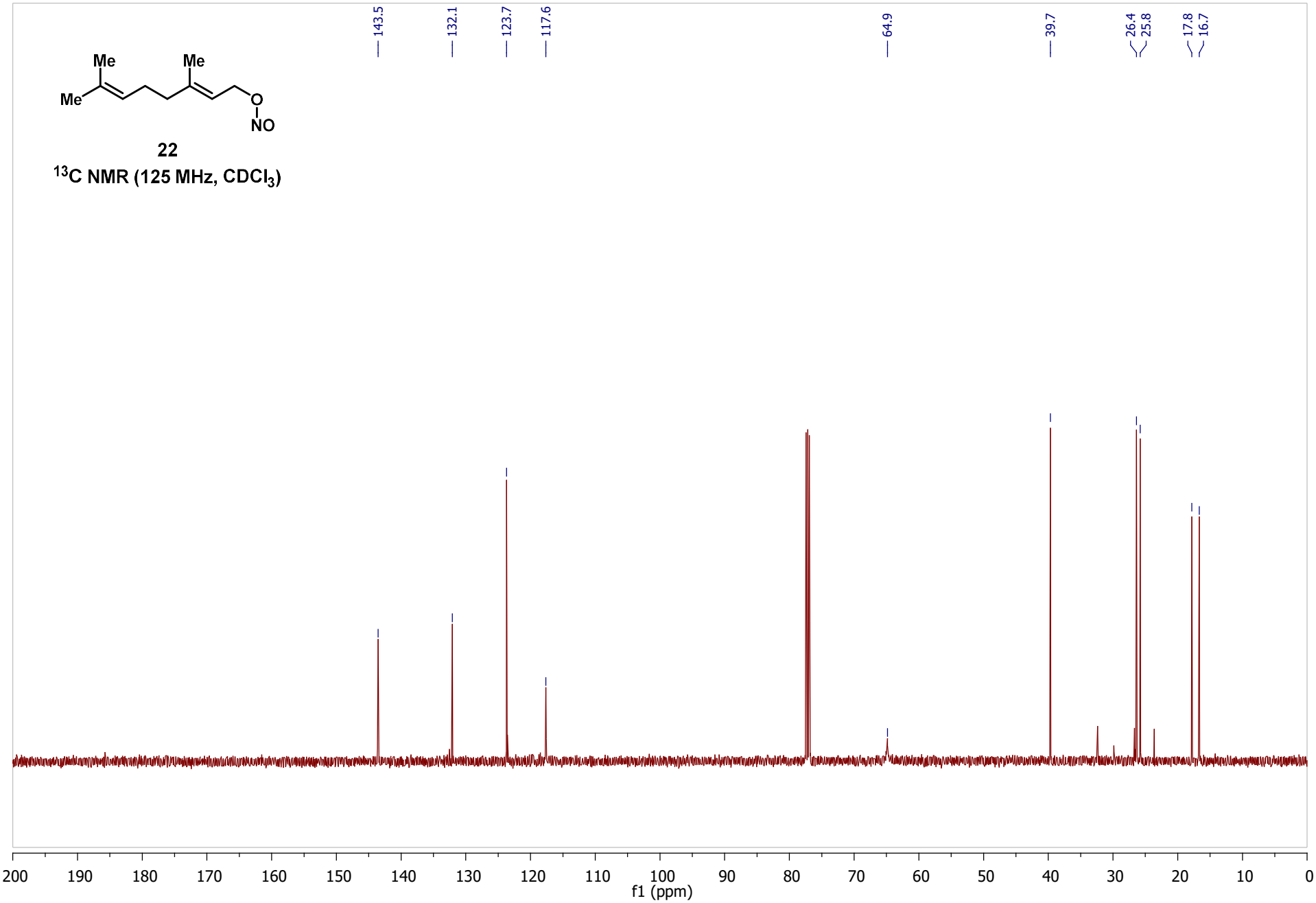
Me
Me
Me
O
NO
22
^{13}C NMR (125 MHz, $CDCl_3$)
143.5
132.1
123.7
117.6
64.9
39.7
26.4
25.8
17.8
16.7
200
190
180
170
160
150
140
130
120
110
100
90
80
70
60
50
40
30
20
10
0
f1 (ppm)

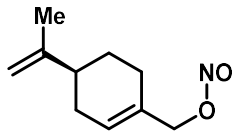

23

^{1}H NMR (400 MHz, $CDCl_3$)

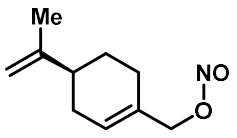

23

^{13}C NMR (100 MHz, $CDCl_3$)

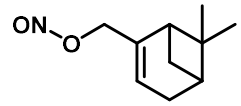

24

^{1}H NMR (500 MHz, $CDCl_3$)

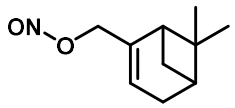

24

^{13}C NMR (125 MHz, $CDCl_3$)

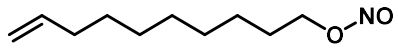

25

^{1}H NMR (500 MHz, $CDCl_3$)

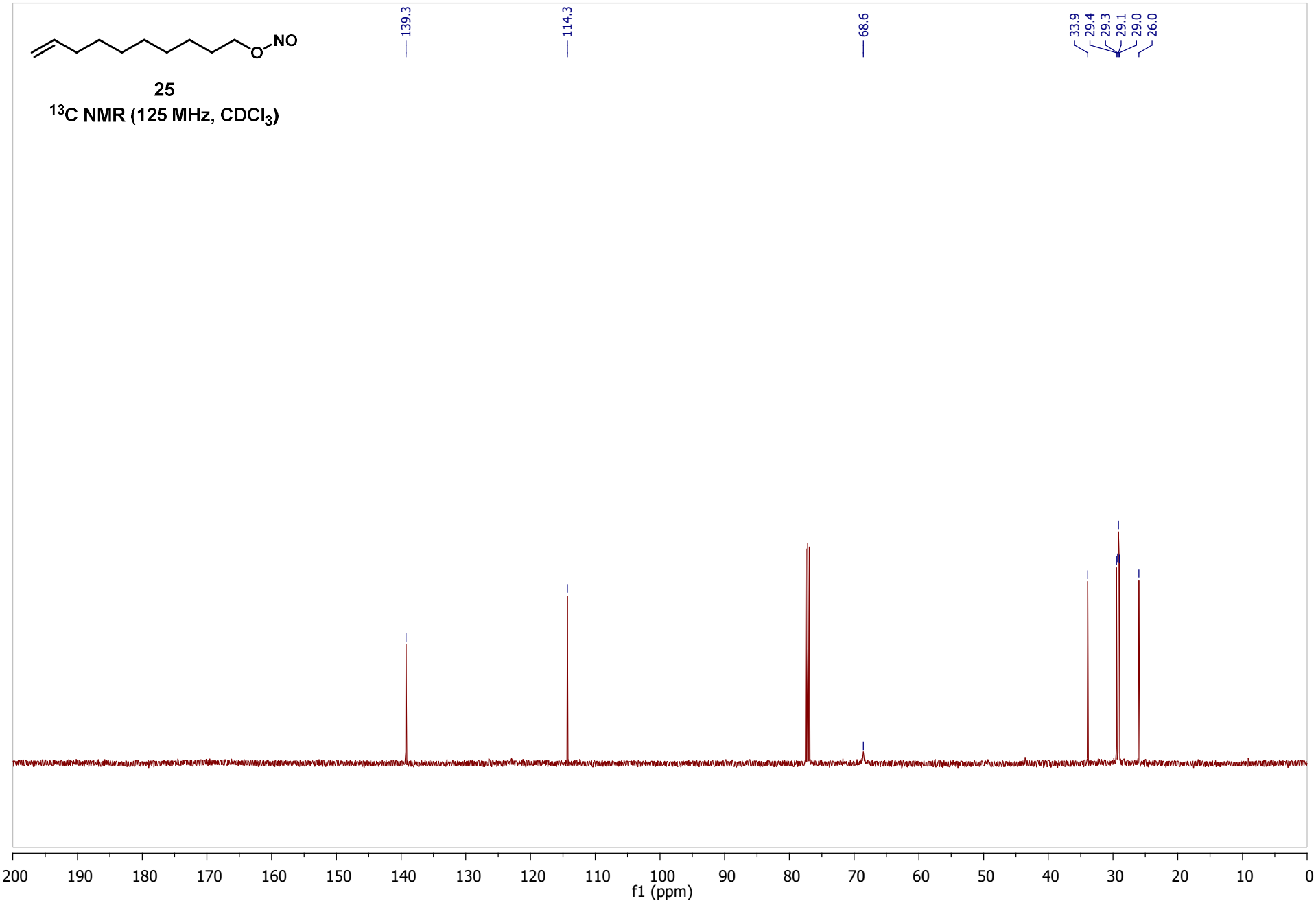

25

^{13}C NMR (125 MHz, $CDCl_3$)

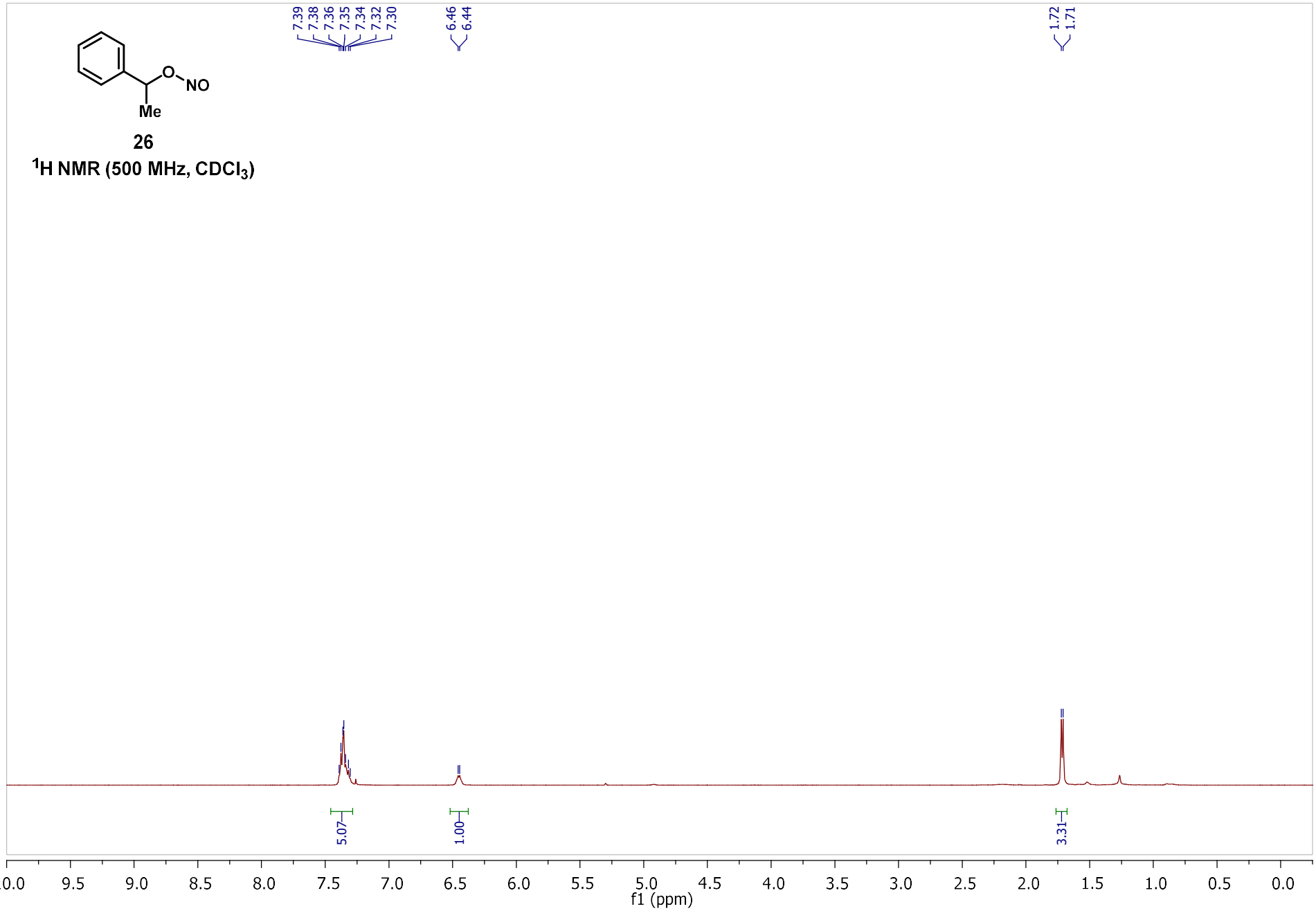

26

^{1}H NMR (500 MHz, $CDCl_3$)

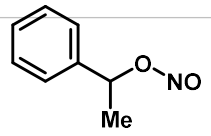

26

^{13}C NMR (125 MHz, $CDCl_3$)

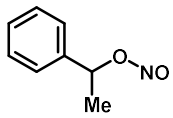

26

^{1}H—^{13}C HSQC NMR (500 MHz, $CDCl_3$)

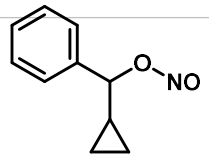

27

^{1}H NMR (400 MHz, $CDCl_3$)

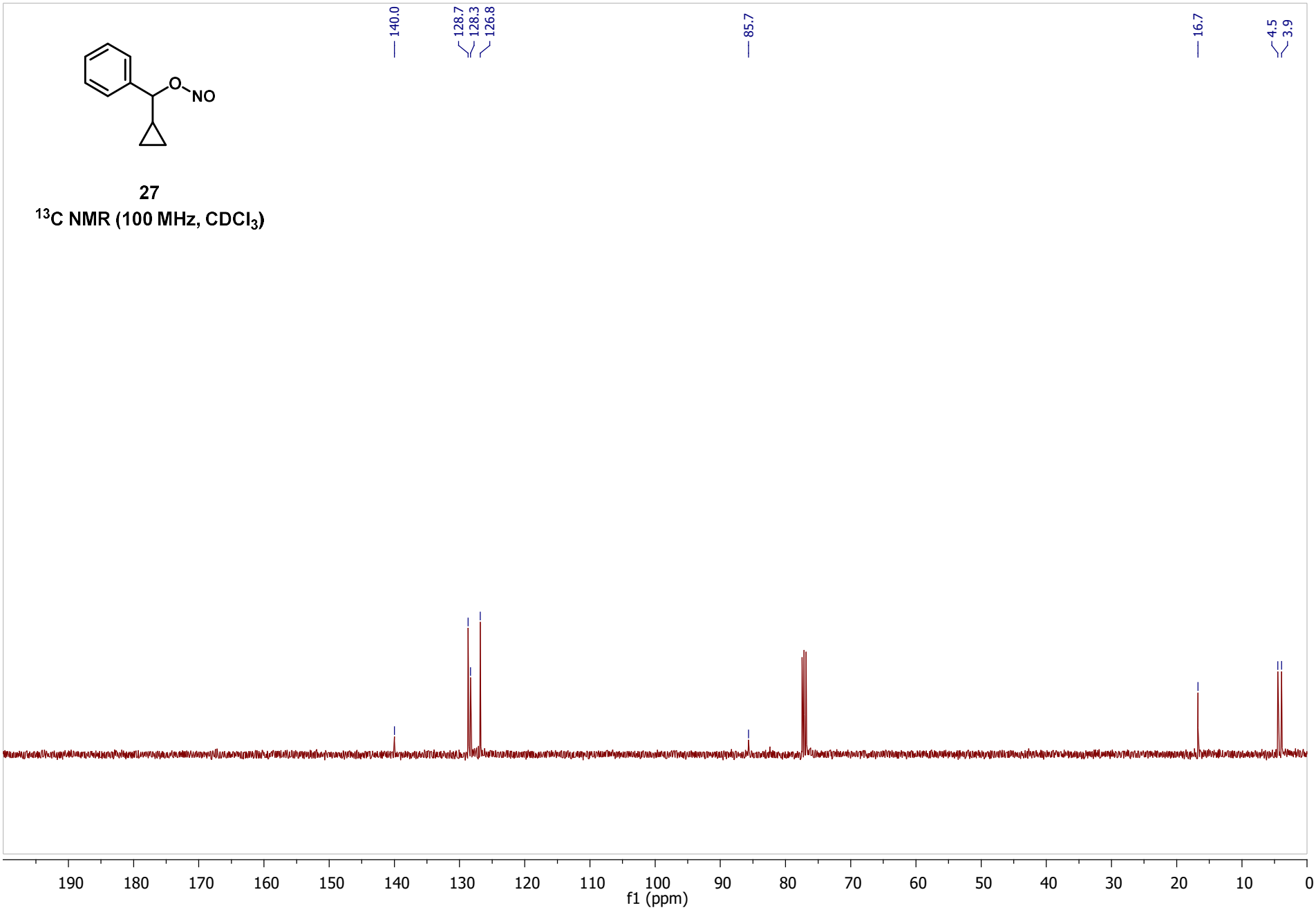

27

^{13}C NMR (100 MHz, $CDCl_3$)

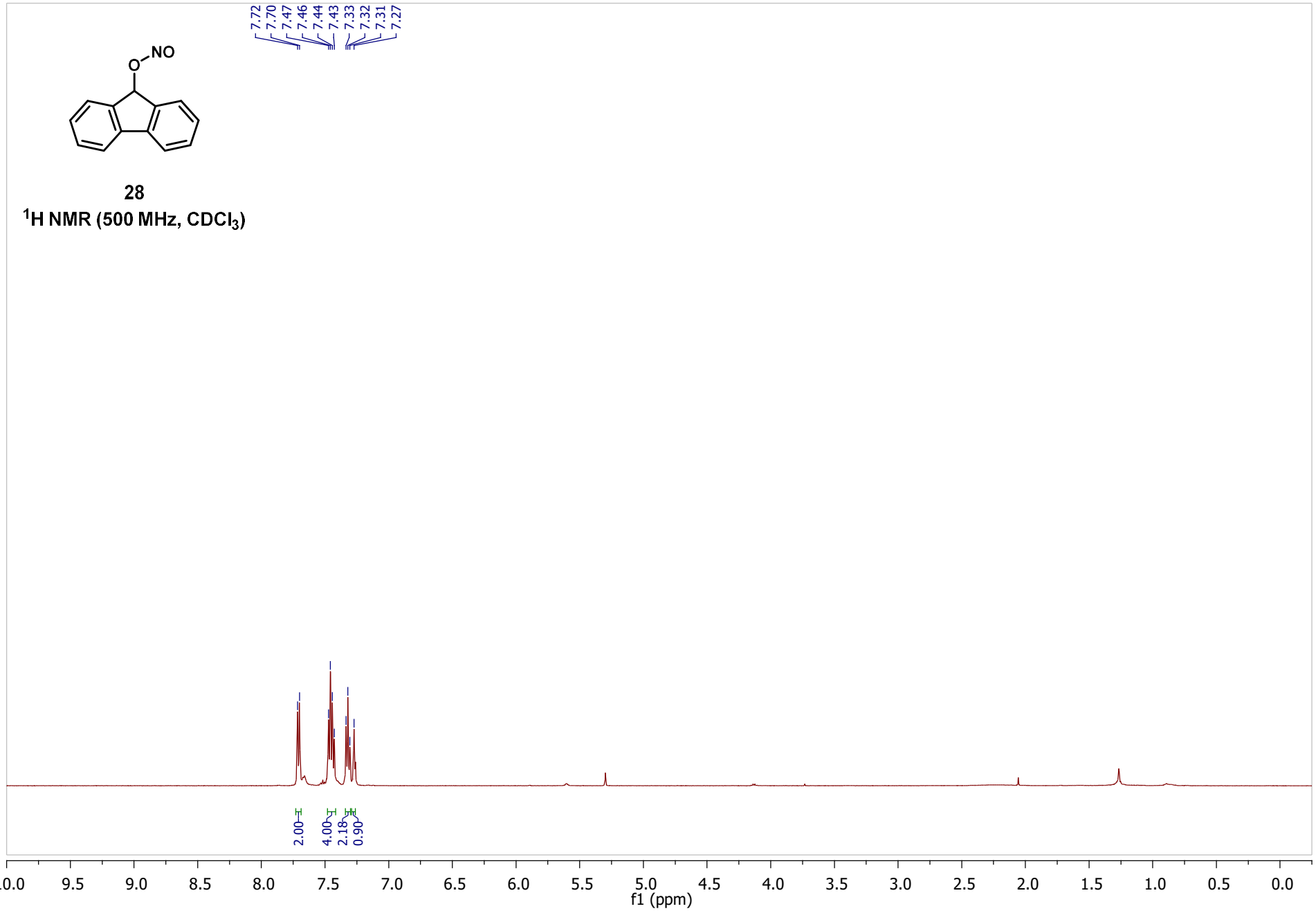

28

^{1}H NMR (500 MHz, $CDCl_3$)

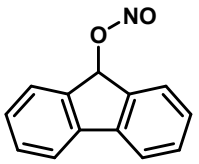

28

^{13}C NMR (125 MHz, $CDCl_3$)

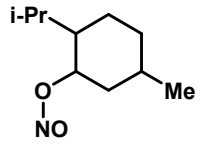

29

^{1}H NMR (400 MHz, $CDCl_3$)

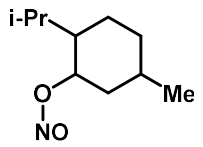

29

^{13}C NMR (100 MHz, $CDCl_3$)

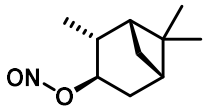

30

^{1}H NMR (500 MHz, $CDCl_3$)

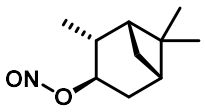

30

^{13}C NMR (125 MHz, $CDCl_3$)

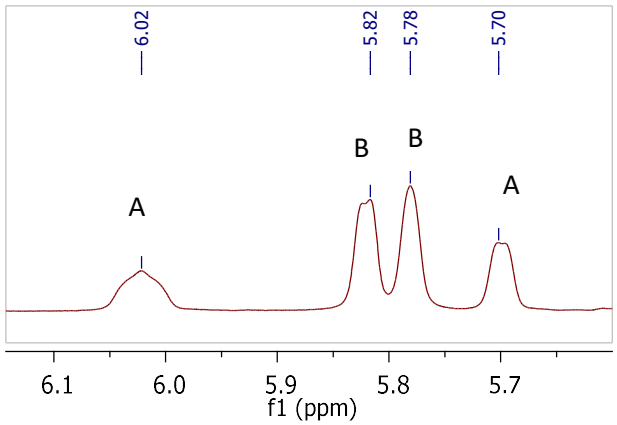

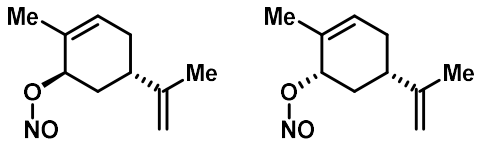

31 (trans) & 31 (cis)
A B
^{1}H NMR (500 MHz, $CDCl_3$)

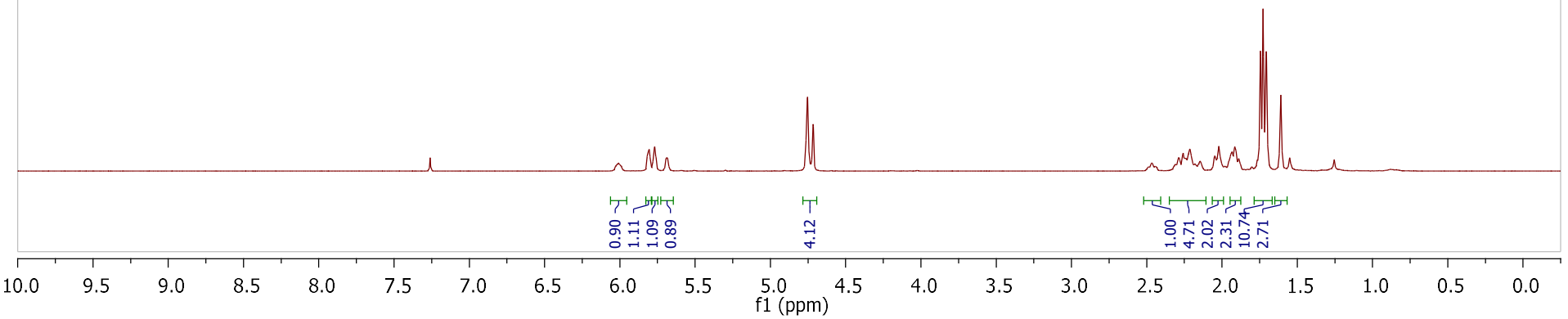

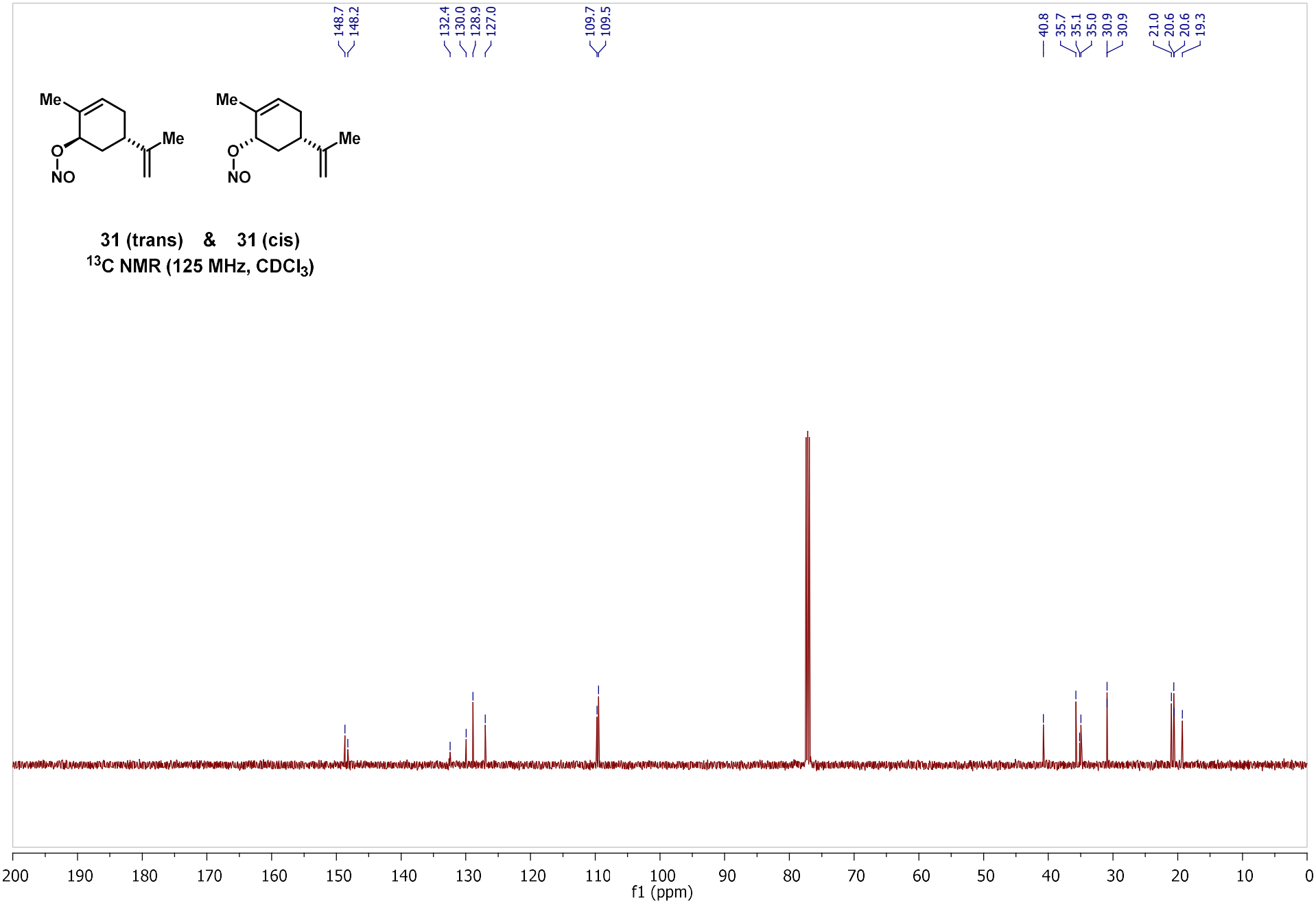

31 (trans) & 31 (cis)

^{13}C NMR (125 MHz, $CDCl_3$)

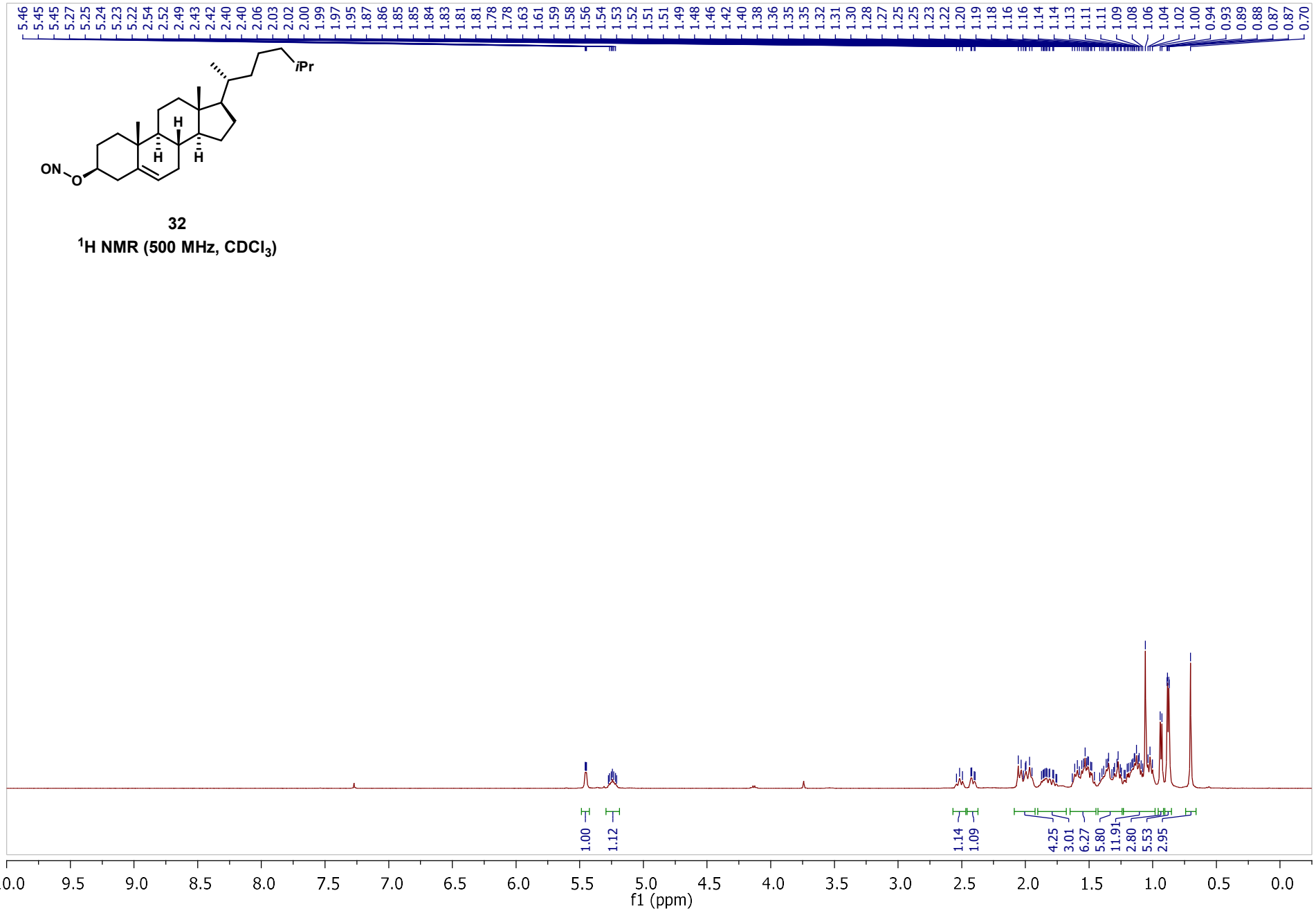

32

^{1}H NMR (500 MHz, $CDCl_3$)

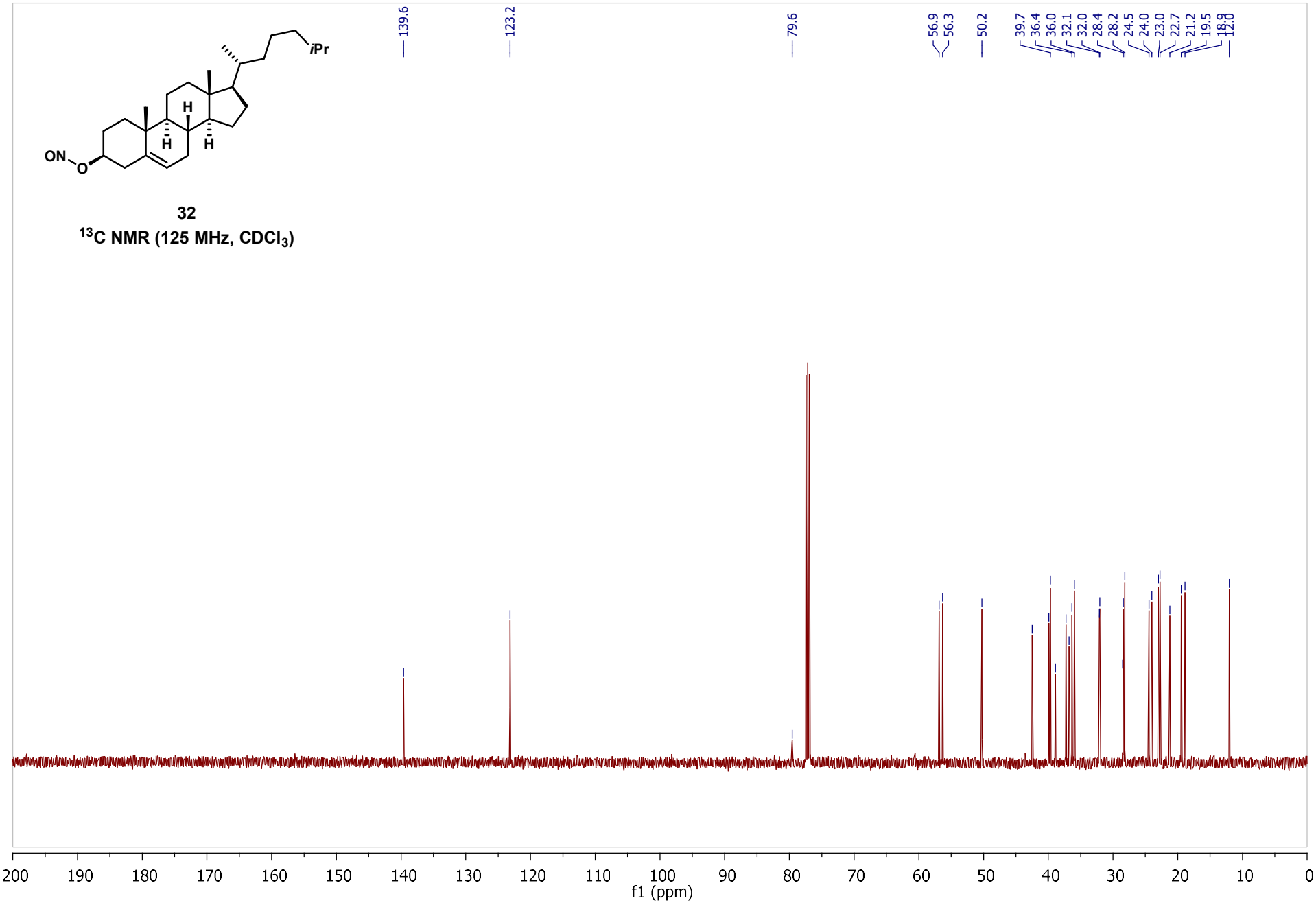

32

^{13}C NMR (125 MHz, $CDCl_3$)

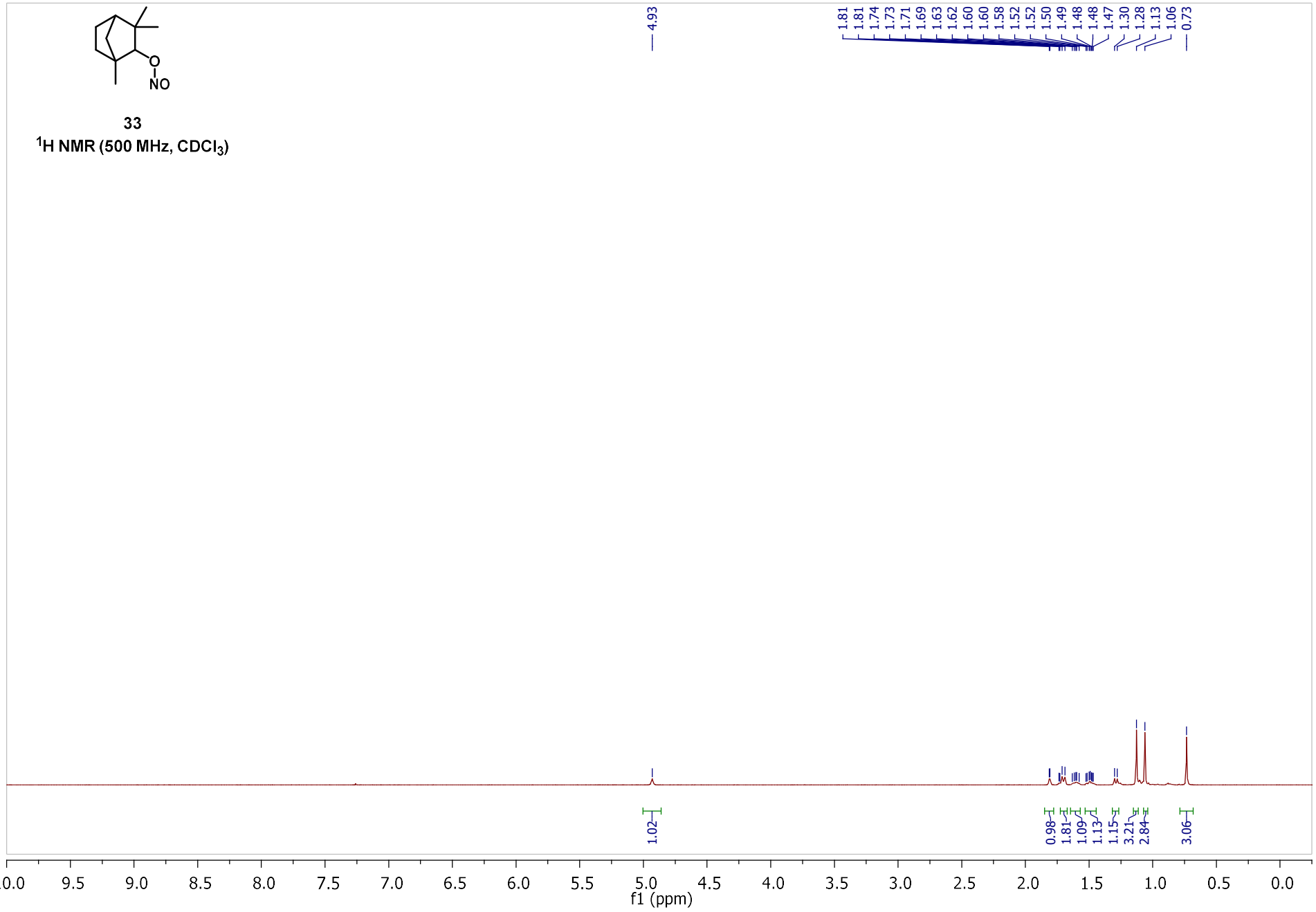
O
NO
33
1H NMR (500 MHz, CDCl3)
4.93
1.81
1.81
1.74
1.73
1.71
1.69
1.63
1.62
1.60
1.60
1.58
1.52
1.52
1.50
1.49
1.48
1.48
1.47
1.30
1.28
1.13
1.06
0.73
1.02
0.98
1.81
1.09
1.13
1.15
3.21
2.84
3.06
10.0
9.5
9.0
8.5
8.0
7.5
7.0
6.5
6.0
5.5
5.0
4.5
4.0
3.5
3.0
2.5
2.0
1.5
1.0
0.5
0.0
f1 (ppm)

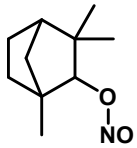

33

^{13}C NMR (125 MHz, $CDCl_3$)

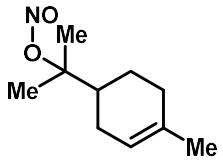

34

^{1}H NMR (500 MHz, $CDCl_3$)

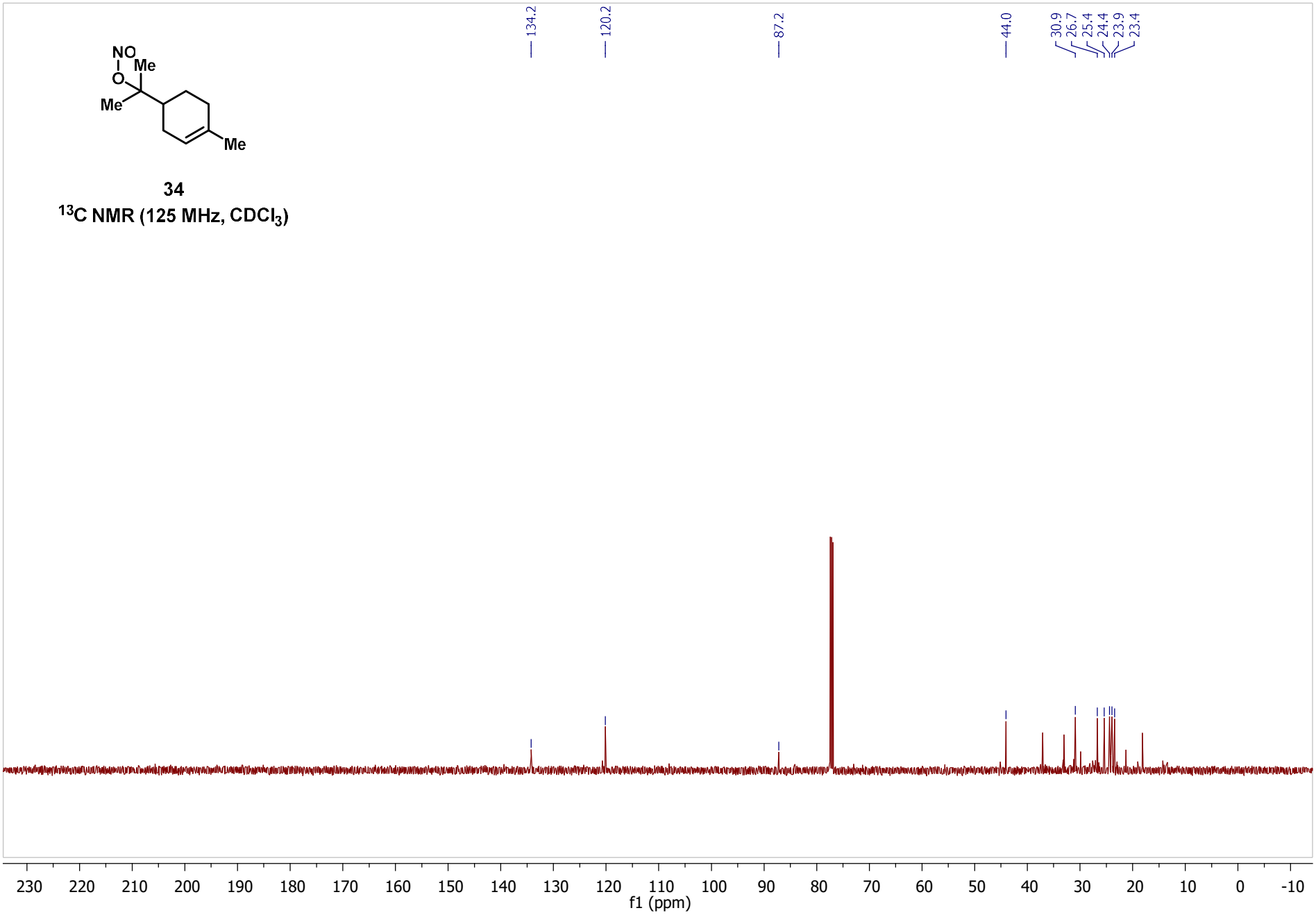

34

^{13}C NMR (125 MHz, $CDCl_3$)

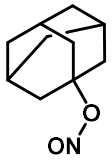

35

^{1}H NMR (500 MHz, $CDCl_3$)

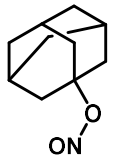

35

^{13}C NMR (125 MHz, $CDCl_3$)

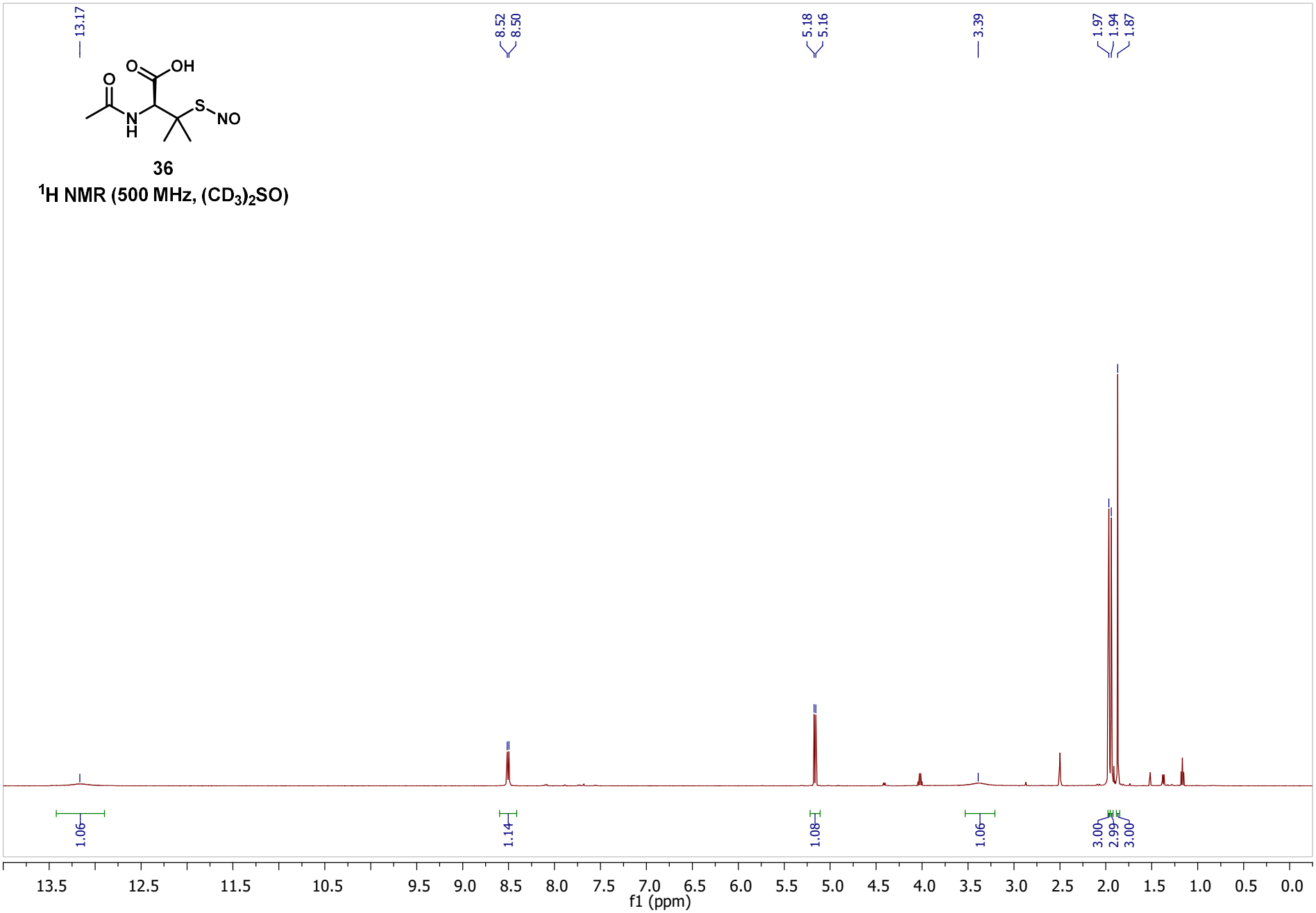

36

^{1}H NMR (500 MHz, $(CD_3)_2SO$)

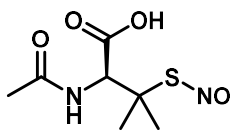

36

^{13}C NMR (125 MHz, $(CD_3)_2SO$)

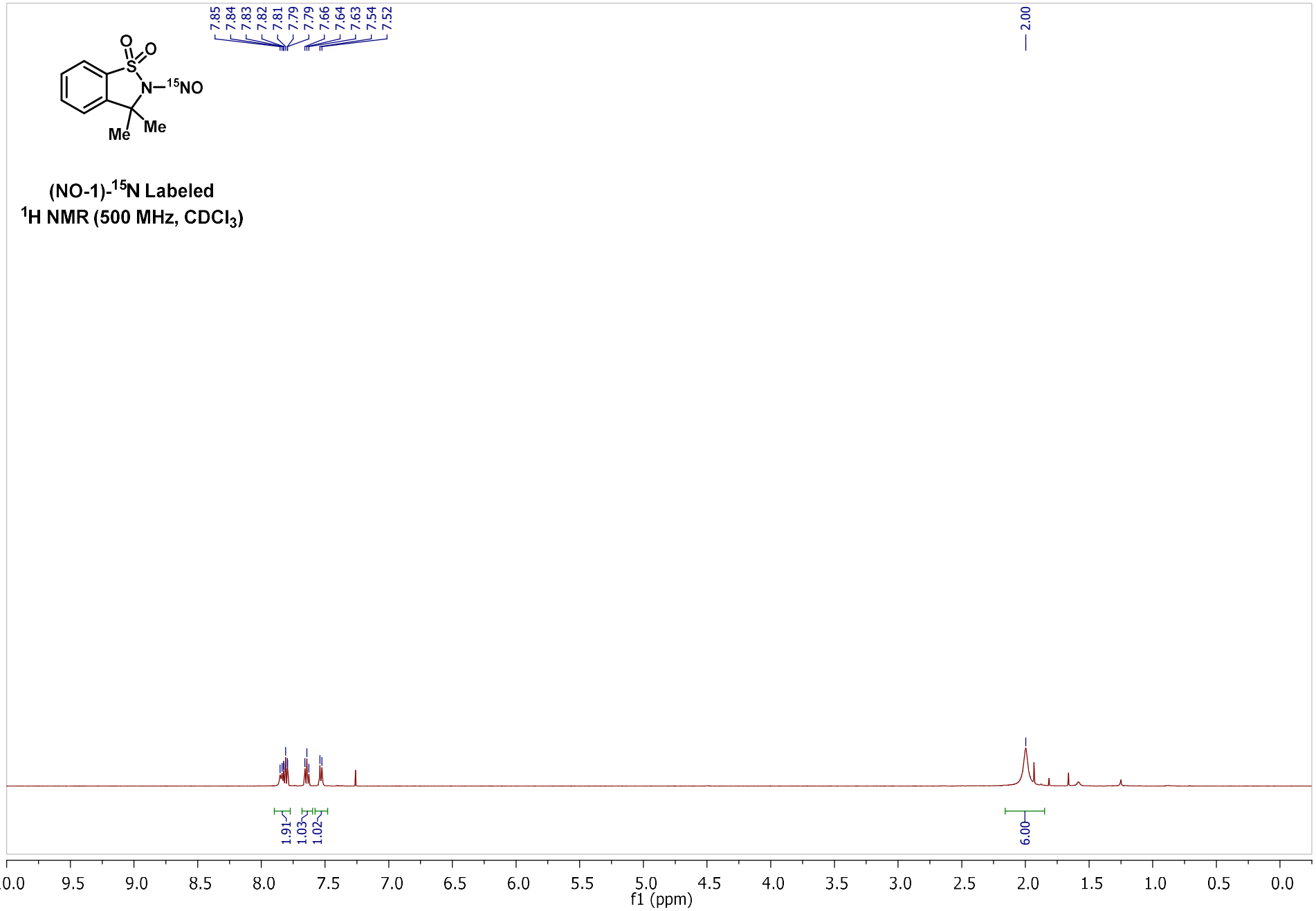
7.85
7.84
7.83
7.82
7.81
7.79
7.79
7.66
7.64
7.63
7.54
7.52
2.00
O
O
S
N—15NO
Me
Me
(NO-1)-15N Labeled
1H NMR (500 MHz, CDCl3)
1.91
1.03
1.02
6.00
10.0
9.5
9.0
8.5
8.0
7.5
7.0
6.5
6.0
5.5
5.0
4.5
4.0
3.5
3.0
2.5
2.0
1.5
1.0
0.5
0.0
f1 (ppm)

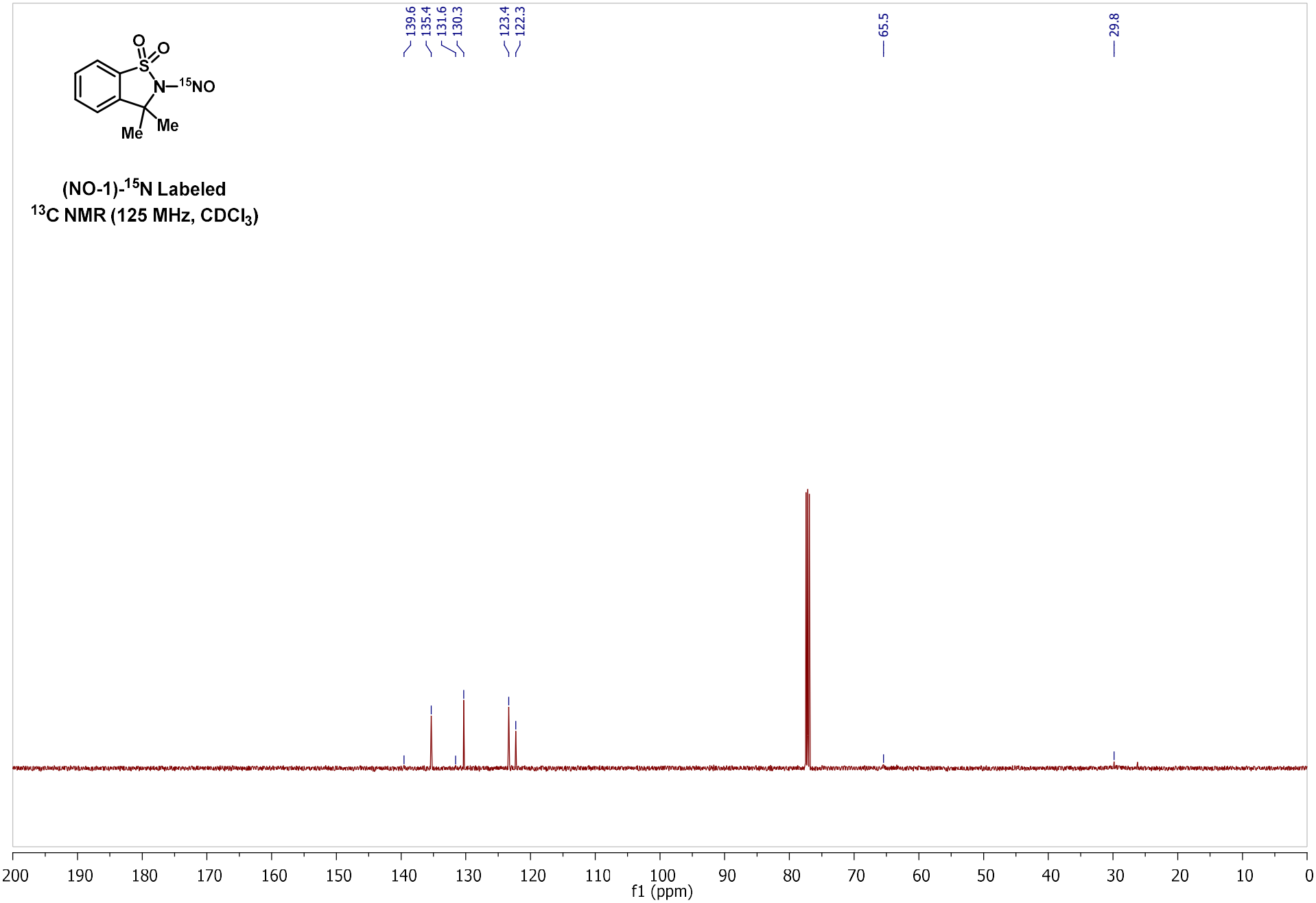
139.6
135.4
131.6
130.3
123.4
122.3
65.5
29.8
O
O
S
N—15NO
Me
Me
(NO-1)-15N Labeled
13C NMR (125 MHz, CDCl3)
200
190
180
170
160
150
140
130
120
110
100
90
80
70
60
50
40
30
20
10
0
f1 (ppm)

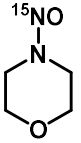

37

^{1}H NMR (500 MHz, $CDCl_3$)

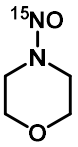

37

^{13}C NMR (125 MHz, $CDCl_3$)

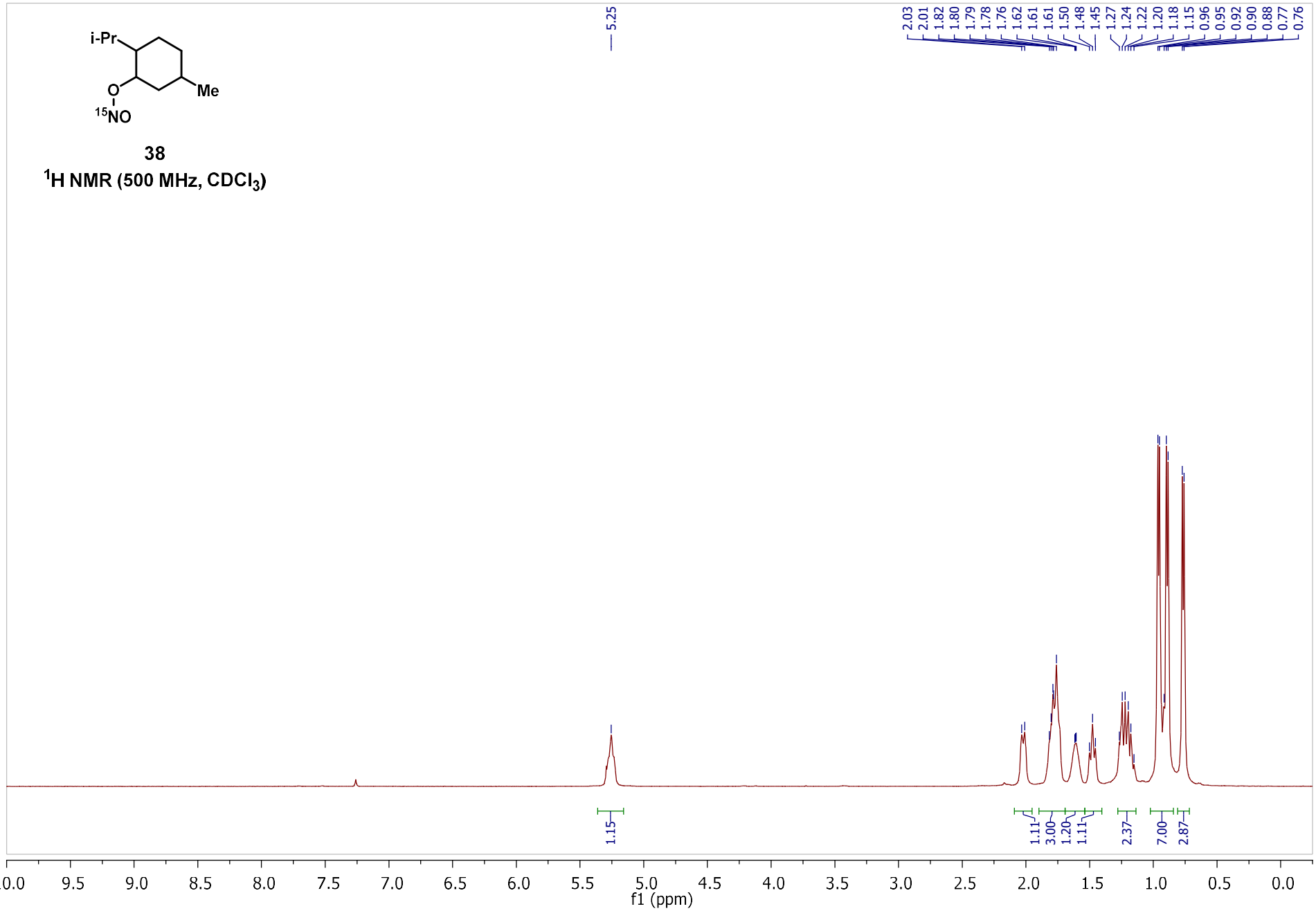
i-Pr
Me
O
15NO
38
1H NMR (500 MHz, CDCl3)
5.25
2.03
2.01
1.82
1.80
1.79
1.78
1.76
1.62
1.61
1.61
1.50
1.48
1.45
1.27
1.24
1.22
1.20
1.18
1.15
0.96
0.95
0.92
0.90
0.88
0.77
0.76
1.15
1.11
3.00
1.20
1.11
2.37
7.00
2.87
10.0
9.5
9.0
8.5
8.0
7.5
7.0
6.5
6.0
5.5
5.0
4.5
4.0
3.5
3.0
2.5
2.0
1.5
1.0
0.5
0.0
f1 (ppm)

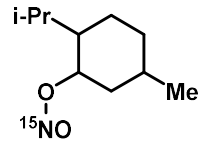

38

^{13}C NMR (125 MHz, $CDCl_3$)

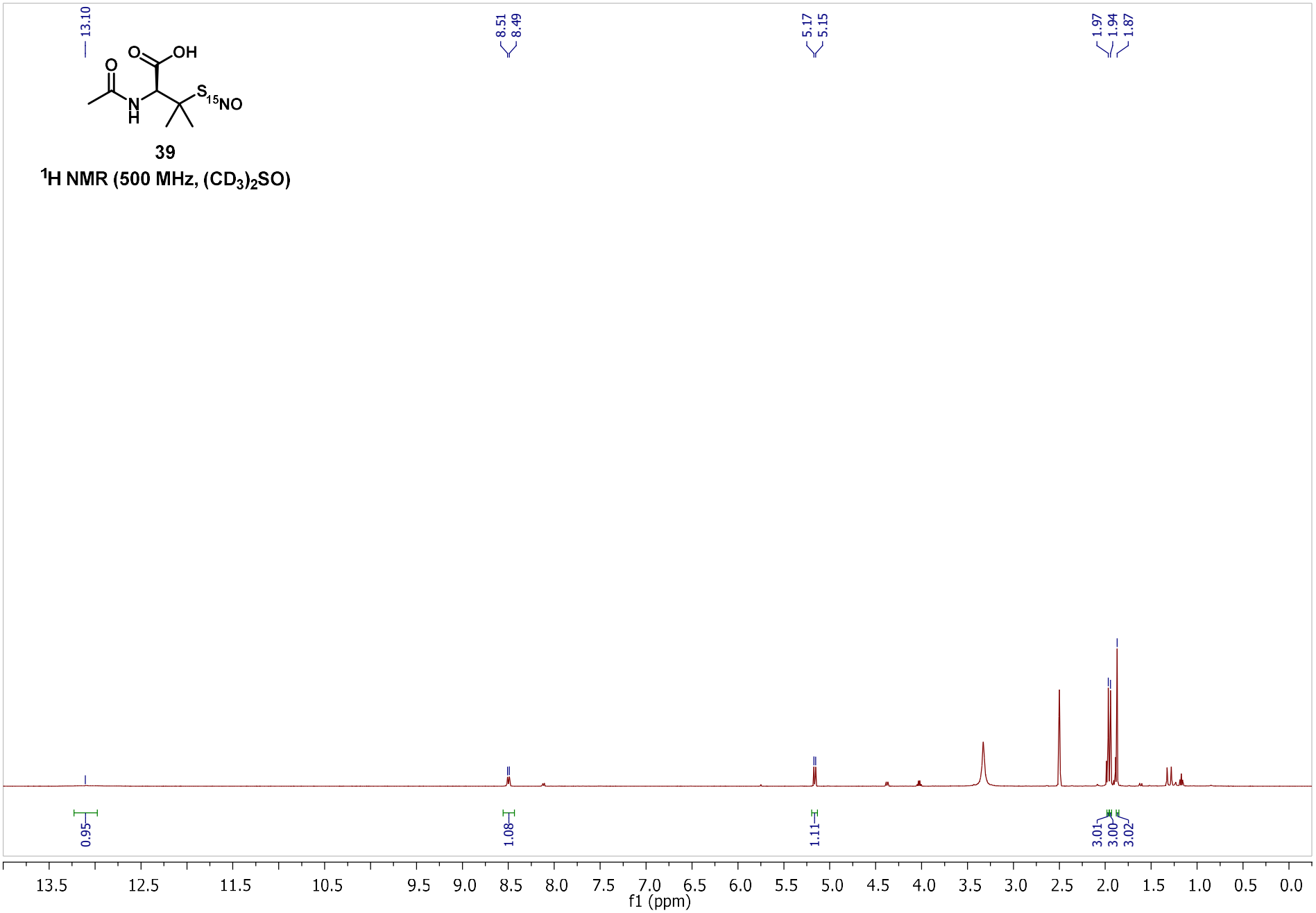

39

^{1}H NMR (500 MHz, $(CD_3)_2SO$)

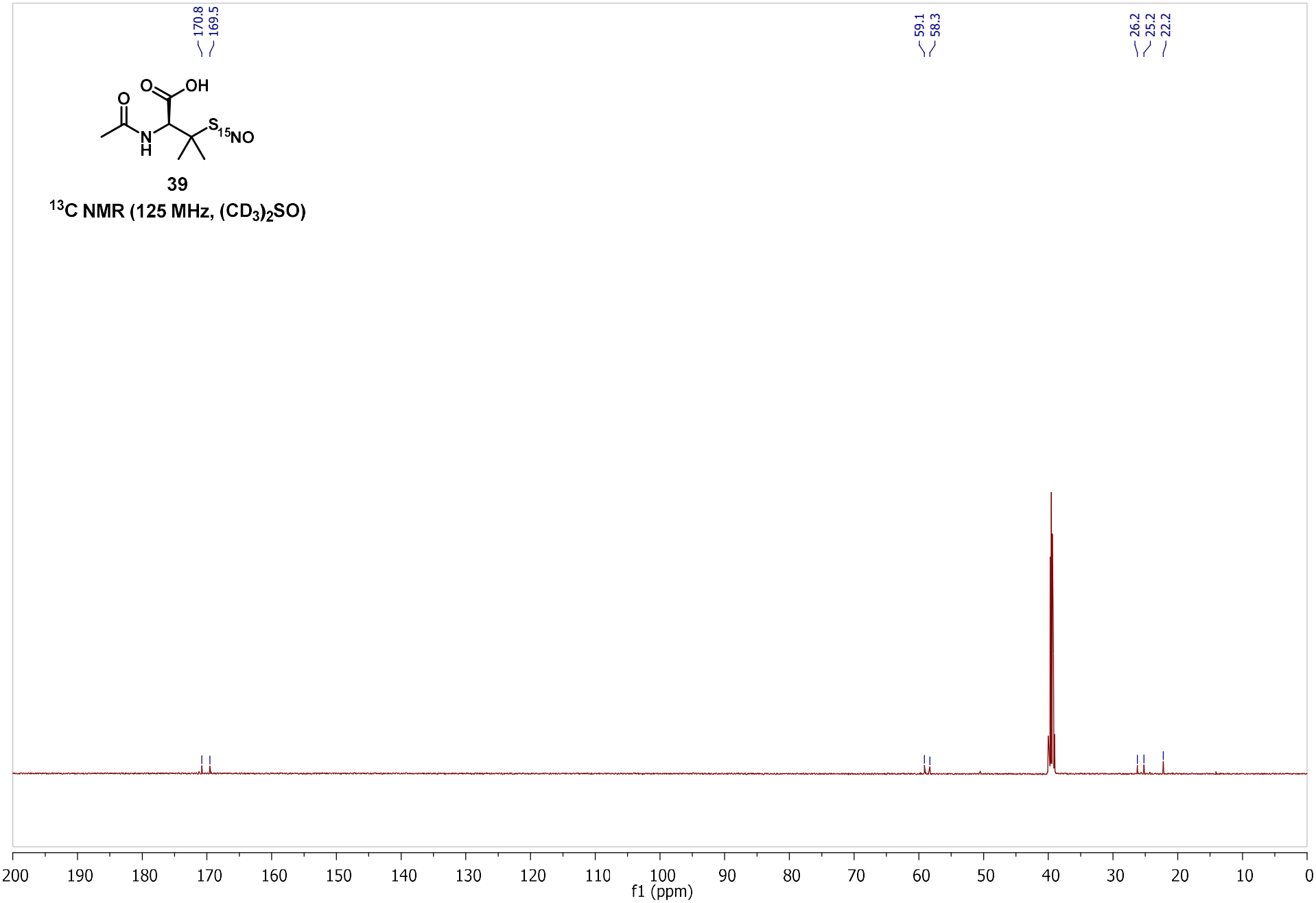

39

^{13}C NMR (125 MHz, $(CD_3)_2SO$)

A Versatile New Reagent for Nitrosation under Mild Conditions

Jordan D. Galloway[1], Cristian Sarabia[1], James C. Fettinger[2], Hrant P. Hratchian[1], and Ryan D. Baxter[1]*

[1]Department of Chemistry and Chemical Biology, University of California, Merced. Merced, California 95343, United States. [2]Department of Chemistry, University of California, Davis. Davis, California 95616.

Supporting Information Placeholder

ABSTRACT: Here we report a new chemical reagent for transnitrosation under mild experimental conditions. This new reagent is stable to air and moisture across a broad range of temperatures, and is effective for transnitrosation in multiple solvents. Compared to traditional nitrosation methods, our reagent shows high functional group tolerance for substrates that are susceptible to oxidation or reversible transnitrosation. Several challenging nitroso-compounds are accessed here for the first time, including ^{15}N isotopologues. X-ray data confirms two rotational isomers of the reagent are configurationally stable at room temperature, although only one isomer is effective for transnitrosation. Computational analysis describes the energetics of rotamer interconversion, including interesting geometry-dependent hybridization effects.

Nitric oxide (NO) is a small molecule of extreme biological importance. It has been implicated in a range of biological processes including; vasodilation[1], immune regulation[2], neurotransmission[3], and the inhibition of platelet aggregation.[4] Because NO is a gaseous molecule with low water solubility, medicinal applications targeting NO pathways predominately involve organic molecules capable of generating NO *in situ* via direct bond cleavage, enzymatic processes, or both. [1b,5] As shown in Figure 1, several small molecules possessing heteroatom–NO or –NO_2 bonds are effective NO donors used to treat multiple medical conditions. While alkyl nitrites and nitrates are most often used as vasodilators, several *N*-nitroso compounds are potent DNA alkylators that effectively halt tumor growth in certain cancers.[6] Interestingly, while *N*-nitrosourea Lomustine has been used to treat brain tumors and Hodgkin lymphoma[7], structurally similar Semustine has been removed from market and rated as a Group I carcinogen by the IARC.[8] This dramatic difference from just a single remote methyl group suggests a sensitive structure-activity-relationship for *N*-nitrosoureas acting as chemotherapeutics. With this in mind, the ability to easily access a variety of structurally diverse nitroso-compounds would benefit the development of next-generation therapeutics that rely on the NO functional group for activity.

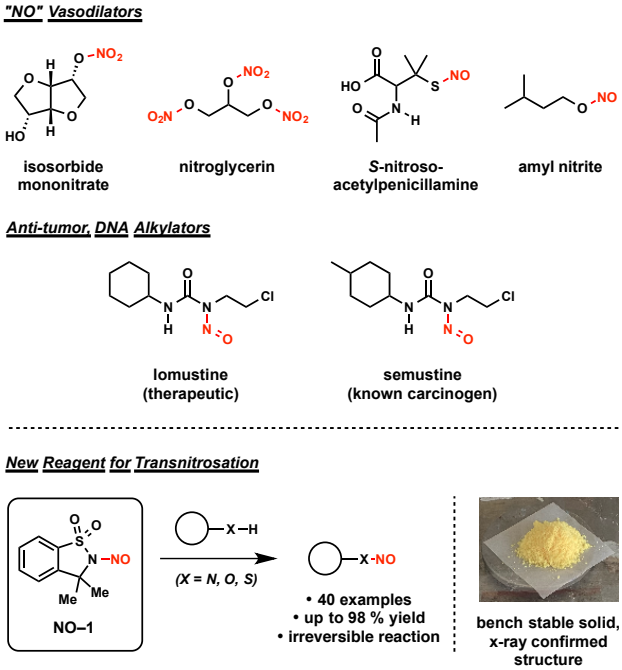

Figure 1. Biologically active "NO" molecules (top), and a new bench-stable reagent for transnitrosation (bottom).

Traditional methods for nitrosation have involved the use of inorganic nitrites, such as $NaNO_2$, under strongly acidic conditions to generate electrophilic sources of NO.[9] These methods can be effective for the nitrosation of amides, secondary amines, and certain alcohols, but lead to rapid diazotization when reacting with primary amines.[10] In addition, $NaNO_2$ decomposes under basic conditions, and the requirement for nitrosation at low pH limits the scope of substrates that can effectively participate. Because of this observed limitation, recent synthetic efforts have shifted to using commercially available *tert*-butyl nitrite (TBN) as an electrophilic transnitrosation reagent.[11] Unlike inorganic nitrites, TBN does not require strongly acidic conditions for transnitrosation, although some nucleophiles require excess TBN to minimize reversible transnitrosation with *tert*-butanol[12]. TBN has been effective for nitrosating amides, secondary amines, and certain alcohols, but is known to oxidize primary alcohols under atmospheric conditions.[13–14] Because TBN has been known to undergo both homolytic thermolysis and air-mediated oxidation at room temperature, cryogenic storage under inert atmosphere is required. As

detailed below, we have developed a new organic reagent that serves as an attractive alternative to TBN for the trans-nitrosation of nucleophiles under mild conditions. *N*-nitrososulfonamide reagent, **NO–1**, is a an easily synthesized crystalline material that maintains long-term integrity under ambient storage conditions (Figure 1).[15] Upon irreversible transnitrosation with a variety of nucleophiles, the sulfonamide byproduct of **NO–1** is easily recovered to regenerate **NO–1** with high fidelity. Alkyl alcohols, amines, amides, ureas, and thiols are all effectively nitrosated irreversibly by **NO–1** under mild conditions, resulting in several nitroso-compounds that are reported here for the first time.

Our interest in transnitrosation came from our work on C–H functionalizations involving radical hydrogen atom abstractions. Based on work from our lab and others, the diazobicyclo radical cation produced via single-electron reduction of Selectfluor has been shown to be an effective C–H abstractor.[16] We sought to explore alternative sources of *N*-centered radicals for C–H abstraction, and became interested in nitrosoamines and nitrosoamides as potential radical precursors. A large body of work by Chow involves the generation of *N*-centered radicals via light-mediated cleavage of *N*–NO bonds.[17] Several *N*-centered radicals derived from simple cyclic nitrosoamides were capable of C–H abstraction in our hands, but with limited synthetic efficiency. In an effort to generate more electron-deficient *N*-centered radicals, we explored *N*-nitrososulfonamides as radical precursors. Boer had previously shown sulfonamidyl radicals capable of abstracting hydrogens from solvent under thermal conditions, and recent reports describe related intramolecular hydrogen atom abstractions.[18]

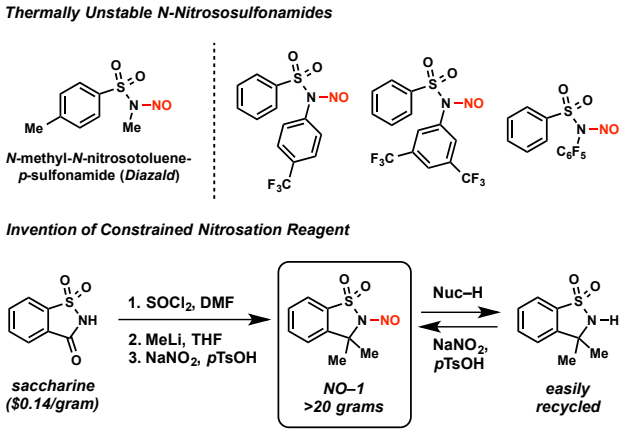

Figure 2. *N*-nitrososulfonamides prone to thermal decomposition (top), and the invention of geometrically constrained **NO–1** (bottom).

During the course of our studies, we found limited success for intermolecular C–H abstraction using *N*-nitrososulfonamides as radical precursors, but found them to be effective transnitrosating reagents. Although this type of reactivity has been reported, a well-known limitation of *N*-nitrososulfonamides as transnitrosating reagents is their propensity for thermal decomposition.[19] In fact, *N*-methyl-*N*-nitroso-*p*-toluenesulfonamide (Diazald) is a well-known commercial reagent that requires only mild heating under basic conditions to generate an equivalent of diazomethane. Several Diazald analogues were explored as alternatives, but were found to be thermally unstable under ambient conditions (Figure 2). In an effort to overcome this limitation, we sought to develop a class of geometrically constrained *N*-nitrososulfonamides that resisted thermal degradation. Beginning with the artificial sweetener Saccharine as starting material, a series of straightforward transformations yield **NO–1** in high yield. This synthetic sequence is amenable to scaling with no appreciable loss in efficiency (see SI for details). In our hands **NO–1** has been shown to be indefinitely bench-stable under ambient conditions with no significant decrease in activity upon standing for several months. Upon successful transnitrosation, the sulfonamide byproduct can be recovered to regenerate **NO–1** in a one-step synthesis. With the new reagent in hand, we explored the scope of nucleophiles that efficiently transnitrosate with **NO–1**.

Scheme 1. Amine and Amide Nitrosation with NO–1

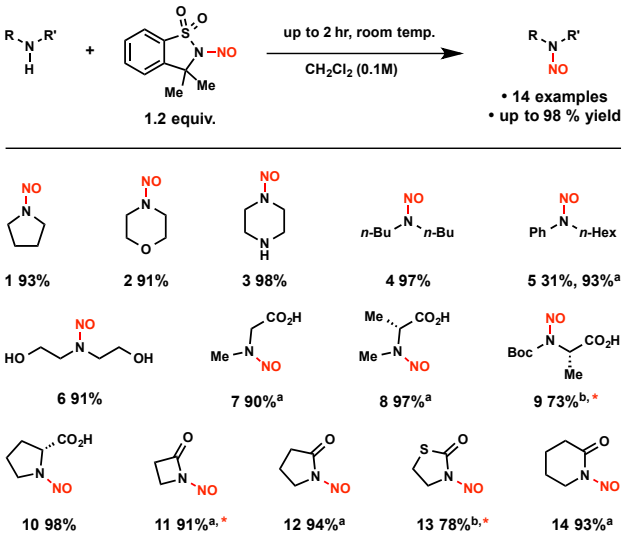

General reaction conditions: Amine/amide (0.2 mmol) and **NO–1** (0.24 mmol) in 2mL CH_2Cl stirred at room temperature. Yields refer to chromatographically pure material. [a]Reaction was heated to 80 °C in 1,2-dichloroethane. [b]Reaction was run at room temperature in CH_3CN with trifluoroacetic acid added (0.04 mmol). *First known report of structure.

Cyclic and acyclic amines are effectively nitrosated by **NO–1** (Scheme 1, entries **1**–**5**). Free alcohols are tolerated (**6**), although it is likely that transnitrosation initially occurs at oxygen prior to intramolecular transnitrosation to the amine. Carboxylic acids are well tolerated, allowing for the direct nitrosation of amino acids (entries **7**–**10**). Finally, cyclic amides are efficiently nitrosated in high yields (entries **11**–**14**). To the best of our knowledge nitroso-compounds **9**, **11**, and **13** are reported here for the first time.

Although reagent **NO–1** is effective for the synthesis of nitrosoamines and nitrosoamides, many of the structures shown in Scheme 1 may be accessed directly by reaction with *tert*-butyl nitrite (TBN). Conversely, alkyl alcohols often require excess TBN to promote transnitrosation, or suffer from unwanted oxidation under ambient conditions. Scheme 2 shows that **NO–1** efficiently nitrosates a variety of alcohol structures. Primary (**15**–**25**), secondary (**26**–**33**), and tertiary (**34**–**35**) alcohols are all effectively nitrosated in good to excellent yields. Activated benzylic or allylic are not susceptible to oxidation, although no effort is made to exclude oxygen from solvents or reaction flasks. In addition, **NO–1** tolerates elevated temperature in the presence of alkynes (**21**) and alkenes (**20, 23**–**25**, **31**–**32, 34**) without evi-

dence of byproducts resulting from homolytic *N–N* cleavage of **NO–1**. *N*-Acetylpenicillamine is also successfully nitrosated to produce *S*-nitroso-*N*-acetylpenicillamine (**36**), a molecule implicated in signaling pathways associated with vasodilation.[20–21] For substrates that do not tolerate elevated temperatures, an alternative experimental procedure involving catalytic trifluoroacetic acid is generally effective. Isolated yields for both procedures are given for the majority of substrates shown in Scheme 2. In many cases, transnitrosation is effective in multiple organic solvents and a brief description of solvent compatibility is provided in the *Supporting Information.*

Scheme 2. Alcohol Nitrosation with NO–1

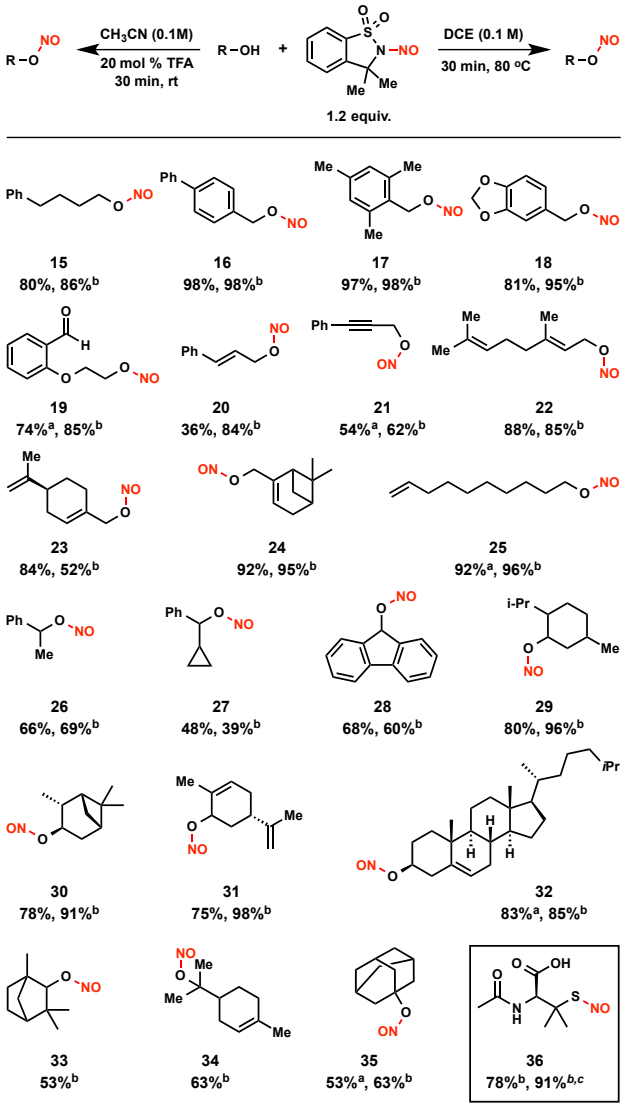

General reaction conditions: Alcohol (0.2 mmol) and **NO–1** (0.24 mmol) in 2mL 1,2-dichloroethane (DCE) stirred at 80 °C for 30 minutes. Yields refer to chromatographically pure material. [a]Reaction was run in CH_3CN at 80 °C. [b]Reaction was run at room temperature in CH_3CN with trifluoroacetic acid added (0.04 mmol). [c]NMR yield using 1,2,4,5-tetramethylbenzene as a standard.

One of the potential strengths of a transnitrosation method is the ability to incorporate radiolabeled ^{15}N into target molecules. Because enriched $Na^{15}NO_2$ is commercially available, we produced **^{15}NO–1** to explore its efficacy in transnitrosation (Scheme 3). To our satisfaction, this reagent behaved analogously to **NO–1** with no loss in stability or reactivity. A secondary amine (**37**), alcohol (**38**), and thiol (**39**) were all successfully nitrosated in high yields to produce enriched materials.

Scheme 3. Nitrosation with Radiolabeled ^{15}NO–1

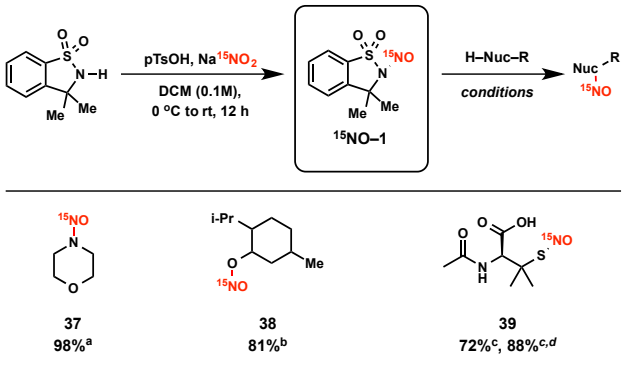

Reaction conditions: [a]Nucleophile (0.2 mmol) and **^{15}NO–1** (0.24 mmol) in 2mL dichloromethane stirred at room temperature for 30 minutes. [b]1,2-Dichloroethane (DCE) stirred at 80 °C for 30 minutes. [c]CH_3CN with trifluoroacetic acid (0.04 mmol) at room temperature for 30 minutes. [d]NMR yield using 1,2,3,4,5-tetramethylbenzene as an internal standard.

Although the efficiency of transnitrosation with **NO–1** is established, early efforts were plagued by batch-to-batch variability and irreproducible yields. Comparison of crystallographic data from multiple synthetic batches of **NO–1** suggested that the rotational configuration of the nitroso-group affected the efficiency of transnitrosation. Data from a batch of **NO–1** that produced low yields for transnitrosation were especially informative (~60% conversion for **1**, Scheme 1). As shown in Figure 3, a poorly performing batch of **NO–1** exists as a mixture of rotational isomers centered around the *N–N–O* bond. Superimposed structures show that molecular geometry is nearly identical throughout both isomers, beyond the orientation of the nitroso *N–O* bond. Interestingly, while ineffective at room temperature, this batch of **NO–1** was still capable of transnitrosation to produce **1** in high yields at elevated temperature. This suggested that both isomers are sufficiently reactive at elevated temperature, or that thermally induced conversion to a single active rotamer was occurring.

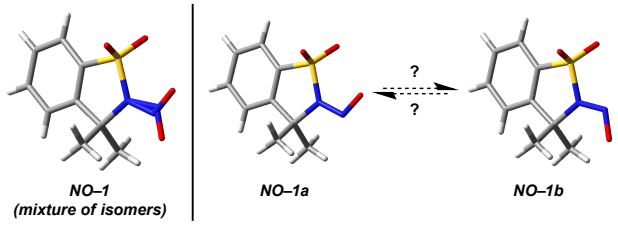

Figure 3. Crystallographic data for **NO–1** as a mixture of rotational isomers (left), and the individual structures (right) found within the crystal lattice.

To better understand the possibility of thermal interconversion between stable rotational isomers, we computed the potential energy of **NO–1** as a function of the *N–N* dihedral angle (Figure 4, red data). Initial results confirmed that structure **NO–1a** was lower in energy than **NO–1b** by approximately -1.2kcal/mol (0° and 180° dihedral angle, respective-

ly). Interestingly, different rotational barriers were calculated rotating between 0–90º than from 180–360º. Discontinuities in the potential energy surface were also noted between 130–140º and 290-300º, which warranted further investigation. Upon analyzing the geometries of **NO–1** at each data point along the energy surface, we noted geometry/hybridization changes of the nitrogen atom within the ring. Additional energy plots were rendered while restricting this nitrogen atom to either sp^2 or sp^3 hybridization (green and blue data, respectively). Taken together, these data describe how changes in hybridization occur during conversion between rotational isomers **NO–1a** and **NO–1b**. Overlap of the red data with either the blue or green curves indicates the hybridization of the energy-minimized structure at a particular dihedral angle. Lack of overlap, coinciding with discontinuities in the unrestricted data (red), indicates a geometry that does not fit neatly into the limiting definitions of sp^2 or sp^3 hybridization.

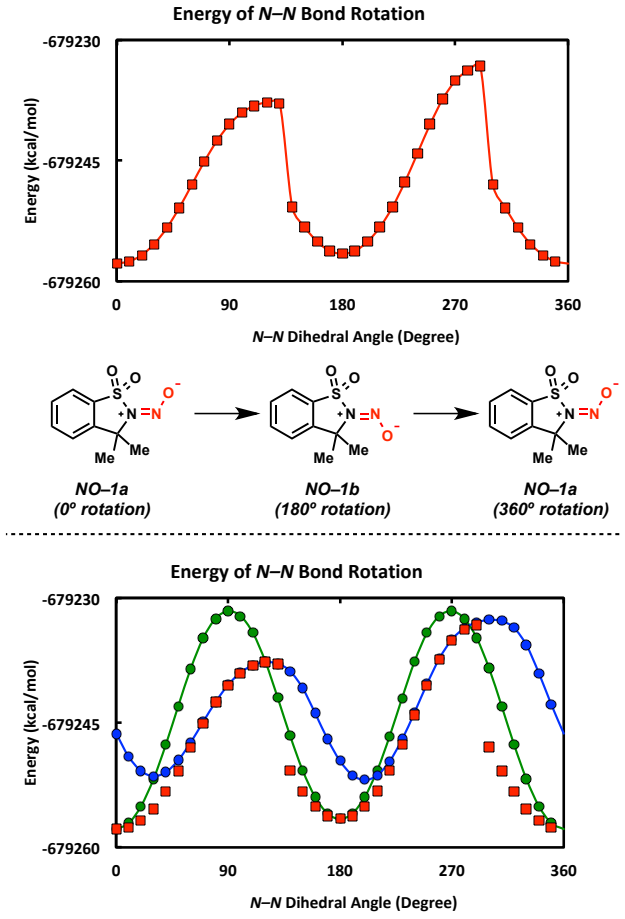

Figure 4. All the calculations were run using the B3LYP/6-311+G(2d, p) model chemistry with MeCN using the Polarizable Continuum Model for solvents. **Top:** red data represent the potential energy surface of an *N–N* dihedral angle scan while the nitrogen in the ring is unconstrained to any hybridization. Representative rotational isomers **1a** and **1b** are the dominant species where indicated. **Bottom:** green data represent a potential energy surface of an *N–N* dihedral angle scan while restricting the nitrogen in the ring to sp^2 hybridization. Blue data represent a potential energy surface of an *N–N* dihedral angle scan while restricting the nitrogen in the ring to sp^3 hybridization. Red data shown overlaid for reference.

Experimental efforts confirmed that **NO–1a** is the active rotational isomer for transnitrosation at room temperature. Simply heating a crude mixture of **NO–1** to 80ºC as a final step in the synthesis yields a reagent that consistently transnitrosates at room temperature and a crystal structure consistent with **NO-1a**. Efforts to identify the source of disparate reactivity between **NO–1a** and **NO–1b** room temperature are ongoing.

We have reported the invention of a new reagent for transnistrosation under mild conditions. This reagent requires no special handling for use or storage, nitrosates nucleophiles irreversibly, and is straightforward to regenerate from the byproducts of a successful reaction. High functional group tolerance and efficiency under a variety of reaction conditions make this an ideal reagent to explore nitrosated molecules that are challenging, or impossible, to make via traditional methods. Two rotational isomers of **NO–1** are stable at room temperature, although theoretical and experimental data suggest a single isomer (**NO–1a**) active for transnitrosation. Future work will involve further exploration of molecules that can be nitrosated by **NO–1** and to identify features that favor reaction from **NO–1a** at room temperature.

ASSOCIATED CONTENT

Supporting Information. Detailed experimental and computational procedures, full characterization and copies of all spectra. This material is available free of charge via the internet at http:pubs.acs.org.

AUTHOR INFORMATION

Corresponding Authors

rbaxter@ucmerced.edu

Author Contributions

†These authors contributed equally to this work.

Notes

The authors declare no competing financial interest.

ACKNOWLEDGEMENT

J.D.G and C.S. gratefully acknowledge NSF Graduate Research Fellowships for funding. This material is based upon work supported by the National Science Foundation under Grants No. 1752821 (R.D.B) and 2019144, 1429783 (H.P.H). We thank the National Science Foundation (Grant 1531193) for the Dual source X-ray diffractometer (J.C.F). Dr. Duy (Peter) Mai is thanked for helpful discussions and edits.

REFERENCES

(1) (a) Zhao, Y.; Vanhoutte, P. M.; Leung, S. W. S., Vascular nitric oxide: Beyond eNOS. *J. Pharmacol. Sci.* **2015,** *129*, 83–94. (b) Wang, P. G.; Xian, M.; Tang, X.; Wu, X.; Wen, Z.; Cai, T.; Janczuk, A. J. Nitric Oxide Donors: Chemical Activities and Biological Applications. *Chem. Rev.*, **2002**, 102, 1091–1134.

(2) (a) Nathan, C. F.; Hibbs, J. B. Role of nitric oxide synthesis in macrophage antimicrobial activity. *Curr. Opin. Immunol.* **1991,** *3*, 65–70. (b) Karpuzoglu, E.; Ahmed, S. A. Estrogen Regulation of Nitric Oxide and Inducible Nitric Oxide Synthase (INOS) in Immune Cells: Implications for Immunity, Autoimmune Diseases, and Apoptosis. *Nitric Oxide*, **2006**, 15, 177–186.

(3) (a) Garthwaite, J. Glutamate, nitric oxide and cell-cell signalling in the nervous system. *Trends Neurosci.* **1991,** *14*, 60–67. (b) Vincent, S. R. Nitric Oxide Neurons and Neurotransmission. *Progress in Neurobiology*, **2010**, 90, 246–255. (c) Yun, H.-Y.; Dawson, V. L.; Dawson, T. M. Nitric Oxide in Health and Disease of the Nervous System. *Mol Psychiatry*, **1997**, 2, 300–310.

(4) (a) Riddell, D. R.; Owen, J. S., Nitric Oxide and Platelet Aggregation. In *Vitamins & Hormones*, Litwack, G., Ed. Academic Press: **1997**; Vol. 57, pp 25-48. (b) Fukumura, D.; Kashiwagi, S.; Jain, R. K. The role of nitric oxide in tumour progression. *Nat. Rev. Cancer* **2006**, 6, 521.

5 Wang, P. G.; Cai, T. B.; Taniguchi, N (Eds). Nitric Oxide Donors for Pharmaceutical and Biological Applications. Wiley-VHC, Weinehim, 2005.

(6) (a) Miller, M. R.; Megson, I. L., Recent developments in nitric oxide donor drugs. *Br. J. Pharmacol* **2007,** *151*, 305–321. (b) Huang, Z.; Fu, J.; Zhang, Y., Nitric Oxide Donor-Based Cancer Therapy: Advances and Prospects. *J. Med. Chem.* **2017**, *60*, 7617–7635. (c) Robbiano, L.; Martelli, A.; Allavena, A.; Mazzei, M.; Gazzaniga, G. M.; Brambilla, G., Formation of the *N*–Nitroso Derivatives of Six β-Adrenergic-blocking Agents and Their Genotoxic Effects in Rat and Human Hepatocytes. *Cancer Res.* **1991,** *51*, 2273–2279.

(7) Lee, F. Y. F.; Workman, P.; Roberts, J. T.; Bleehen, N. M., Clinical pharmacokinetics of oral CCNU (Lomustine). *Cancer Chemoth. Pharm.* **1985,** *14*, 125–131.

(8) (a) Gastrointestinal Tumor Study Group. Radiation therapy and fluorouracil with or without semustine for the treatment of patients with surgical adjuvant adenocarcinoma of the rectum. *J. Clin. Oncol.* **1992,** *10*, 549–557. (b) IARC Working Group on the Evaluation of Carcinogenic Risks to Humans. A review of human carcinogens. Part A: Pharmaceuticals. International Agency for Research on Cancer, Lyon, 2012.

(9) For a review on the applications of $NaNO_2$ to organic synthesis, see: (a) Mukhopadhyay, S.; Batra, S., Applications of Sodium Nitrite in Organic Synthesis. *European Journal of Organic Chemistry* **2019,** 38, 6424–6451. (b) McCullough, K. J.; Bessieres, B.; Wei, L.; Sodium Nitrite. In *Encyclopedia of Reagents for Organic Synthesis*, pp 1-11. (c) Williams, D. L. H. *Nitrosation*; Cambridge University: Cambridge, 1988; pp 95. (c) Challis, B. C.; Challis, J. A. *The Chemistry of Functional Groups*; Patai, S., Ed.; Wiley: New York, 1982; Suppl. F, pp 1151. (d) Chaskar, A. C.; Langi, B. P.; Deorukhkar, A.; Deokar, H. Bismuth Chloride–Sodium Nitrite: A Novel Reagent for Chemoselective N-Nitrosation. *Syn. Comm.* **2009**, *39*, 604–612. (e) Párkányi, C.; Célariès, B. Tin(IV) Chloride-Sodium Nitrite as a New Nitrosating Agent for *N*-Nitrosation of Amines, Amides and Ureas under Mild and Heterogeneous Conditions. *Synthesis.* **2006**, 2371–2375. (f) Borikar, S. P.; Paμl, V. N-Nitrosation of Secondary Amines Using *p*-TSA-$NaNO_2$ as a Novel Nitrosating Agent Under Mild Conditions. *Syn. Comm.* **2010**, *40*, 654–660.

(10) Ridd, J. H., Nitrosation, diazotisation, and deamination *Q. Rev., Chem. Soc.* **1961**, *15*, 418.

(11) For a review on various modes of reactivity for TBN, including transnitrosation, see: (a) Dahiya, A.; Sahoo, A. K.; Alam, T.; Patel, B. K., tert-Butyl Nitrite (TBN), a Multitasking Reagent in Organic Synthesis. *Chemistry – An Asian Journal* **2019,** *14*, 4454–4492. (b) Li, P., Jia, X., tert-Butyl Nitrite (TBN) as a Versatile Reagent in Organic Synthesis. *Synthesis*. **2018**, 50, 711–722. (c) Chaudhary, P.; Gupta, S.; Muniyappan, M.; Sabiah, S.; Kandasamy, J. An efficient synthesis of N-nitrosamines under solvent, metal and acid free conditions using tert-butyl nitrite. *Green.Chem.* **2016**, *18*, 2323–2330.

(12) Jaman, Z.; Sobreira, T. J. P.; Mufti, A.; Ferreira, C. R.; Cooks, R. G.; Thompson, D. H., Rapid On-Demand Synthesis of Lomustine under Continuous Flow Conditions. *Organic Process Research & Development* **2019,** *23*, 334-341.

(13) Hamasaki, A.; Kuwada, H.; Tokunaga, M. Tert-Butylnitrite as a Convenient and Easy-Removable Oxidant for the Conversion of Benzylic Alcohols to Ketones and Aldehydes. *Tetrahedron Letters*, **2012**, 53, 811–814.

(14) (a) 8.1 Recent Developments in Catalytic Alcohol Oxidation Using Nitroxyl Radicals. In Catalytic Oxidation in Organic Synthesis; Muñiz, Ed.; Georg Thieme Verlag, 2018. (b) Ghaffari Khaligh, N. Recently Applications of Tert-Butyl Nitrite in Organic Synthesis-Part I. COC, 2018, 22 (11), 1120–1138.

(15) Removed from solvent upon standing for 60 days under ambient conditions, **NO-1** showed no signs of decomposition.

(16) (a) Galloway, J. D.; Mai, D. N; Baxter, R. D. Radical Benzylation of Quinones via C–H Abstraction. *J. Org. Chem.,* **2019**, *84*, 1213–12137. *ChemRxiv*., 2019, doi: 10.26434/chemrxiv.7959368.vi. (b) Hua, A. M.; Bidwell, S. L.; Baker, S. I.; Hratchian, H. P.; Baxter, R. D. Experimental and Theoretical Evidence for Nitrogen–Fluorine Halogen Bonding in Silver-Initiated Radical Fluorinations. *ACS Catalysis*, **2019**, *9*, 3322–3326.

(17) (a) Chow, Y. L. Chemistry of *N*-Nitrosamides and Related *N*-Nitrosamino Acids. *ACS Symp. Ser. Am. Chem. Soc.* **1979**; 101, 13–37. (b) Chow, Y. L.; Perry, R. A. Chemistry of Amidyl Radicals: Intramolecular Reactivities of Alkenyl Amidyl Radicals. *Can. J. Chem.* **1985**, *63*, 2203–2210.

(18) (a) Dekker, E. E. J.; Engberts, J. B. F. N.; de Boer, T. J. Photolysis of Some *N*-Cycloalkyl-N-Halosulfonamides. *Recl. Trav. Chim. Pays Bas.,* **2010**, *97*, 39–41. (b) Qin, Q.; Yu, S. Visible-Light-Promoted Remote C(sp3)–H Amidation and Chlorination. *Org. Lett.* **2015**, *17*, 1894–1897. (c) Chu, J. C. K.; Rovis, T. Amide-Directed Photoredox-Catalysed C–C Bond Formation at Unactivated sp3 C–H Bonds. *Nature.* **2016**, *539*, 272–275. (d) Choi, G. J.; Zhu, Q.; Miller, D. C.; Gu, C. J.; Knowles, R. R. Catalytic Alkylation of Remote C–H Bonds Enabled by Proton-Coupled Electron Transfer. *Nature*. **2016**, *539*, 268–271.

(19) (a) W. A.; Yates, M. C.; Boese, B. J.; Barbeau, N. R. Electronic and Steric Effects in Thermal Denitrosation of N-Nitrosoamides. *J. Org. Chem.* **2001**, 66, 5679–5686. (b) Zhu, X.-Q.; Hao, W.-F.; Tang, H.; Wang, C.-H.; Cheng, J.-P. Transnitrosation of Thiols from Aliphatic N-Nitrosamines: S-Nitrosation and Indirect Generation of Nitric Oxide *J. Am. Chem. Soc.* **2005**, 127, 2696-2708.

(20) (a) Zhang, Y.; Hogg, N. S-Nitrosothiols: Cellular Formation and Transport. Free Radical Biology and Medicine, 2005, 38 (7), 831–838. (b) Lindkvist, M.; Fernberg, U.; Ljungberg, L. U.; Fälker, K.; Fernström, M.; Hurtig-Wennlöf, A.; Grenegård, M. Individual Variations in Platelet Reactivity towards ADP, Epinephrine, Collagen and Nitric Oxide, and the Association to Arterial Function in Young, Healthy Adults. Thrombosis Research, 2019, 174, 5–12.

(21) Other, less substituted, thiols produced *S*-nitrosothiols that decomposed under ambient conditions to yield disulfides.

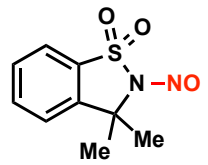

new reagent for transnitrosation

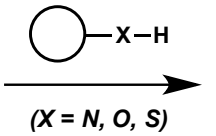

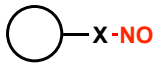

- 40 examples
- up to 98 % yield
- irreversible reaction

bench stable solid, x-ray confirmed structure